

A Comparative Study of Physiological Feature Selection Methods for Emotion Recognition

Andreas De Lille

Supervisors: Prof. dr. ir. Joni Dambre, Dr. ir. Pieter van Mierlo
Counsellor: Ir. Thibault Verhoeven

**Master's dissertation submitted in order to obtain the academic degree of
Master of Science in Computer Science Engineering**

Department of Electronics and Information Systems
Chair: Prof. dr. ir. Rik Van de Walle
Faculty of Engineering and Architecture
Academic year 2015-2016



A Comparative Study of Physiological Feature Selection Methods for Emotion Recognition

Andreas De Lille

Supervisors: Prof. dr. ir. Joni Dambre, Dr. ir. Pieter van Mierlo
Counsellor: Ir. Thibault Verhoeven

**Master's dissertation submitted in order to obtain the academic degree of
Master of Science in Computer Science Engineering**

Department of Electronics and Information Systems
Chair: Prof. dr. ir. Rik Van de Walle
Faculty of Engineering and Architecture
Academic year 2015-2016



Preface

This work was completed with the help of several people, I would like to thank. First of all my supervisors, prof. dr. ir. Joni Dambre and my counsellor ir. Thibault Verhoeven for their guidance and patience during the year. They gave me the freedom to steer the direction of my thesis, while still ensuring that the end result has scientific value. Secondly, I would also like to thank my thesis colleges, Nina, Bjorn and Thijs for giving me suggestions and ideas for my research as well as their support during this work.

This preface wouldn't be complete without thanking my parents, stepparents, brothers and sister for giving me their support, not only this year, but throughout all my years as a student. I would also like to mention my mother and father for giving me the opportunity to study.

Last but not least, I would also like to thank my friends, among others, Cedric, Patrick, Michiel, Thomas and Wouter for supporting me during the year and creating an pleasant working atmosphere.

Andreas De Lille
Ghent, 1 June 2016

This work is licensed under a Creative Commons “Attribution 4.0 International” license.



Persmission for Usage

“The author(s) gives (give) permission to make this master dissertation available for consultation and to copy parts of this master dissertation for personal use. In the case of any other use, the copyright terms have to be respected, in particular with regard to the obligation to state expressly the source when quoting results from this master dissertation.“

“De auteur geeft de toelating deze scriptie voor consultatie beschikbaar te stellen en delen van de scriptie te kopiëren voor persoonlijk gebruik.
Elk ander gebruik valt onder de beperkingen van het auteursrecht, in het bijzonder met betrekking tot de verplichting de bron uitdrukkelijk te vermelden bij het aanhalen van resultaten uit deze scriptie.”

Andreas De Lille
Ghent, 1 June 2016

A Comparative Study of Physiological Feature Selection Methods for Emotion Recognition

by

Andreas DE LILLE

Supervisors: Prof. J. DAMBRE and Dr. Ir. P. BUTENEERS

Counsellor: Ir. T. VERHOEVEN

Master's dissertation submitted in order to obtain the academic degree of
Master of Science in Computer Science Engineering

Department of Electronics and Information Systems

Chair: Prof. dr. ir. Rik Van de Walle

Faculty of Engineering and Architecture

Academic year 2015-2016

Summary

An emerging field of research is the field of emotion recognition. Emotion can be observed in many ways, but the most reliable method is to use physiological signals. This method uses machine learning to classify emotions based on characteristics or features extracted from the signals. To do so, good, reliable features are needed. This work compares a wide range of features and feature selection techniques to study the physiological responses triggered by emotion.

Keywords

Emotion recognition, Physiological Signals, Machine Learning, Feature Selection

Contents

Preface	iii
Permission for Usage	iv
Overview	v
Table of Contents	vii
List of Figures	viii
List of Tables	xi
1 Introduction	1
1.1 Emotion recognition	1
1.1.1 Physiological signals	2
1.2 Machine learning	6
1.2.1 Over- and underfitting	8
1.2.2 Feature selection	10
1.3 Problem statement	11
1.4 Goal of the thesis	11
2 Methods	13
2.1 Dataset	13
2.2 Features	16
2.2.1 EEG-features	16
2.2.2 non-EEG features	18
2.2.3 Overview	20
2.3 State of the art	21
2.3.1 DEAP method	21
2.3.2 Stable emotion recognition over time	21
2.3.3 EEG-based emotion recognition in music listening	23
2.3.4 Comparing selected methods for feature extraction and classification	23
2.3.5 Advanced RF feature selection	24
2.4 Feature selection methods	25
2.4.1 Filter methods	25
2.4.2 Wrapper methods	29
2.4.3 Embedded methods	33

3 Results - Person specific	38
3.1 Used approach	38
3.2 Performance	40
3.3 Correlation probability and level of valence/arousal	43
3.4 Selected features	45
3.5 Important EEG channels	56
3.6 Stability	60
4 Results - Cross-subject	62
4.1 Approach	62
4.2 Performance	62
4.3 Correlation probability and level of valence/arousal	64
4.4 Selected features	66
4.5 Important EEG channels	74
4.6 Stability	74
5 Conclusion	76
5.1 Person specific	76
5.2 Cross-subject	77
6 Future Research	78
6.1 Applications for emotion recognition	78
Bibliography	82

List of Figures

1.1	The arousal - valence model maps emotions in a two dimensional plane[1]	2
1.2	EEG measurements is a trace electrical potentials of different channels over time.[2]	3
1.3	The electrode placement of a 23 channel system[3].	4
1.4	Placement of the 32 electrodes in this thesis.	5
1.5	In optical character recognition, a computer uses machine learning to find characters in an image[4].	6
1.6	The price of a house is determined by its total area.	7
1.7	Overfitting versus underfitting[5].	9
1.8	Cross validation	10
2.1	The images used for the SAM[6].	16
2.2	The plethysmograph before smoothing.	18
2.3	The local optima in the plethysmograph.	19
2.4	Pearson correlation coefficients for different sets of (x,y) points. Note that many coefficients are zero, while there clearly is some correlation. Source: Wikipedia .	27
2.5	Distance correlation coefficients for different sets of (x,y) points. Note the difference with the Pearson correlation coefficients in Figure 2.4. - Source: Wikipedia	28
2.6	One possible separation border.	30
2.7	A separation with maximal boundary.	30
2.8	There exists no possible line that can separate the red balls from the blue ones. .	31
2.9	Transformation to a new features space where the balls can be separated by a hyperplane.	31
2.10	Separation boundary in the original feature space.	32
2.11	LDA finds a projection of the data where the separation of the data is clear. . .	33
2.12	The structure of a random forest, found at [7]	34
2.13	A decision tree for the data in Table 2.3	35
2.14	Suppose a three-dimensional feature space, where all points lie in the ellipsoid in the left.	37
3.1	The used approach of this thesis.	39
3.2	Comparison of different feature selection methods for arousal recognition. The y-axis shows the test accuracy averages over all persons as well as the standard deviation. The x-axis shows the different models, each number corresponds to the number in Table 3.1. Blue bars correspond to filter selection methods, red bars correspond to wrapper methods and green bars are used for the embedded methods.	41

3.3	Comparison of different feature selection methods for valence recognition. The y-axis shows the test accuracy averages over all persons as well as the standard deviation. The x-axis shows the different models, each number corresponds to the number in Table 3.2. Blue bars correspond to filter selection methods, red bars correspond to wrapper methods and green bars are used for the embedded methods.	42
3.4	The pearson correlations between the model's prediction probability and the distance between the subject's level of arousal and the separation boundary, see Table 3.3 for more details.	44
3.5	The pearson correlations between the model's prediction probability and the distance between the subject's level of valence and the separation boundary, see Table 3.3 for more details.	44
3.6	The distribution of the selected features for arousal classification of all persons combined of different feature selection methods. It is clear that the most valuable features are the asymmetry features combined with the power features. Furthermore, all feature selection methods agree that EEG features are dominant.	47
3.7	The distribution of the selected features for valence classification of all persons combined of different feature selection methods. It is clear that the most valuable features are the asymmetry features combined with the power features. Furthermore, all feature selection methods agree that EEG features are dominant.	48
3.8	The average and standard deviation of the test accuracies of arousal classification for all, EEG and non-EEG features, see also Table 3.4	49
3.9	The average and standard deviation of the test accuracies of valence classification for all, EEG and non-EEG features, see also Table 3.4	50
3.10	The distribution of the selected features for arousal classification of all persons combined of different feature selection methods. The feature set was limited to EEG features only.	52
3.11	The distribution of the selected features for valence classification of all persons combined of different feature selection methods. The feature set was limited to EEG features only.	53
3.12	The distribution of the selected features for arousal classification of all persons combined of different feature selection methods. The feature set was limited to non-EEG features only.	54
3.13	The distribution of the selected features for valence classification of all persons combined of different feature selection methods. The feature set was limited to non-EEG features only.	55
3.16	All EEG channels were grouped in 4 regions: left-front (blue), right-front (red), left-back (black), right-back (purple) and midline (yellow).	57
4.1	Comparison of different feature selection methods' test accuracies for arousal recognition in a cross-subject setting. The blue bars correspond to filter selection methods. Red bars correspond to wrapper methods and green bars are used for the embedded methods.	63
4.2	Comparison of different feature selection methods' test accuracies for valence recognition in a cross-subject setting. The blue bars correspond to filter selection methods. Red bars correspond to wrapper methods and green bars are used for the embedded methods.	64

4.3	The pearson correlations of the model's prediction probability versus the distance between the subject's level of arousal and the separation boundary in a cross-subject setting.	65
4.4	The pearson correlations of the model's prediction probability versus the distance between the subject's level of valence and the separation boundary in a cross-subject setting.	66
4.5	The distribution of the selected features for arousal classification in a cross-subject setting for different feature selection methods. It is clear that the most valuable features are the asymmetry features combined with the power features. Furthermore, all feature selection methods agree that EEG features are dominant.	68
4.6	The distribution of the selected features for valence classification in a cross-subject setting for different feature selection methods. It is clear that the most valuable features are the asymmetry features combined with the power features. Furthermore, all feature selection methods agree that EEG features are dominant.	69
4.7	The performance of arousal prediction for all, EEG and non-EEG features on the test set in a cross-subject setting.	70
4.8	The performance of valence prediction for all, EEG and non-EEG features on the test set in a cross-subject setting.	71
4.9	The distribution of the selected features for arousal classification in a cross-subject setting for the different feature selection methods. The feature set was limited to non-EEG features only.	72
4.10	The distribution of the selected features for valence classification in a cross-subject setting for the different feature selection methods. The feature set was limited to non-EEG features only.	73
6.1	The basic components of a BCI system[8]	78
6.2	Different parts of the P300 speller, found at [9].	79

List of Tables

1.1	total area of different houses and their corresponding asking prices.	7
1.2	Six different papers on emotion recognition, six different feature sets.	11
2.1	The available signals in the DEAP dataset.	14
2.2	An overview of the different features that were compared in this thesis.	20
2.3	suppose the following training examples for a decision tree.	35
2.4	Some feature are not significant on its own, but a might be part of a combination of features.	36
3.1	A comparison of the accuracy of different feature selection methods for arousal. The reported scores are test accuracies averaged over the different persons with their standard deviation..	41
3.2	A comparison of the accuracy of different feature selection methods for valence. The reported scores are test accuracies averaged over the different persons with their standard deviation.	42
3.3	This table gives the Pearson R correlation coefficients between the prediction probability and the distance between the level of arousal and the separation boundary, i.e. level 9 arousal lies at a distance —9-5— = 4, while an arousal of level 7 lies at distance 2. The assumption is that larger distances are easier to recognise, and thus be predicted with a higher confidence. The correlation should thus ideally be positive.	43
3.4	The average and standard deviation of the test accuracies (over the different persons) for the different feature sets, using the random forest feature selection model.	50
3.5	P-values for the comparison of the performance of different feature sets.	50
3.6	The region for each EEG channel	57
3.7	the region for each DASM and RASM channel pair	58
3.8	The region for each corresponding DASM and RASM channel pair.	59
3.9	The Jaccard index of two consecutive features sets for the random forest feature selection method. The indexes are averaged over all persons.	61
4.1	A comparison of the test accuracy of different feature selection methods for both arousal and valence. The reported scores are test accuracies averaged over	63
4.2	The correlations between the prediction probability of the different feature selection methods and the distance to the separation boundary.	65
4.3	The test accuracies for both arousal and valence, using different feature sets.	71
4.4	The Jaccard index of two consecutive features sets for the random forest feature selection method.	75

1

Introduction

This chapters introduces the masterthesis. It starts by introducing the basic concepts of emotion recognition based on physiological signals, machine learning. Then it explains the problem statement and the goal of the thesis, followed by an overview of the next chapters.

1.1 Emotion recognition

Human-to-machine communication, where humans communicate with machines or computer agents, is becoming more and more common[10]. Fully understanding human communication is a complex problem. In addition to verbal communication, non-verbal communication is also used to exchange information[11]. To better understand human-to-machine communication, more insight in the non-verbal communication is needed. Emotion recognition is becoming an increasingly important field as a result[12].

Emotion recognition is the proces of recognizing a subject's emotional state. In psychology a clear distinction between physiological behavior and the conscious experience of an emotion, called expression[13] is made. Expression consists of many parts, including facial expression, body language and voice concern[14]. Unlike expression, the physiological aspect of an emotion, e.g. heart rate, skin conductance and pupil dilation, is much harder to control. This makes emotion recognition based on physiological signals more robust to social masking[15]. Social masking is the process where an individual masks or hides their emotions to conform to social pressure. To really know one's emotions, it seems, one has to research the physiological aspect of the emotion.

Before emotions can be recognized, an objective class model describing different emotions is needed. A simple way of achieving this is using several discrete emotions, e.g. anger, joy, sad and pleasure. A more convenient model to classify emotions is the bipolar arousal-valence model[13, 12], which places emotions in a two dimensional space. The main advantage of using a continuous multidimensional model, is that all emotions are modelled in its space, even when no particular discrete label can be used to define the current feeling. Figure 1.1 shows the mapping of different emotions for this model.

The valence-arousal model consists of two dimensions. Arousal indicates how active a person is and ranges from inactive/bored to active/excited. The valence indicates if the emotion is perceived as positive or negative. Even though arousal and valence describe emotions quite well, a third dimension, dominance, can also be added. This third dimension indicates how strong the emotional feeling was and ranges from a weak feeling to an empowered, overwhelming feeling. The dominance component can aid to filter out samples of strong feelings, since feelings with low dominance are less likely to show significant effects.

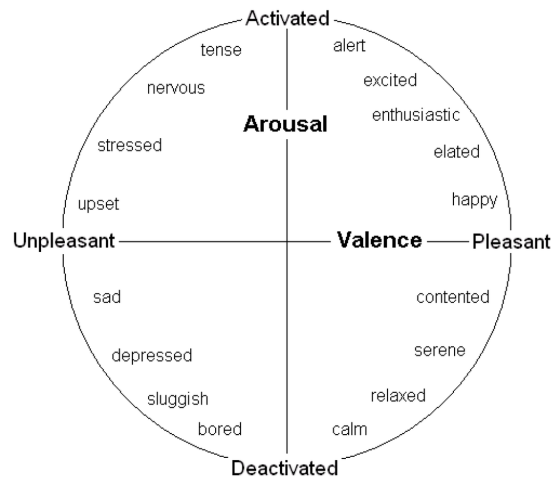


Figure 1.1: The arousal - valence model maps emotions in a two dimensional plane[1]

1.1.1 Physiological signals

Now that the classification model is defined, the different physiological signals will be explained. As mentioned before, these signals are used to do automatic emotion recognition. Physiological signals can be divided in two subgroups: brain activity and other signals, e.g. heart rate, respiration rate, etc. Different technologies exist to record brain activity. The most convenient method is electroencephalography (EEG), since it is a non-invasive method. Non-invasive methods, in contrast to invasive methods require no surgery. In case of EEG, they simply measure electrical activity using electrodes placed on the scalp.

Electrical activity in the brain is generated when an incoming signal arrives in a neuron. This triggers some sodium ions to move inside the cell, which in turn, causes a voltage rise[13]. When this increase in voltage reaches a threshold, an action potential is triggered in the form of a wave of electrical discharge that travels to neighbouring neurons. When this reaction occurs simultaneously in a lot of neurons, the change in electrical potential becomes significant enough, it is measured by the EEG surface electrodes. EEG can thus only capture synchronized activity of many, many neurons[13]. This explains why EEG signals have low spatial resolution capabilities. EEG measurements consist of electrical potentials of different channels, measured over time, like shown in Figure 1.2.



Figure 1.2: EEG measurements is a trace electrical potentials of different channels over time.[2]

Signals originating from the cortex, close to the skull, are easier to measure, while signals originating deeper in the brain cannot be observed directly. Even for signals originating close to the cortex, EEG is far from precise as the bone between the cortex and electrodes distorts the signal. Additionally, other artifacts like eye and muscle movement add a lot of noise to the signal. This explains why EEG signals are very noisy by nature. Noise removal techniques are therefore advised[16]. Note that even though EEG data contains a lot of noise and has a low spatial resolution, it still provides significant insight into the electrical activity of the cortex while offering excellent temporal resolution[17].

To ensure that experiments are replicable, standards for locations of electrodes have been developed. One of these systems is the 10/20 system, an internationally recognized method to describe the location of scalp electrodes[18]. The numbers 10 and 20 refer to the distances between the electrodes, which are either 10% or 20% of the total front-back or left-right distance of the scalp, this is depicted in Figure 1.3.

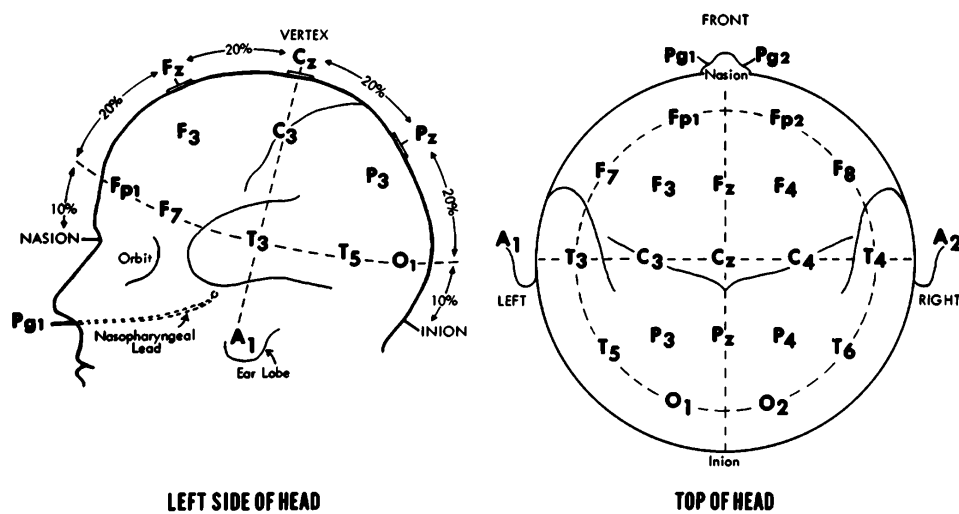


Figure 1.3: The electrode placement of a 23 channel system[3].

Each site is identified with a symbol that determines the lobe and a number that determines the hemisphere location.

- **F:** Frontal
- **T:** Temporal
- **C:** Central
- **P:** Parietal
- **O:** Occipital

Note that no central lobe exists; the C letter is only used for identification purposes. The letter z indicates that the electrode is placed on the central line. Even numbers are used for the right hemisphere, while odd numbers are used for the left hemisphere. Note that the 10/20 system does not require a fixed number of channels. Some experiments may use a different set of channels, but they all follow the same naming convention. In this work, a 32 channel EEG cap is used. The corresponding electrode locations are shown in Figure 1.4

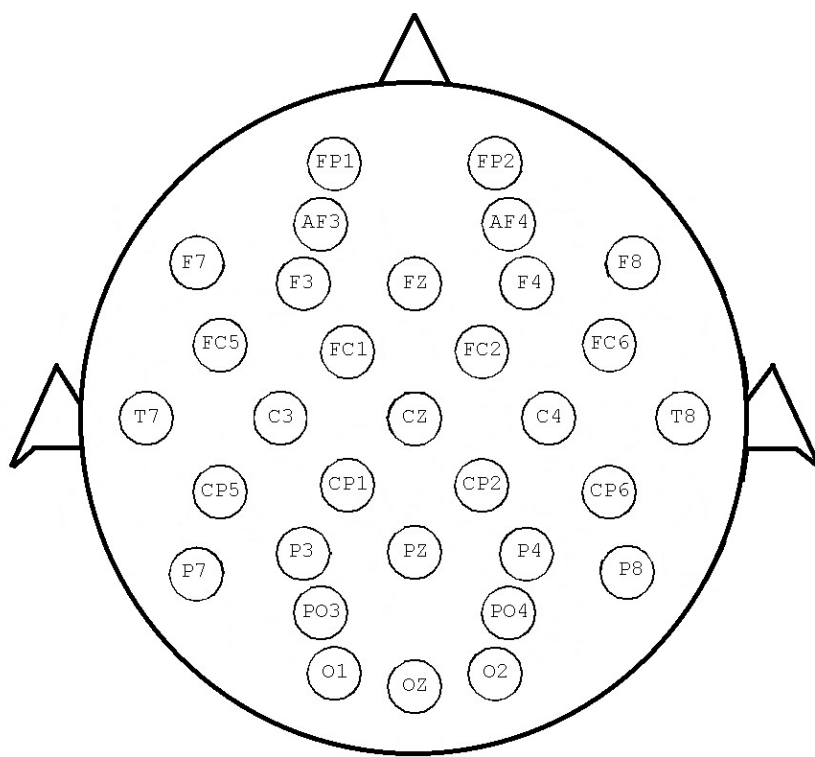


Figure 1.4: Placement of the 32 electrodes in this thesis.

In the frequency domain, brain waves are usually split up into different bands[11, 19], with a different medical interpretation for each band. These wavebands are:

1. **Alpha:** 8-13Hz, indicate how relaxed and/or inactive the brain is.
2. **Beta:** 13-30Hz, indicate a more active and focused state of mind.
3. **Gamma:** 30-50Hz, relate to simultaneous processing of information from different brain areas.
4. **Delta:** 0-4hz, these waves are generated during dreamless sleep and meditation.
5. **Theta:** 4-8Hz, occurs during dreaming.

Even though EEG is used in this thesis, alternative methods to measure brain activity exist. What follows is an overview of some of these techniques.

- Magnetoencephalography (MEG) use magnetic fields to measure brain activity[20]. Since MEG is more prone to noise from external magnetic signals, i.e. the earth's magnetic field and electromagnetic communication, a magnetic shielded room is required, making this method very expensive and not mobile.
- Functional magnetic resonance (fMRI) [21]: works by detecting changes in blood oxygenation and blood flow. An active area of the brain consumes more oxygen and has an increased blood flow.

- Computed tomography (CT) [22]: uses X-rays to create an image of the brain.
- Positron emission tomography (PET) [23]: this method uses trace amounts of short-lived radioactive material. When this material undergoes decay, a positron is emitted that is picked up by a detector.
- Near infrared spectroscopy (NIRS) [24]: an optical technique to measure blood oxygenation in the brain. This technique works by shining light in the near infrared part of the spectrum through the skull and measuring how much remerging light is attenuated.

In addition to brain activity, other physiological signals are also used in this work. The most known signal is the heart rate, which measures the number of contractions per minute. Respiration rate gives the number of breaths a human takes in one minute[6]. Another physiological signal is the galvanic skin response. The galvanic skin response measures the electrical characteristics of the skin[25, 6]. In addition to the electrical characteristics, the temperature of the skin can also be measured. A plethysmograph is another physiological signal, that measures changes in volume within an organ[6]. A plethysmograph can be used to measure a subject's blood pressure and heart rate.

1.2 Machine learning

Machine learning is the missing link between the physiological signals and the emotion recognition. It is, in short, an input output model, that takes physiological signals and maps them to an emotional state. Machine learning is a very broad domain. As a result, this discussion will be limited to an introduction of the basic machine learning concepts with the focus on the application of machine learning and machine learning techniques used in this thesis.

A possible definition for machine learning is: "the science of getting computers to act without being explicitly programmed"[26]. To do so, machine learning uses pattern recognition to find patterns or structure in the data. A simple example of machine learning is the Optical Character Recognition (OCR), where a computer recognises characters in pictures[27]. An example of OCR is shown in Figure 1.5.

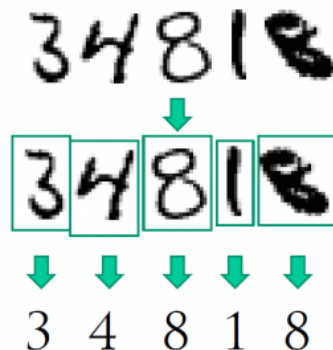


Figure 1.5: In optical character recognition, a computer uses machine learning to find characters in an image[4].

To further explain how machine learning works, have a look at the following example. Suppose one has a price list of houses that are for sale combined with their total area, shown in Table 1.1. Logic sense dictates us that a bigger house will have a higher price than a smaller house. The total area is a characteristic of the house that helps us in determining the price. In the context of machine learning, the characteristic 'total area', will be called a feature as the asking price of a house is correlated to the total area.

Table 1.1: total area of different houses and their corresponding asking prices.

Area of the house (m^2)	Price (x 1000 EUR)
70	312
73	429
76	174
79	410
82	334
:	:

One possible way of predicting the asking price of a house is machine learning. Machine learning works in several steps, first you train the machine learning algorithm with a list of asking prices and the corresponding area of the house. This process is called training or fitting and gives the machine learning component an idea to what price corresponds to a house with a certain area. Once trained, the algorithm's output will look like Figure 1.6. The black dots represent the data points from Table 1.1. The blue line represents the predicted price for different area. The predicted price is simply defined by the total area of the house multiplied by some weight.

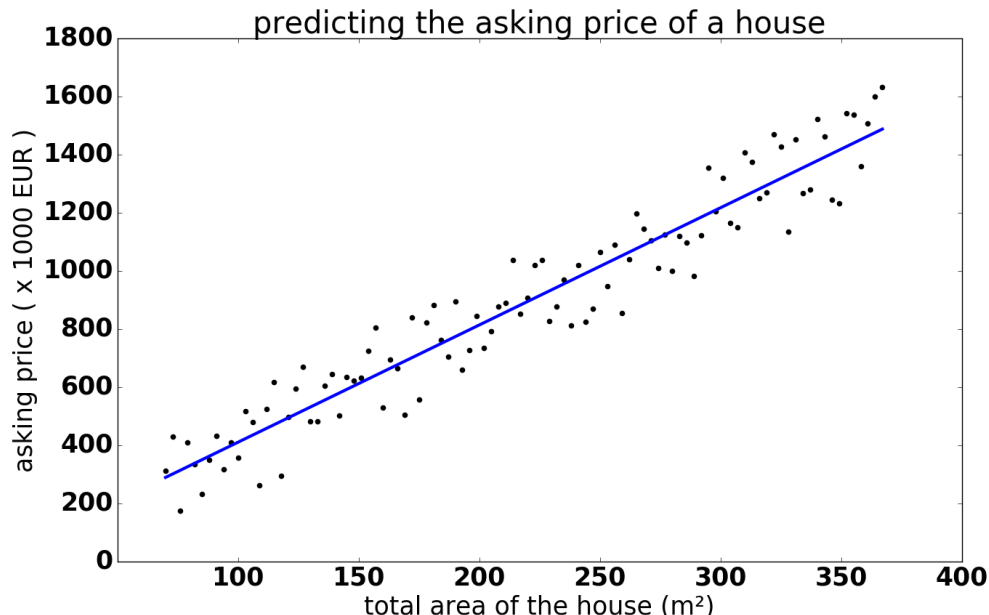


Figure 1.6: The price of a house is determined by its total area.

Even though, the blue line looks reasonable, there is sometimes a big difference between the predicted value and the actual value. This is due to the fact that the area of the house is only one feature that determines the price. Other features, like the number of bedrooms or the location of the house, were not taken into consideration. Adding additional features, gives more insight into the data, e.g. a house with 5 bedrooms is more expensive than a house with only 3 bedrooms. Having more features is thus likely to improve the performance of the machine learning algorithm.

There are many machine learning algorithms. One way to group these algorithms is to look at the produced output. In the asking price examples above, the output is a price, which is (more or less) a continuous value. Machine learning problems that require the output of a continuous value, are called regression problems[28]. In the OCR example above, a picture of a character is classified as a character. This means that OCR is a classification problem, as there are only a limited number of characters in an alphabet[28].

Another way to group algorithms is based on their training data[28]. In the asking price examples above, the training data consists of labelled results. Labelled training data corresponds to data where the correct output (in this case the asking price) is given for each input (the area). This type of machine learning is referred to as supervised machine learning[28]. The alternative is unsupervised machine learning[28]. Unsupervised learning often results in finding groups of similar data points (clustering), without knowing the actual labels. Note that the combination of supervised and unsupervised data, known as semi-supervised learning, is also possible[29]. Imagine a dataset with 5000 webpages that need to be grouped into 10 distinct categories, e.g. science, nature, cooking, Only 100 of the 5000 pages in the train set are labelled. An approach to solve this problem could be to first cluster the pages in similar groups using unsupervised learning. As soon as a group contains a single labelled page, all pages in the group can be labelled accordingly. This is possible because clustering returns groups of similar samples. Semi supervised learning has the advantage that one can also use unlabelled data, which is often easier and cheaper to obtain, unlike labelled data which is usually quite rare; if there was a fast and easy way to label the data then there would not be a need for machine learning.

1.2.1 Over- and underfitting

Over and underfitting is a common problem in many machine learning projects[28]. Suppose the example in Figure 1.7, where one tries to find a good function to fit the given data points. The green line corresponds to the generator function, the 'actual' function that generated the outputs. The blue line is the line represents the machine learning algorithm's fit of the data. Looking at the three proposed functions, one can easily see that the middle figure corresponds to the best fit of the sample points.

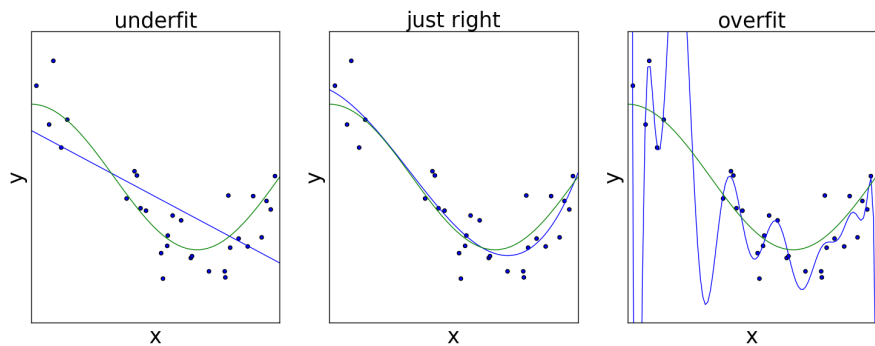


Figure 1.7: Overfitting versus underfitting[5].

The figure on the left corresponds to an underfit, where the proposed function is not able to capture sufficient detail of the points. The function is not complex enough to approach the generator function. As a result the best fit will always contain a relatively big error.

The function on the right corresponds to an overfit. The function is trying too hard to fit each point exactly, which results in low train error for these data points. However, one can see that the behaviour of the hypothesis function in between data points is not what one would expect. This is the result of using a too complex function to fit the data. As a result the error is very low error for these points.

Part of a good machine learning algorithm is finding the right tradeoff between overfitting and underfitting. In case of the aforementioned overfitting, it would be better to lower the performance of the algorithm on the sample datapoints, to gain performance on the 'unseen' datapoints. Different techniques exist to estimate how good an algorithm performs on unseen points. To evaluate how good a designed machine learning algorithm performs on unseen data a part of the sample points is put in a test set. This test set is neglected during training and only used after the training of the algorithm is complete. The performance on the test set will indicate how well the algorithm generalises, since these are all unseen points. It is only the performance of the test set that gives a fair estimation of the performance of a machine learning algorithm.

Sometimes it might be important to estimate generalisation during training to prevent overfitting. One way to do this, is cross validation. Cross validation (CV) is a technique that separates the data in N folds, as shown in Figure 1.8. The algorithm is then trained on N-1 blocks and tested on the remaining blocks. This is done N times and the average of the performance is then reported as cross validation error. Note that the test set, displayed in red, is not used during cross validation. The test set is kept completely separate to ensure that a fair estimate of the generalisation is achieved.

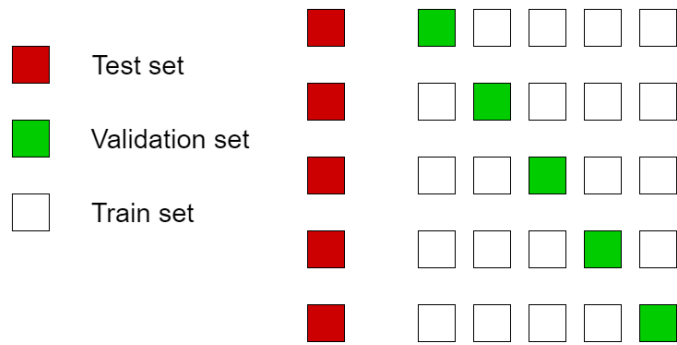


Figure 1.8: Cross validation

1.2.2 Feature selection

Feature selection is a technique that aims at selecting the features that perform well, while trying to remove irrelevant features[30]. The advantages of having a smaller features set are twofold. First having fewer features, will lower the risk of overfitting[30]. Second, knowing which features are important makes it possible for humans to interpret the machine learning model. In this thesis, knowing which features are relevant might help in gaining insight in the processing of emotion by the brain.

There exist several approaches to do feature selection. The first one is to simple use a statistical metric and remove all features with low correlation to the output. Another approach is to look at the weights of a model. When a machine learning model gives a large weight to a feature, then that feature is considered more important than a feature with an assigned weight close to zero. Embedded methods also exist, they rely on the build in feature selection mechanisms of some machine learning algorithms. A more thorough overview of the different feature selection techniques is given in Section 2.4.

1.3 Problem statement

A lot of different physiological features are reported in the literature. Unfortunately, the literature does not fully agree on a specific set of features nor does it agree on what EEG channels and/or frequency bands are most important for emotion recognition. The features that are reported in different studies are often quite different, as you can see in Table 1.2 below.

Table 1.2: Six different papers on emotion recognition, six different feature sets.

study	features used
[31]	Alpha and beta power
[32]	PSD and asymmetry features
[33]	PSD
[34]	discrete wavelet transform of alpha, beta and gamma band
[13]	alpha/beta ratio, Fpz beta and alpha band power
[35]	PSD, RCAU, DCAU, DASM, RASM, DE

Another related problem with physiological signals is that they are very personal by nature. Features that work well for one person might not work well for another person[6]. Finding a set of features that works well for all persons is hard, but it might make the system more robust against personal differences.

The last problem is that is hard to compare the performance of different physiological feature studies, as they do not share the same dataset.

1.4 Goal of the thesis

The first goal is finding relevant features for emotion recognition in a person specific setting. This is already quite challenging as there are fuzzy boundaries and individual variation of emotion[36]. To do so, the output of different feature selection methods is compared. In a successful scenario, good features are found. These features could be used by a machine learning algorithm to accurately predict the emotions of one person. Some attention will also be spend on comparing non-EEG and EEG features to see which whether it is useful or not to include EEG and/or non-EEG signals in the emotion recognition.

The second goal is finding features for emotion recognition in a cross-subject setting. In this setting features should generalise well across different persons, thus the algorithm should be able to recognize emotions from unseen persons. The comparison for non-EEG and EEG features will also be done here. Emotion recognition is harder in a cross-subject setting, since physiological signals are very personal[6].

Both goals are tackled by comparing a large range of different feature selection methods combined with a huge feature set. Additionally, the accuracy on the DEAP, a dataset designed to compare different emotion recognition studies[6] will be reported. This will ensure that the results obtained in this thesis can serve as a benchmark for future research. This is important as performance of emotion recognition algorithms based on physiological signals often varies a lot for different datasets[15].

The contents of this thesis are as follows. The next chapter gives an overview of the dataset, features and feature selection methods that are used in this thesis. It also gives an overview of similar state of the art emotion recognition studies.

Chapter 3 and 4 give an overview of the obtained results for person specific and cross-subject emotion recognition respectively. Chapter 5 gives the conclusion of this work. Chapter 6 gives an overview of future research that is possible.

2

Methods

This chapter starts by explaining the used dataset and features. Next some state of the art methods are briefly discussed, to give an idea of similar research. After that the contributions of this thesis are explained. Next different feature selection methods are explained. The last part of this section explains the used approach in this thesis.

2.1 Dataset

One of the most used datasets in the context of emotion recognition is the Dataset for Emotion Analysis using Physiological Signals (DEAP)[6]. This dataset consists of several parts, the first part is a rating of 120 music videos by 14 - 16¹ persons. Each video is rated for valence, arousal and dominance on a scale ranging from 1 to 9 using self-assessment manikins (see later). This part of the dataset is not used during this thesis, because it contains no physiological signals.

The next part of the dataset is the physiological experiment that contains emotional reactions of 32 subjects. The emotional reactions were triggered using music video excerpts. Each subject watched 40 one-minute videos, while several physiological signals were recorded. These physiological signals consist of 32 channel, 512Hz EEG signals combined with peripheral physiological signals like respiration rate, skin temperature, etc. More concretely, this dataset contains following signals:

¹2 persons did not complete all the necessary ratings.

Table 2.1: The available signals in the DEAP dataset.

Channel	Name	Category	Channel	Name	Category
1	Fp1	EEG	21	F8	EEG
2	AF3	EEG	22	FC6	EEG
3	F3	EEG	23	FC2	EEG
4	F7	EEG	24	Cz	EEG
5	FC5	EEG	25	C4	EEG
6	FC1	EEG	26	T8	EEG
7	C3	EEG	27	CP6	EEG
8	T7	EEG	28	CP2	EEG
9	CP5	EEG	29	P4	EEG
10	CP1	EEG	30	P8	EEG
11	P3	EEG	31	PO4	EEG
12	P7	EEG	32	O2	EEG
13	PO3	EEG	33	hEOG	non-EEG
14	O1	EEG	34	vEOG	non-EEG
15	Oz	EEG	35	zEMG	non-EEG
16	Pz	EEG	36	tEMG	non-EEG
17	Fp2	EEG	37	GSR	non-EEG
18	AF4	EEG	38	respiration belt	non-EEG
19	Fz	EEG	39	plethysmograph	non-EEG
20	F4	EEG	40	skin temperature	non-EEG

A preprocessed version of the physiological experiment database is also available. In this version, the EEG recordings were downsampled to 128Hz and noise and EOG artifact removal was performed. A bandpass filter was applied to filter out frequencies below 4Hz and above 40-45Hz. This was done to remove noise, since most muscle and eye artifacts have a frequency around 1.2Hz and artifacts caused by nearby power lines, have a frequency around 50Hz[13]. This thesis uses the preprocessed version of the DEAP since it is the most practical version to use.

Additionally facial video for 22 of the 32 subjects was recorded, so research of facial expressions is also possible with this dataset. All videos are rated on 4 scales: arousal, valence, dominance and liking. The liking component indicates how much each person liked each video excerpt. It is important not to confuse the liking component with the valence component, as it inquires information about the participants' tastes, not their feelings. For instance, a person can like a video that triggers angry or sad emotions². The liking rates are mentioned here for completeness and are not used in this work as they are not part of the emotion space.

For assessment of these scales self-assessment manikins (SAM) were used[6]. SAM visualizes the valence, arousal and dominance scales with pictures. Each picture corresponds to a discrete value. The user can click anywhere in between the different figures, which makes the scales continuous. All dimensions are given by a continuous value between 1 and 9. This thesis focusses on a classification problem, rather than a regression problem. As a results, the valence and arousal are divided into low and high valence/arousal, using binary classification. All valence

²However strong correlations between the liking and valence ratings were observed[6].

or arousal values above 5 are labelled as high valence/arousal respectively. The other values are labelled as low valence/arousal.

The used SAM figures are shown in Figure 2.1. The first row gives the valence scale, ranging from sad to happy. The second row shows the arousal scale, ranging from bored to excited. The last row represents the different dominance levels. The left figure represents a submissive experience, while the right figure corresponds with a dominant experience.

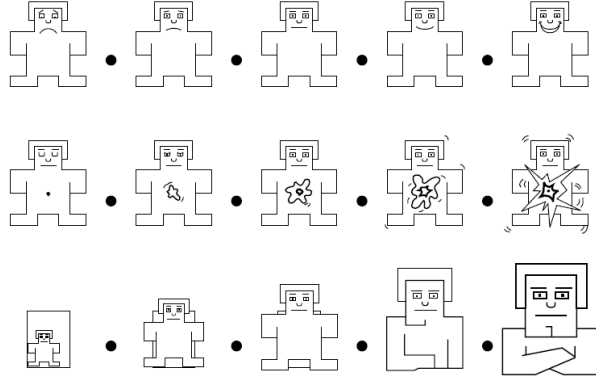


Figure 2.1: The images used for the SAM[6].

2.2 Features

Machine learning algorithms require good features to perform well³. In the context of this thesis, good features should be correlated with the subject's emotional state. Two categories of features are observed in this work: EEG features and non-EEG features. Both categories are covered in the following sections.

2.2.1 EEG-features

EEG features are extracted from the electroencephalography measurements from the subject's scalp. From these signals a lot of different signals can be extracted. The power spectral density (PSD) of a signal gives the distribution of the signal's energy in the frequency domain. By calculating the spectral density for different frequency bands of the signal, one can determine how much power of each frequency band is in the signal.

Differential entropy (DE) is defined as follows [35]

$$DE_{channel} = - \int_{-\infty}^{\infty} \frac{1}{\sqrt{2\pi\sigma^2}} \exp\left(\frac{(x-\mu)^2}{2\sigma^2}\right) \log\left(\frac{1}{\sqrt{2\pi\sigma^2}}\right) \exp\left(\frac{(x-\mu)^2}{2\sigma^2}\right) dx$$

It is proven that the differential entropy of a certain band is equivalent to the logarithmic power spectral density for a fixed length EEG sequence[38]. This simplifies the calculations significantly.

$$DE_{channel} = \log(PSD_{channel})$$

³There are some exceptions, for instance some types neural networks are capable of 'designing' their own features[37]. But these algorithms were not used in this thesis.

The most used feature for valence recognition is the frontal asymmetry of the alpha power[17]. The right hemisphere is generally speaking, more active during negative emotion than the left hemisphere. The left hemisphere is in turn more active during positive emotions[12, 39, 35]. The asymmetry can be calculated in different ways. First, one can calculate the differential asymmetry (DASM) , where the left alpha power is subtracted from the right alpha power.

$$DASM = DE_{left} - DE_{right}$$

Another way to measure the asymmetry is by division. The Rational Asymmetry (RASM) does exactly this and is given by:

$$RASM = \frac{DE_{left}}{DE_{right}}$$

With DE_{left} and DE_{right} being the left and right differential entropy respectively. Another reported feature in literature is the caudality, or the asymmetry in fronto-posterior direction[40]. Caudality measures the difference in power between the front and the back of the scalp. This can again be calculated in two ways. The first method is the differential Caudality (DCAU) , defined as:

$$DCAU = DE_{front} - DE_{post}$$

The second method to determine the Caudality is the Rational Caudality (RCAU) , which is defined as:

$$RCAU = \frac{DE_{front}}{DE_{post}}$$

With DE_{front} and DE_{post} being the frontal and posterior power respectively. Arousal is usually determined, by looking at the different frequency bands[13]. Each frequency and has their own medical interpretation, see 1.1.1. Alpha power corresponds to a more relaxed brain, while Beta power corresponds to a more active brain. The alpha / beta ratio therefore seems a good indicator for the arousal state of a person.

The Alpha/ Beta ratio is limited to comparing two frequency bands. Other frequently used features are fractions of PSD. These fractions indicate what proportion of power a certain frequency band has. They are defined for a channel, given by:

$$frac_{band,channel} = \frac{power_{band,channel}}{power_{total,channel}}$$

These fractions give insight in the distributions of wavebands at different channel locations.

2.2.2 non-EEG features

The aforementioned EEG features are just one class of physiological features, the DEAP dataset contains several other physiological measurements[6]. For each of these measurements the average, standard deviation, variation, median, minimum and maximum are calculated.

The Galvanic Skin Response uses two electrodes on the middle and index finger of the subjects left hand to measure the skin resistance. The skin resistance is one way to measure the perspiration of a subject. It has been reported that the mean value of the GSR is related to the level of arousal[25, 6].

The respiration belt (RSP), indicates the user's respiration rate. Slow respiration is linked to relaxation (low arousal). Fast and irregular respiration patterns corresponds to anger or fear, both emotions have low valence and high arousal[6].

A plethysmograph is a measurement of the volume of blood in the subject's left thumb. This can be used to determine the blood pressure of a subject. Blood pressure offers valuable insight into the emotional state of a person. For instance, stress is known to increase blood pressure[6].

The heart rate is not directly available in the DEAP dataset. fortunately, it can be extracted from the plethysmograph, by looking at local minima and maxima[6]. This is visible when looking at the plethysmograph's output, shown in Figure 2.2.

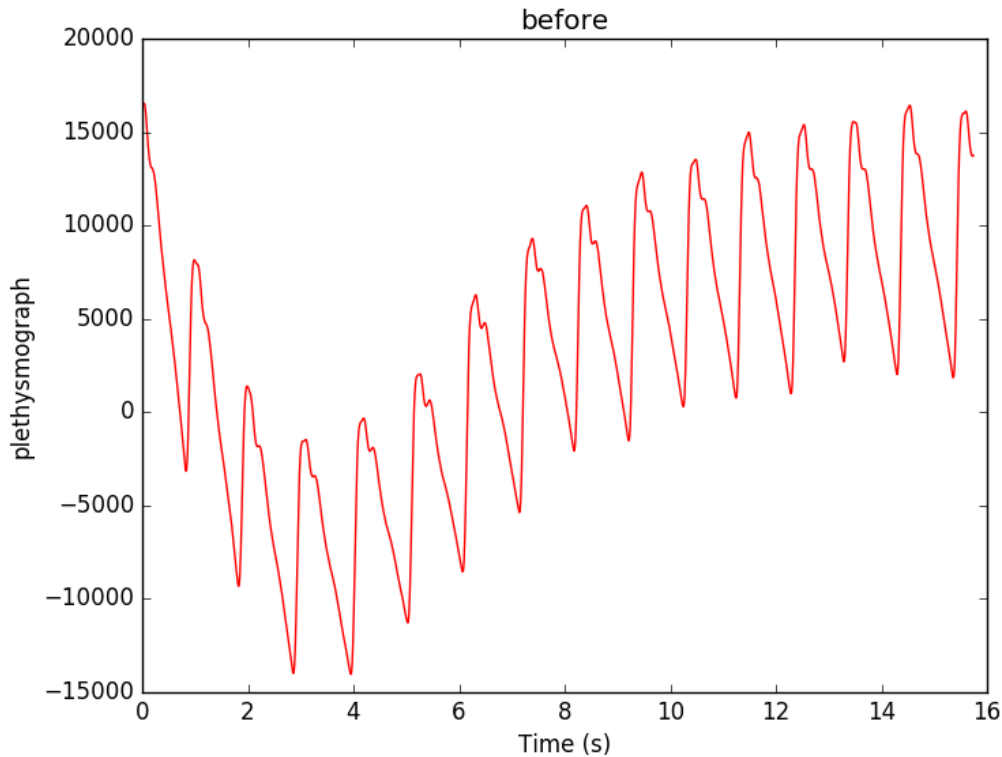


Figure 2.2: The plethysmograph before smoothing.

The heart rate extraction is done in two steps. In the first step the plethysmograph's output is smoothed to filter out high frequency components. This is done to avoid that noise is selected as a local optima. In the second step the local extrema are located, as shown in Figure 2.3

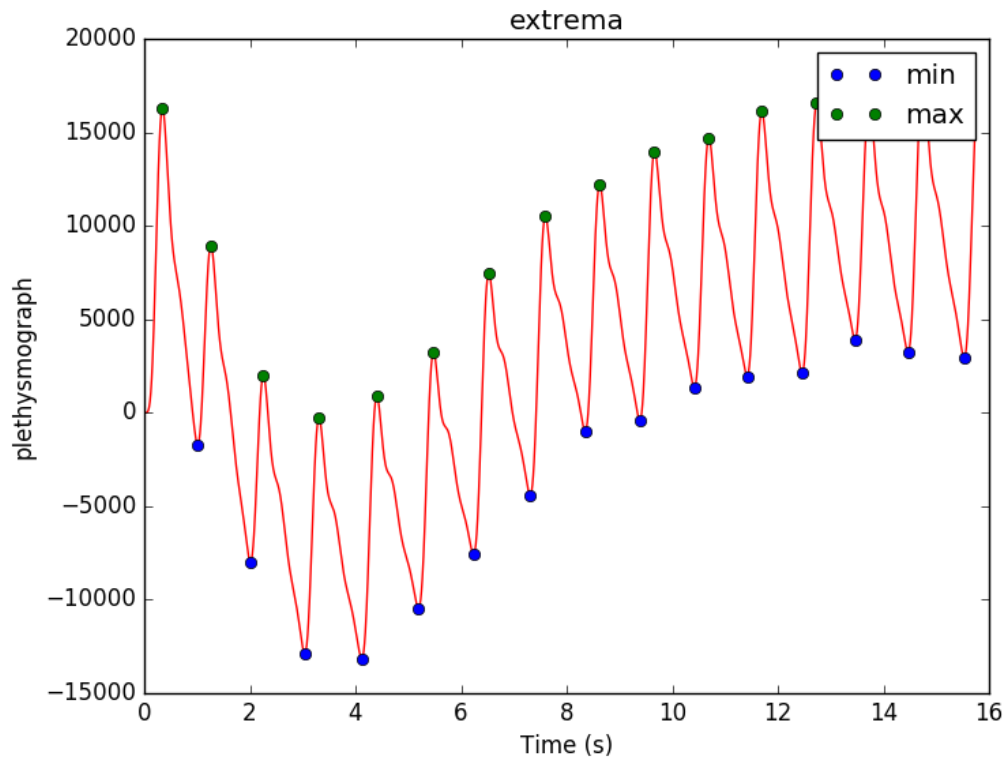


Figure 2.3: The local optima in the plethysmograph.

The combination of a local minimum and maximum correspond to a heart beat[6]. Therefore, the time between two consecutive local minima or maxima correspond to the time between two heart beats, known as the interbeat interval. Getting the average heart rate from the interbeat interval is straight forward. Lastly, the skin temperature of the subject is also available.

2.2.3 Overview

Table 2.2 gives an overview of the different feature types and their sizes. The 32 EEG channels can be found in Table 2.1. As mentioned in Section 1.1.1, there are 6 frequency bands: Alpha, Beta, Gamma, Delta, Theta and All. All refers to taking the total power of a channel. Note that the fractions only have 5 different frequency bands, as the percentage of all power would always be 100%.

Table 2.2: An overview of the different features that were compared in this thesis.

Name	Type	no. Channels	no. Frequency bands	Total
PSD	EEG	32	6	192
DE	eeg	32	6	192
DASM	eeg	13	6	78
RASM	eeg	13	6	78
DCAU	eeg	11	6	66
RCAU	eeg	11	6	66
Frac	eeg	32	5	160
Alpha / Beta	eeg	32	1	32
EEG Total				864
Name	Type	no. Statistics		
HR	non-eeg	6		
Plethysmograph	non-eeg	6		
GSR	non-eeg	6		
ST	non-eeg	6		
RSP	non-eeg	6		
non-EEG Total		30		
Overall Total		894		

The feature set has a size of 894, which is huge considering that there are only 40 samples for each person. Using this many features in combination with the low sample count, will quickly result in overfitting[28]. To solve this problem, one can either increase the number of samples or decrease the number of features. Increasing the number of samples is hard. Since EEG data is very personal [6], several recordings of the same subjects are required.

Reducing the feature set in size is another possibility. Two methods exists, dimension reduction and feature selection. The difference between dimensionality reduction and feature selection is that dimensionality reduction methods consider all information in the feature space. Feature selection methods, on the other hand, take a subset of the information[15].

This problem is even more severe in cross-subject emotion recognition system. Here, it is not possible to simply take a limited subset of features. Physiological signals are very personal by nature [6]. Selecting features that work for one person, might therefore not work well on different persons.

2.3 State of the art

This section will give an overview of similar studies and their conclusions. Some of these studies also did some research on cross-subject emotion recognition. Emotion recognition is still in its infancy[36] and subject independent features are hard to find [6]. Therefore, research is aimed more towards person specific emotion recognition systems.

2.3.1 DEAP method

The first method of emotion recognition is the DEAP method, described in the DEAP paper[6], the paper that introduces the DEAP dataset used in this thesis. The research found that Valence shows the strongest correlations with the EEG signals. Additionally the study found correlations in all frequency bands, with an increase in power for the lower range wavebands for an increase in valence. These effects occur in the occipital regions of the brain, above the visual cortices. This might indicate that the subject is focussing on a pleasurable sound. A central decrease in beta power was observed together with a occipital and right temporal increase in power for positive emotions. The research conclude that these observed correlations concur with other neurological studies. The absolute value of the correlations are seldom bigger than 0.1 for a cross person setting. This indicates that cross person emotion recognition is a non trivial problem. The absolute values of the person specific correlations were around 0.5.

The DEAP paper also propose their own classification method for person specific emotion classification. They start by performing feature selection using the Fisher's linear discriminant for feature selection. The Fisher's linear discriminant is defined as:

$$J(f) = \frac{|\mu_1 - \mu_2|}{\sigma_1^2 + \sigma_2^2}$$

With μ and σ being the mean and standard deviation of feature f. The Fisher's discriminant was calculated for each feature, before a threshold of 0.3 was applied to filter out irrelevant features. The used classifier was a Naive Bayes classifier, which assumes independence of features. The Naive Bayes classifier is a simple classifier that uses the following equation:

$$G(f_1, \dots, f_n) = \operatorname{argmax}_{cp}(C = c) \prod_{i=1}^n p(F_i = f_i | C = c)$$

With F being the set of features and C the classes. $p(F_i = f_i | C = c)$ is estimated by assuming Gaussian distributions of features and modelling these from the training set.

2.3.2 Stable emotion recognition over time

EEG patterns are not only subject dependent, they are also dependent on the subjects mood and thus might vary in time[35]. This work starts by researching different EEG features: PSD, DE, DASM, RASM, DCAU, RCAA⁴. The different features are tested on the DEAP dataset. Afterwards, they develop a new dataset, where subjects have repeated trial sessions with some time in between. This dataset is then used to measure the performance of their time independent, subject specific, emotion recognition system.

⁴Note that these features are explained in more detail in Section 2.2.

Their machine learning set-up is as follows, first they perform feature extraction of the aforementioned features. Then feature smoothing is done using a Linear Dynamic system (LDS) , that can be expressed by:

$$\begin{aligned} x_t &= z_t + w_t \\ z_t &= Az_{t-1} + v_t \end{aligned}$$

x_t denotes the observed variables or features, while z_t denotes the hidden emotion variables. A is a transformation matrix and w_t is Gaussian noise. The need for a linear dynamic system is supported by the assumption that emotion change gradually over time. The LDS filters out components that are not associated with emotional states.

The list of features at this point is too big and may contain uncorrelated features that might lead to performance degradation of the classifier. Two methods for this are compared, principal component analysis (PCA) and minimal redundancy maximal relevance (MRMR).

PCA uses an orthogonal transformation to create a lower dimensional feature space starting from the original higher dimensional feature space. It does so by minimizing the loss of information, i.e. the principal component should have the largest possible variance. PCA is explained later in Section 2.4.3.

PCA cannot preserve original domain information like channel and frequency, therefore the paper also uses the MRMR method. MRMR uses mutual information in combination with maximal dependency criterion and minimal redundancy. The algorithm starts by searching features satisfying:

$$\max D(S, c), D = \frac{1}{|S|} \sum_{x_d \in S} I(x_d; c)$$

Where S is the feature subset to select. When two features are highly correlated, the maximal dependency is not likely to change when one of the correlated features is removed. This is expressed by the minimal redundancy condition.

$$\min R(S), R = \frac{1}{|S|^2} \sum_{x_{di}, x_{dj} \in S} I(x_{di}, x_{dj})$$

The two conditions are then combined to form the Maximal Relevance Minimum Redundancy, which can be expressed as:

$$\max \varphi(D, R), \varphi = D - R$$

Note that incremental search methods exists and are often used in practice. After performing the dimensionality reduction, the samples from the DEAP data set are classified in high / low valence and high/low arousal, giving a total of four classes. All values close to the separation border are removed from the training data, as they might confuse the classifier.

For the classification, three conventional and one newly developed pattern classifiers were compared. k-nearest neighbors (KNN) , logistic regression (LR), Support Vector Machines (SVM) and Graph regularized Extreme Learning Machine (GELM) . Extreme Learning Machine (ELM) is a single layer feed forward neural network[41]. GELM is based on the idea that similar shapes should have similar properties and obtains better results for face recognition [42] and as the paper concludes, also for emotion classification.

The study found then performed a study on the different features and concluded that DE features are the most suitable EEG features, followed by the asymmetry features (RASM, DASM, DCAU and RCAAU). The LDS smoothing was also found to be the better feature smoothing method.

2.3.3 EEG-based emotion recognition in music listening

This study[36] uses EEG features to recognize 4 different discrete emotions (joy, anger, sadness, pleasure) induced by music. They compared four different feature sets on 6 different wavebands: RASM and DASM of 12 channelpairs, raw PSD of the 24 channels and PSD of 30 channels (including 6 midline channels). The compared set of wavebands consists of: alpha, beta, gamma, delta, tetha and all wavebands. These features were fed to two different classifiers, one Multilayer perceptron (MLP) and an SVM.

Their main results were that the DASM features worked better than the RASM features and even better than using the corresponding 24 PSD features. They also did research to person independent EEG features and found that their accuracy remained consistent. Note that while these results sound promising, they were unfortunately not performed on the DEAP dataset. Performance of emotion recognition algorithms is known to vary a lot between datasets[15].

2.3.4 Comparing selected methods for feature extraction and classification

In this comparative study four distinct emotions (joy, anger, sadness and pleasure) were classified [15]. The emotions were triggered by songs that were selected for each subject. The subjects were instructed to select songs themselves, that trigger memories. These memories should in turn, trigger the desired emotions. The four emotional states were mapped in the valence-arousal model. The used features were typical statistical values of physiological signals (Skin Conductivity (SC), Electrocardiogram (ECG), Electromyography (EMG) and Respiration rate (RSP)).

Several feature selection techniques were compared. The first one is the analysis of Variance (ANOVA) where the best D features were taken. Sequential forward selection (SFS) , where the algorithm starts with an empty feature set and then introduces a new feature in each iteration. Sequential backward selection (SBS) is an alternative, where a feature is removed in each iteration. These feature selection methods were also compared to two dimensionality reduction methods: PCA and Fisher projection.

The newly formed feature space was then fed to three different classifiers: K-nearest neighbors, Multilayer perceptron and Linear discriminant function. The results indicated that it is easier to classify arousal than valence. This might indicate that non-EEG features might be features for arousal classification, as this work only contains non-EEG features. SFS in combination with

fisher seems to give the best classification performance, closely followed by LDF and ANOVA, a less computationally intensive method.

The paper also concludes that joy was characterized by a faster heart rate, while sadness was identified by low SC and EMG signals. There was also a higher breathing rate for negative valence emotions. They reported limited similarities for the selected features between subjects.

2.3.5 Advanced RF feature selection

One advanced method for feature selection is the two-step method using random forest[30]. There are two possible motivations for feature selection. The first motivation is to do interpretation, find out which features are important and use them for research. In the context of this work, feature interpretation could help neuroscientist find out which parts of the brain are affected by emotion. The second motivation is to improve machine learning techniques. Having fewer features will not only speed up training and prediction times, it also reduces the complexity. Reducing complexity often has a good influence on the generalisation property of a machine learning algorithm[28, 30]. Additionally in the context of EEG data gathering, using fewer electrodes means less preprocessing time; mounting 32 electrodes to the brain of a subject is a time consuming task.

The selection procedure itself consists of two steps. In the first step, data is fitted to a random forest and the importance values for each feature are determined. The importance values are then averaged and the standard deviation of the importances over all trees is calculated. All features are then ranked based on their importance ranking. Next features with small importance values are cancelled.

Then, depending on the motivation of feature selection, one of two possible second steps is performed. For feature interpretation the second step starts by fitting a random forest using a single feature. The OOB is then averaged over multiple runs. The runs are needed because a random forest has an element of randomness; fitting the same data twice to a random forest, will not give you the same random forest. To get an accurate estimate of the performance of a random forest, fitting the data several times is required. The average OOB score and its standard deviation is then used to determine an initial OOB score.

$$OOB_{init} = AVG(OOB) - STD(OOB)$$

The standard deviation is used to avoid noisy results. This means that a result is only regarded as better, when it is better from a statistical point of view. Next features are added iteratively, when a larger features set has a better average OOB score (taking the standard deviation into account), the feature set is replaced by the larger feature set. Note that the whole set of features is always considered; it is not possible to leave a feature out and include the next feature.

The other possible second step is used for prediction, here the algorithm starts similarly, by determining an initial average OOB score and standard deviation. The idea behind the standard deviation is the same as with the interpretation step, noise removal and stability.

$$OOB_{init} = AVG(OOB) - STD(OOB)$$

The next part is different, in each iteration a feature is introduced. When the average OOB score and standard deviation of the feature are better, the feature is added to the feature set, otherwise it is neglected. This is a greedy forward selection algorithm, once a feature is selected, it remains selected. The difference between the interpretation and prediction step is that here single features are added to the feature set, while step two-interpretation always takes the whole feature set, meaning all features before the last feature, as a replacement. The prediction version of step two is able to select a distinct set of features out of the results from step one.

In the end the paper notes several observations, the step two-prediction method provides better OOB scores using fewer features. Additionally they mention that highly correlated features might confuse the algorithm, as correlated features have lower importances.

2.4 Feature selection methods

Feature selection is the process of selecting good features from a set of features. The need for this is twofold: first reducing the number of features, is a protection mechanism against overfitting[30]. This is important when a smaller dataset is used. Second, reducing the number of features can speedup the learning process of a learning algorithm as fewer parameters need to be optimized. Additionally, in the context of research, looking at which features are important might give more insight in how emotion is processed by the brain. For example, knowing what features are relevant can help neuroscientists understand the working of the brain better. There is also a practical use of feature selection, limiting the physiological signals to fewer channels, can help the set-up time. Mounting an EEG cap to a subject is a time consuming process. Using fewer electrodes can make the system more convenient to use as it would save time.

Several approaches for feature selection exists: filter methods, wrapper methods and embedded methods. What follows is an explanation of how each approach works, combined with the used methods of each approach in this thesis.

2.4.1 Filter methods

Filter feature selection methods use an independent metric or statistical test to filter out features with low importance. The most simple example of to simple look at the correlation between each feature and the output. Afterwards, all features with low correlation can be removed.

Pearson correlation

The Pearson correlation coefficient measures the linear relationship between two variables. The output is a value r , that lies between -1 and 1, corresponding to perfect negative correlation and perfect positive correlation respectively. A correlation value of 0 means that there is no correlation.

More formally[43], the Pearson product-moment coefficient of correlation, r between variables X_i and Y_i of datasets X and Y is defined as:

$$r = \frac{SS_{xy}}{\sqrt{SS_{xx}SS_{yy}}}$$

with

$$SS_{xy} = \sum_i (X_i - \tilde{X})(Y_i - \tilde{Y})$$

and

$$\begin{aligned} SS_{xx} &= \sum_i (X_i - \tilde{X})^2 \\ SS_{yy} &= \sum_i (Y_i - \tilde{Y})^2 \end{aligned}$$

The Pearson correlation coefficient is fast and simple to calculate, but has some major shortcomings. First off, it can only see linear relationships and will not see the correlation between a value x and x^2 .

In the context of this thesis, whether the correlation is positive or negative is not important; a learning algorithm needs features that have a significant correlation. As a result the absolute value of the r value is used as this allows for a more convenient comparison of correlations.

Normalized mutual information

Mutual information is a more robust option for correlation estimation. The mutual information, MI, of two variables X and Y is defined as [44]:

$$MI(X, Y) = \sum_{y \in Y} \sum_{x \in X} p(x, y) \log\left(\frac{p(x, y)}{p(x)p(y)}\right)$$

Using the mutual information directly for feature ranking might be inconvenient because its results does not lie in a fixed range. Fortunately, normalized variants of the mutual information score exists. The normalized mutual information, NMI, of variables X and Y is given by:

$$NMI(X, Y) = \frac{I(X, Y)}{\sqrt{H(X)H(Y)}}$$

With $H(X)$ and $H(Y)$ being the Shannon entropy of variable X and variable Y , defined as:

$$\begin{aligned} H(X) &= \sum_{i \in X} p_i \log\left(\frac{1}{p_i}\right) = -\sum_i p_i \log(p_i) \\ H(Y) &= \sum_{i \in Y} p_i \log\left(\frac{1}{p_i}\right) = -\sum_i p_i \log(p_i) \end{aligned}$$

Distance correlation

Distance correlation solves some shortcomings the Pearson correlation has. The Pearson correlation coefficient might give a correlation of zero for dependent variables, as shown in Figure 2.4.

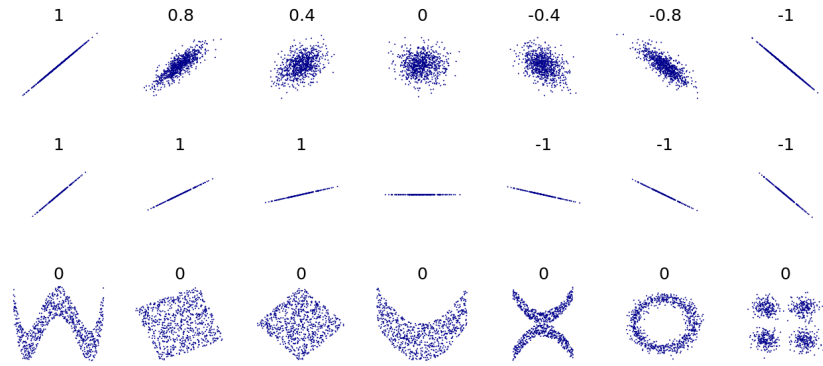


Figure 2.4: Pearson correlation coefficients for different sets of (x,y) points. Note that many coefficients are zero, while there clearly is some correlation. Source: Wikipedia

The distance covariance, sometimes referred as the Brownian covariance, addresses this problem[45]. Its main idea is that a good measurement for dependence is the 'distance' between the joint distribution f_{XY} and the product of the marginal distributions f_X and f_Y weighted by a weight function W . This gives the following theoretical function:

$$dCorr_{X,Y} = W(||f_{XY} - f_X f_Y||)$$

The result is that the distance correlation metric gives very different results, as you can see when comparing the distance correlation outputs in Figure 2.5 with the Pearson correlation outputs in Figure 2.4.

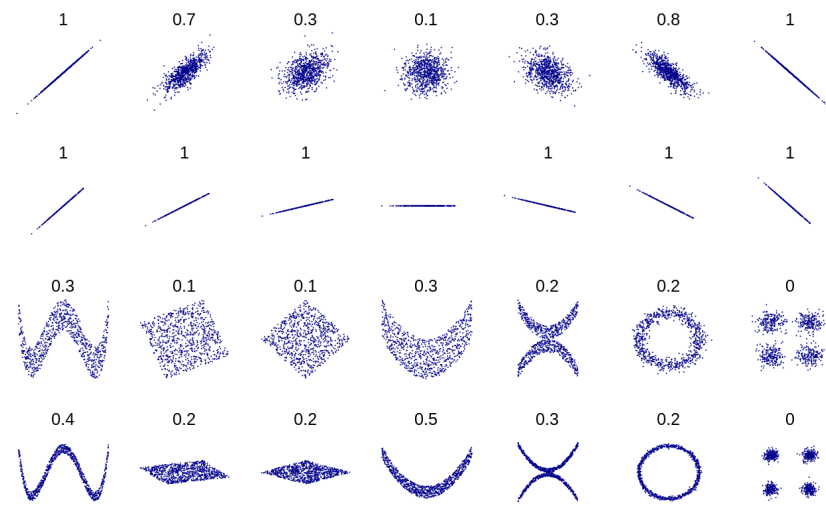


Figure 2.5: Distance correlation coefficients for different sets of (x,y) points. Note the difference with the Pearson correlation coefficients in Figure 2.4. - Source: Wikipedia

Without going further into the theory, the distance correlation between two variables X and Y, each with n data points can be calculated as follows.

First compute all pairwise Euclidean distances for both variables.

$$\begin{aligned} [D_x]_{j,k} &= \|X_j - X_k\| \\ [D_Y]_{j,k} &= \|Y_j - Y_k\| \\ j, k &= 1, 2, \dots, n \end{aligned}$$

The result is two n by n distance matrices D_x and D_y . Next, both matrices are centered:

$$\begin{aligned} S_x &= C_n D_x C_n \\ S_y &= C_n D_y C_n \end{aligned}$$

Finally, the covariance is computed.

$$\nu^2(X, Y) = \frac{1}{n^2} \sum_l \sum_k [S_x]_{k,l} [S_y]_{k,l}$$

This is the distance covariance, which is not normalized. The distance correlation is the normalized version of the distance covariance, $dCorr$, which is defined by:

$$dCorr(X, Y) = \frac{dCov(X, Y)}{\sqrt{dVar(X)dVar(Y)}}$$

With $dCov(X, Y)$ being the aforementioned distance covariance, $dVar(X)$ and $dVar(Y)$ are the distance standard deviations. The distance correlation has the disadvantage that is much slower than mutual information or Pearson correlation, but in return, the distance correlation is able to detect more complex relationships between two variables.

Analysis of variance

Analysis of variance (ANOVA) is a statistical test to analyse differences between groups. The idea is that the total variance, found in the samples consists of two parts. The first part is the variance within a single group, the second part is the variance between groups.

Suppose you want to test the influence of caffeine on the reaction speed⁵. To do so, you take two groups of each 10 persons. The first group has to drink a large cup of coffee, the second group is the control group that only drinks water. Next the reaction times of all persons in both groups are measured. From these results it is possible to calculate the total variance as well as the variance within each group and the variance between the groups.

If the variance within each group is much larger than the variance in between the groups, one concludes that the groups are similar. The reaction time is thus dependent on the person and not on the caffeine. However should the variance between the groups be much bigger than the variance within each group, than one concludes that the variance in reaction time is caused by the caffeine and not by personal difference.

2.4.2 Wrapper methods

These methods select features by applying an arbitrary machine learning technique and looking at the coefficients of the features. The idea is that features with high coefficients have more influence on the end results than features with a lower coefficients and are therefore more important. Again absolute values are used, since a perfectly negative correlated variable is as useful as a perfectly positively correlated variable.

Linear regression

A first method is simple linear regression, where a linear combination of features is searched that produce a good estimate of the output value. Linear regression can achieve good results when the data does not contain a lot of noise and the features are (relatively) independent. When the set of features contains correlated features, the model becomes unstable. As a result, small changes in input data might lead to huge differences in output coefficients. for example assume the 'real output' is given by $Y = X_1 + X_2$ and the dataset contains output in the form of $Y = X_1 + X_2 + \epsilon$ with ϵ being some random noise. Further more assume that X_1 and X_2 are linearly correlated, meaning that $X_1 \approx X_2$. The suspected output of the model should be $Y = X_1 + X_2$, but since noise is added the algorithm might end up with arbitrary combinations of X_1 and X_2 , e.g. $Y = -X_1 + 3X_2$. the result will rate one feature much higher than another one, while in reality they are of equal importance. This is due to the noise. While maximizing the performance, the algorithm will minimize the influence of noise on the output, which results in unstable behaviour.

⁵This example was based on the following video: <https://www.youtube.com/watch?v=ITf4vHhyGpc>

SVM

A Support vector machine (SVM) is a well known and proven method for machine learning. It has been used in several emotion recognition studies. An SVM works in essence by creating a hyperplane that separates two classes. Shown in Figure 2.6 is a simple line separating the red from the blue balls.

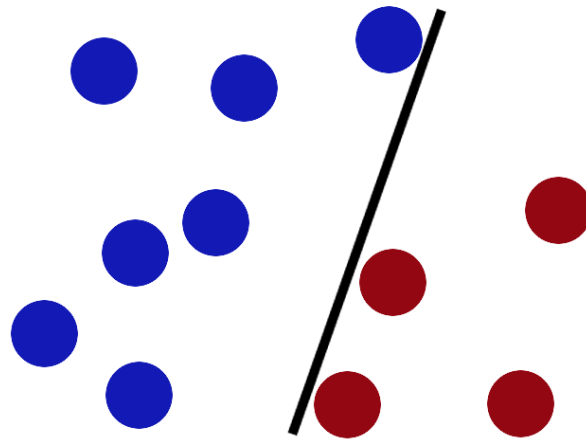


Figure 2.6: One possible separation border.

This is one possible solution, but note that an SVM will always search for a decision boundary that maximizes the boundary between the two classes, shown in Figure 2.7.

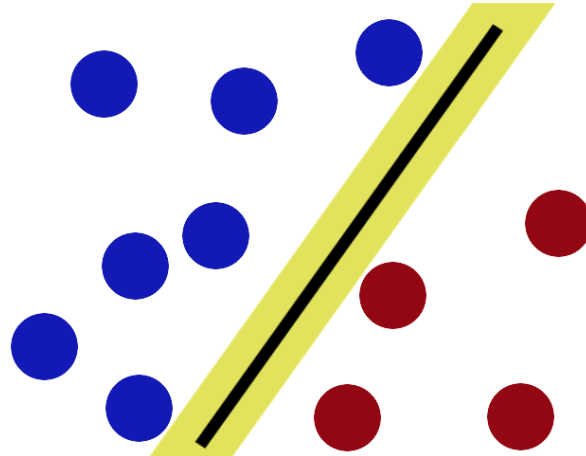


Figure 2.7: A separation with maximal boundary.

This all works well, as the balls are separable using a single straight line. This is not always the case though. Shown in Figure 2.8 is a scenario where it is not possible to separate the red balls from the blue ones using a single straight line.

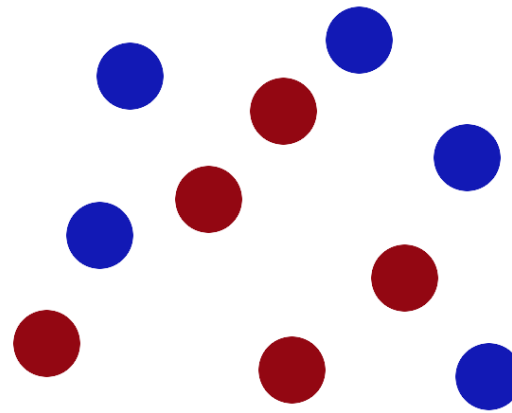


Figure 2.8: There exists no possible line that can separate the red balls from the blue ones.

A solution for this is to transform the input space to the feature space, where it is possible to separate the balls using a hyperplane, this is shown in Figure 2.9. Different transformations are possible. Each transformation corresponds to a different kernel, the component of an SVM that handles the transformation.

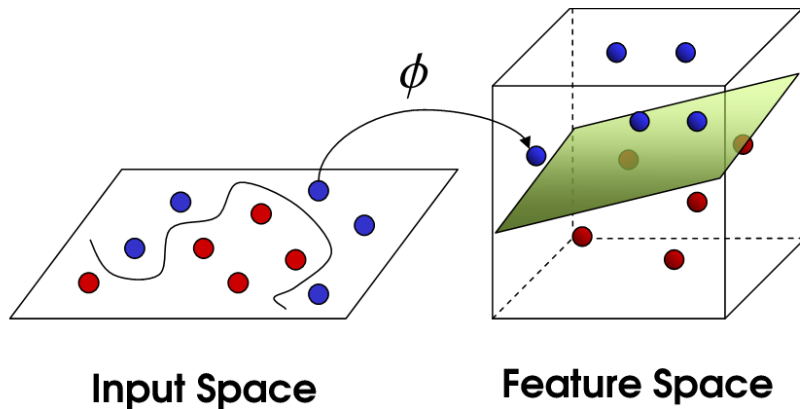


Figure 2.9: Transformation to a new features space where the balls can be separated by a hyperplane.

Back in the original feature space the separation boundary might look like Figure 2.10.

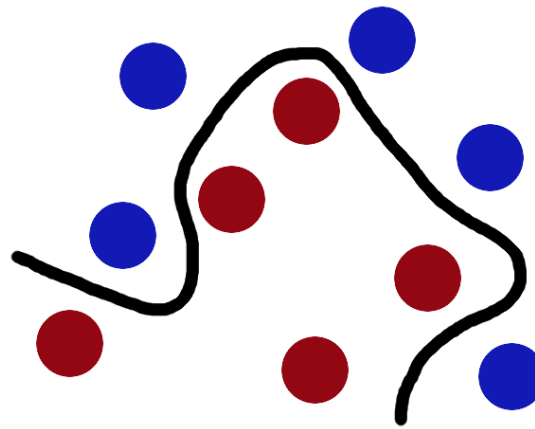


Figure 2.10: Separation boundary in the original feature space.

In this work a Radial Basis Function (RBF) was used. This kernels is sometimes called the Gaussian kernel. The RBF kernel K for two input vectors x and y is given by[?]:

$$K(x, y) = \exp\left(\frac{-x-y^2}{2\sigma^2}\right)$$

The numerator can be recognized as the squared Euclidean distance between two sample points in the feature space. The σ is a parameter. The kernel can be interpreted as a similarity measure[?]. Furthermore, this kernel has an infinite number of dimensions[?], this is visible when the kernel is expanded. For $\sigma = 1$ the kernels becomes:

$$\exp(-\frac{1}{2}x - y^2) = \sum_{j=0}^{\infty} \frac{(x^T y)^j}{j!} \exp(-\frac{1}{2}x^2) \exp(-\frac{1}{2}y^2)$$

Linear discriminant analysis

Linear Discriminant Analysis (LDA), is a machine learning technique often used in combination with CSP[46, 47, 48]. LDA looks for a projection of the data where the data is linearly separable, as shown in Figure 2.11. Looking at the coefficients of the LDA model, one can again determine the importance of the different features.

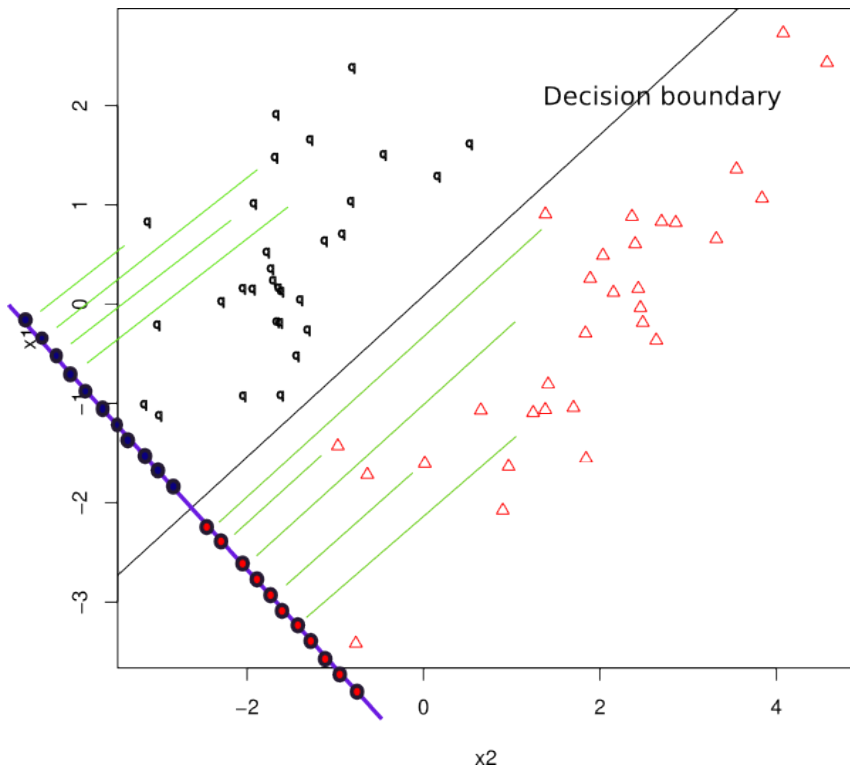


Figure 2.11: LDA finds a projection of the data where the separation of the data is clear.

2.4.3 Embedded methods

Embedded feature selection methods are methods that are build-in for some machine learning algorithms.

Lasso regression

Lasso regression uses L1 regularization, that adds a penalty $\alpha \sum_{i=1}^n |w_i|$ to the loss function. the result is that the coefficients of weak features are forced to zero, as each non-zero feature adds to the penalty. This form of regularization is thus quite aggressive, it removes weak features completely and selects the good features. The problem with this is, similar to linear regression, stability. Coefficients can vary significantly, even for small changes in training data, when there are correlated features.

Ridge regression

Ridge regression uses L2 regularization, which adds a L2 norm penalty to the loss function, given by $\alpha \sum_{i=1}^n w_i^2$. Where the L1 norm forces the coefficients to zero, the L2 regularization forces the coefficients to be spread out more equally. The result is that correlated features tend to get similar coefficients, as this minimizes the loss function, which in turn results in a more stable model. The disadvantage of ridge regression is that bad features still have low weights. This means that they still have an influence on the output.

Random forests

A random forest (RF) is an efficient learning algorithm based on model bagging and aggregation ideas[30]. The Random forests work by creating different decision trees. On their own, decision trees are very prone to overfitting. Random forests solve this problem by creating an aggregation of trees.

The word random in random forest indicates that some randomness is included. Each tree in a random forest looks at a random subset of the samples and a random subset of the features. This principle is shown in Figure 2.12. This random subset of samples is called the bootstrap sample and is selected out of N samples, by picking N samples with replacement. This results, on average, in 2/3 of the samples being selected (with some doubles). The other 1/3 of the samples are then used as out of bag (oob) set. Averaging the performance of each tree on the out of bag set, offers an indication of the generalisation of the random forest.

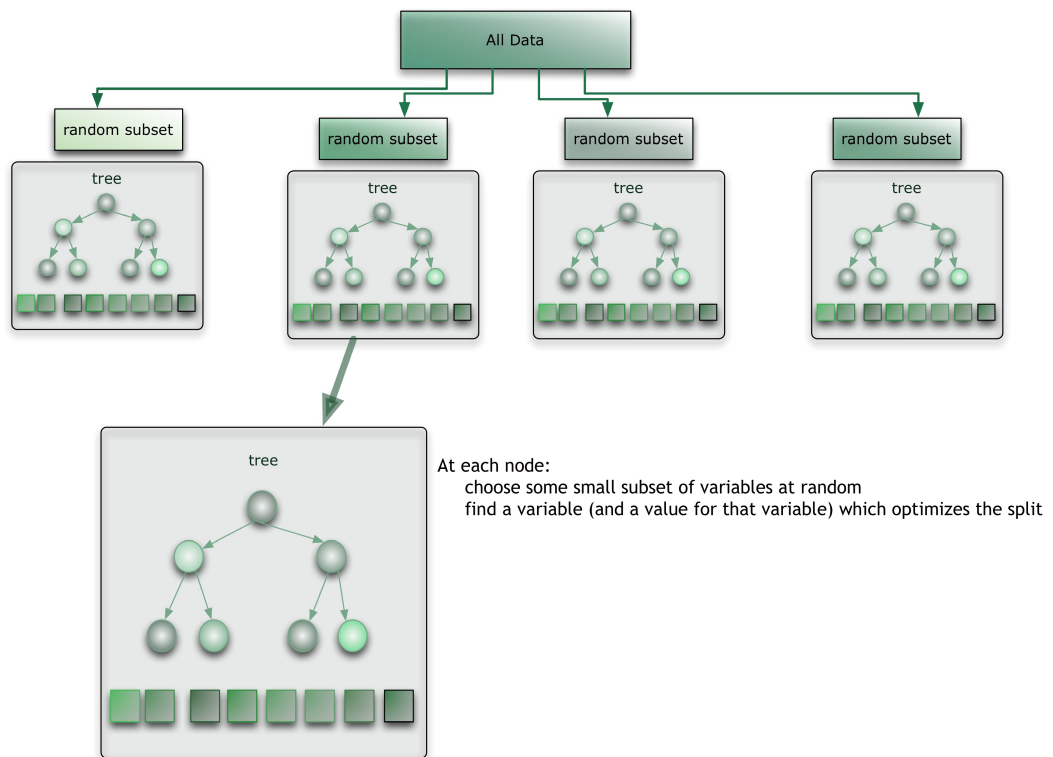


Figure 2.12: The structure of a random forest, found at [7]

To understand which features are good, one needs to understand the internal workings of a decision tree. Suppose the following example⁶, where one tries to find an algorithm to predict whether or not a person will play tennis on a given day. Suppose the training data is given by Table 2.3 and a prediction for the 15th sample needs to be made.

⁶This example is based extensively on this youtube video: <https://www.youtube.com/watch?v=eKD5gxPPeY0>

Table 2.3: suppose the following training examples for a decision tree.

Day	Outlook	Humidity	Wind	Play tennis
1	sunny	high	weak	no
2	sunny	high	strong	no
3	overcast	high	weak	yes
4	rain	high	weak	yes
5	rain	normal	weak	yes
6	rain	normal	strong	no
7	overcast	normal	strong	yes
8	sunny	high	weak	no
9	sunny	normal	weak	yes
10	rain	normal	weak	yes
11	sunny	normal	strong	yes
12	overcast	high	strong	yes
13	overcast	normal	weak	yes
14	rain	high	strong	no
15	rain	high	weak	?

A decision tree will take a feature and split the data based on the possible outcomes of this feature. In case the features are continuous values, ranges are selected. In some cases the leafs will be pure, meaning that all samples in this leaf belong to a single class. The pure leaves in Figure 2.13 are displayed in green. In case the leave is not pure, another split is needed. Note that not all random forests split until all leaves are pure; random forest can be limited in depth, in that case the output is chose by a majority voting of the samples.

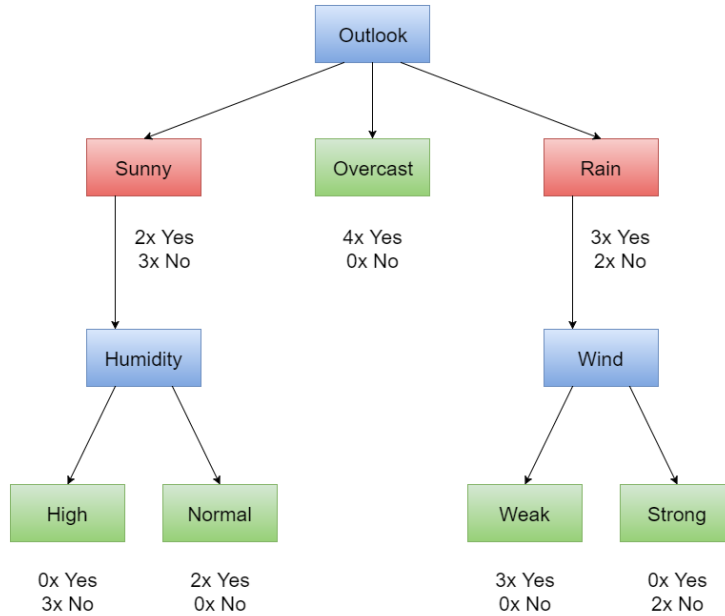


Figure 2.13: A decision tree for the data in Table 2.3

Once the tree is constructed it becomes clear that the predicted output of sample 15 is 'Yes'. This is obtained simply by following the tree branches. Even though the features are selected at random, they have influence on the accuracy. Good features will reduce the impurity significantly, thus the impurity reductions are a good indication for how important a feature is.

The importance is averaged over different nodes and different trees. As a result, random forest are also capable of detecting combinations of features that work well. One feature may not be important on its own, but might be a very good feature when combined with other features. Suppose the following example in Table 2.4:

Table 2.4: Some features are not significant on its own, but might be part of a combination of features.

label	feature A	feature B
Happy	+	+
Happy	-	-
Sad	-	+
Sad	+	-

It is clear that feature A and B are very important when it comes to predicting whether or not a person is happy or sad. When both features have the same sign, the person is happy, otherwise he is not. Combinations of features are often not found by feature selection methods as they look for correlations between a single feature and the output.

This problem does not occur for random forest though, as combinations of features are also 'tested' in the sense that a tree might split on them in different stages. Once the combination of features occurs randomly in a decision tree, the impurity will drop significantly, which will result in higher importance rankings.

Random forest have an element of randomness, which might make them unstable in the sense that running this method several times might give different features. One way to measure how similar the outputs of different runs are is the Jaccard index. The Jaccard index measures similarity between two sets. The Jaccard index J , between set A and B is given by:

$$J_{A,B} = \frac{|A \cap B|}{|A \cup B|}$$

The Jaccard index ranges from zero to one. A value of zero corresponds to no similarity, while a value of 1 indicates that the two sets are identical.

Several ways are available to make random forest more stable for feature selection. First, one can increase the number of trees used. In this thesis 2000 trees were used to estimate the importance. Second, taking an average of the importance values over several runs will also increase the stability. In this work, the random forest were run 30 times to ensure stability.

Principal Component Analysis

Principal Component Analysis (PCA) is a technique to do dimension reduction. Intuitively, PCA can be seen as fitting an n-dimensional ellipsoid to the data. The Principal components

are then the axes of the ellipsoid. Less variation in one direction, corresponds to a smaller axis. Removing that axis, will only remove a small fraction of the information, as there is only little variation in that direction. This is shown in Figure 2.14, where the ellipsoid covers a three dimensional features space. The ellipsoid has three axes: a,b and c. Intuitively, one can see that there is more variation (information) in the c and b direction, while the a axis is relatively small.

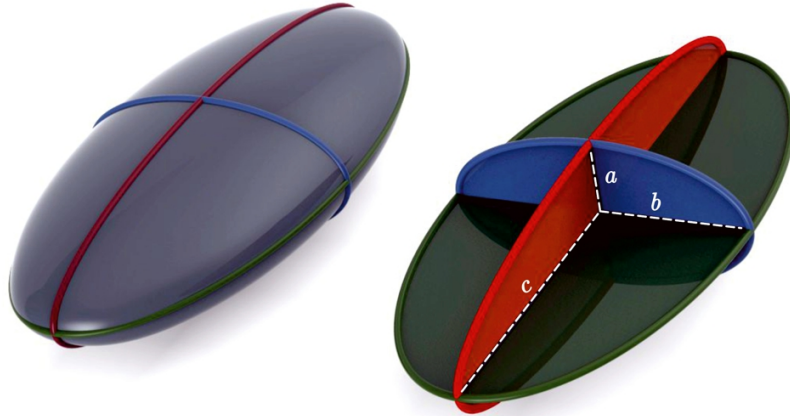


Figure 2.14: Suppose a three-dimensional feature space, where all points lie in the ellipsoid in the left.

Removing the a axis by projecting the data on the plane given by vectors b and c, will result in a two dimensional projection of the data in the form of an ellipse. This would be the black plane in Figure 2.14. This process can be repeated for higher dimensional features spaces. In other words, PCA will thus, without going into too much detail, start with an n-dimensional ellipsoid and iteratively remove the smallest axis in each iteration until the desired number of dimensions is obtained. Note that the ellipsoid should be adjusted in each step.

The major disadvantage of PCA is that the algorithm is unsupervised, meaning that it does not look at the corresponding labels of the given samples. Suppose the difference between two classes was clearly given by looking at the a axis in Figure 2.14. Applying PCA would, in that case, result in a total loss of all information.

3

Results - Person specific

This section explains the result found in a person specific setting. It starts by explaining the used approach before proceeding with a performance comparison of the different classifiers. Next the certainty of the classifiers is investigated, combined with the selected features and EEG channels. This chapter ends with a discussion about the stability of the different methods.

3.1 Used approach

The first part of this work is looking at features in a person specific setting. This means that the algorithm is trained and tested on data from the same person. The main goal was to find features that give insight in the arousal and valence state of a person. This was done by comparing the aforementioned features and feature selection methods. For this a two stepped algorithm, inspired by the advanced random forest method, explained in Section 2.3.5, was used. In short, the first step is to rank all the features and only take the top X of the features. This threshold is applied to limit computation times and cancel features with low or zero importance. The next step is to build a model by selecting features out of the remaining feature set. This approach is depicted in Figure 3.1.

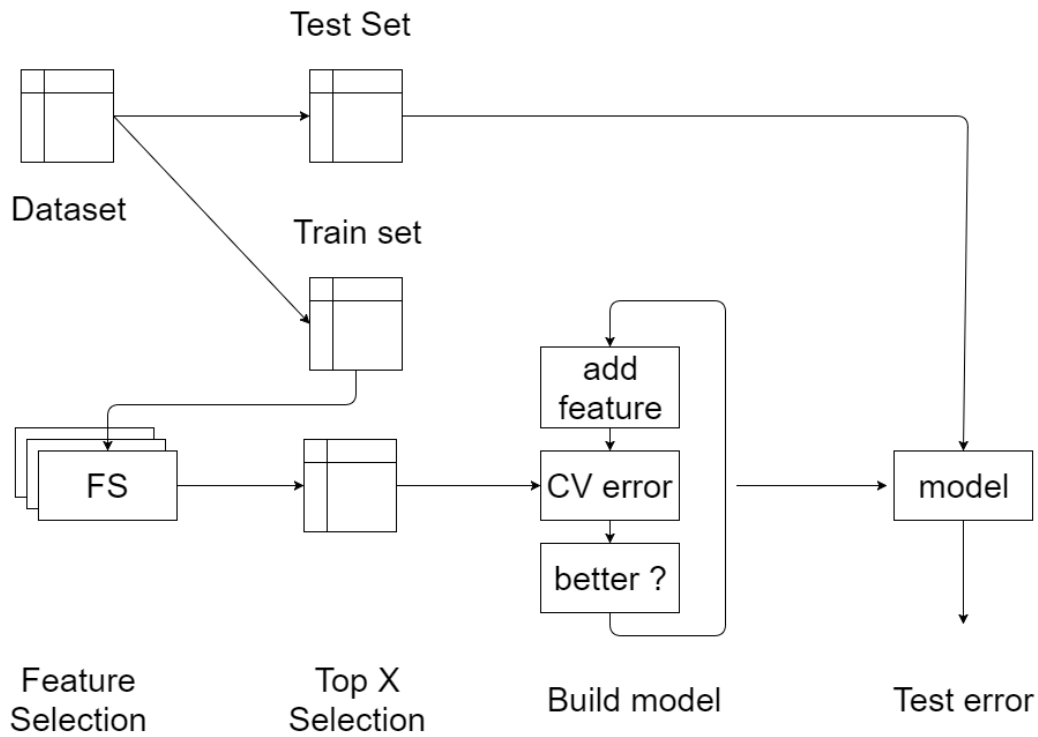


Figure 3.1: The used approach of this thesis.

As you can see in Figure 3.1, the approach starts by separating a test set to evaluate the final performance of the algorithm. This test set contains 10 of the 40 samples. Next, the aforementioned feature selection methods are applied to the train set. A top X of the features is then kept, all other features are cancelled.

In the next step a model is build with the selected features. This is done iteratively by starting with an empty feature set. In the add step, a feature is added to this set and the cross validation error is determined. This step is important because it ensures that chosen features have good generalisation properties. Next the average of the cross validation errors and the standard deviation is calculated. The average cross validation minus the standard deviation is then compared to the previous best performance. If the performance is better, the feature is kept in the feature set. If the performance is not better, the feature is neglected. This is repeated for all the features and is known as greedy forward selection in literature [49]. The standard deviation is included to increase the stability of the algorithm, by avoiding that small differences in averages lead to a different model. This was used rather than a statistical test, as it already provided good results in the original algorithm2.3.5.

In the final step the performance of the test set is determined by the accuracy metric. Accuracy is chosen as metric, because this metric gives a clear and intuitive measurement of performance.

The first parameter of this flow is the threshold parameter, indicated in the figure as X . This threshold cancels features with low importance, by simply taking the best X features from the feature ranking. Assigning a high value to the threshold will increase calculation times as more

features are available for the building phase. The performance of the model, will not be better though. Most of the additional features will have low importance values and are not likely to improve performance. Setting a low threshold might cancel out important features. In this work, the threshold parameter was fixed to 30 for all feature selection methods for the following two reasons. First, considering that there are 30 samples in the feature set, having 30 features is already more than enough. Note that a well-known rule of thumb is to have at least 10 times more samples than features[50, 51]¹. Second, looking at the features that were selected during training, one can see that usually around 5-7 features remain. The last selected feature usually has a rank around 20, meaning that the last 10 available features in the building phase are rarely used.

A second parameter of this model is a model to estimate the performance. For this, an SVM with a radial basis functions (RBF) kernel is used as model. This kernel model was chosen because it has proven itself in multiple emotion recognition studies[35, 36? ?]. SVMs look for a separation boundary between two classes, and thus only look at points close to that boundary. This gives this method an advantage in this experiment, as the dataset only contains 40 samples for each person, only 30 of them are available for training. Another advantage of the marginalization maximization and the regularization is that SVMs are capable of handling large features sets[? ?], which concurs with this work's problem statement.

Some feature selection methods use a machine learning technique as basis. These methods were not used in the final building phase. This was done because some underlying methods are actually regression algorithms, meaning that they will produce a continuous output. This is in contrast with the classification problem that is solved in this work². To ensure that all final models were capable of classification, one classification model was used in the final step. This ensures that the comparison between feature selection methods was possible.

3.2 Performance

When looking at the accuracies of the different feature selection models in combination with the SVM, it is clear that there is not a lot of difference. For each feature selection method, the test accuracy and standard deviation are shown in Table 3.1 and Table 3.2 for valence and arousal respectively. The accuracies are also plotted in in Figure 3.2 and Figure 3.3 for arousal and valence respectively.

¹Note that this is just a rule of thumb, and therefore not proven theoretically. In practice however, it turns out to work quite well.

²Several tests in the early stage of this work indicated that even though continuous valence and arousal values are available, classification was more designated. The current state of the art emotion recognition systems is still limited to classification, because regression proves to be a difficult problem. One possible reason for this might be that each person has his/her own interpretation of the valence / arousal scales. A positive feeling with valence level 6 of one person does not correspond to the exact same feeling of another person.

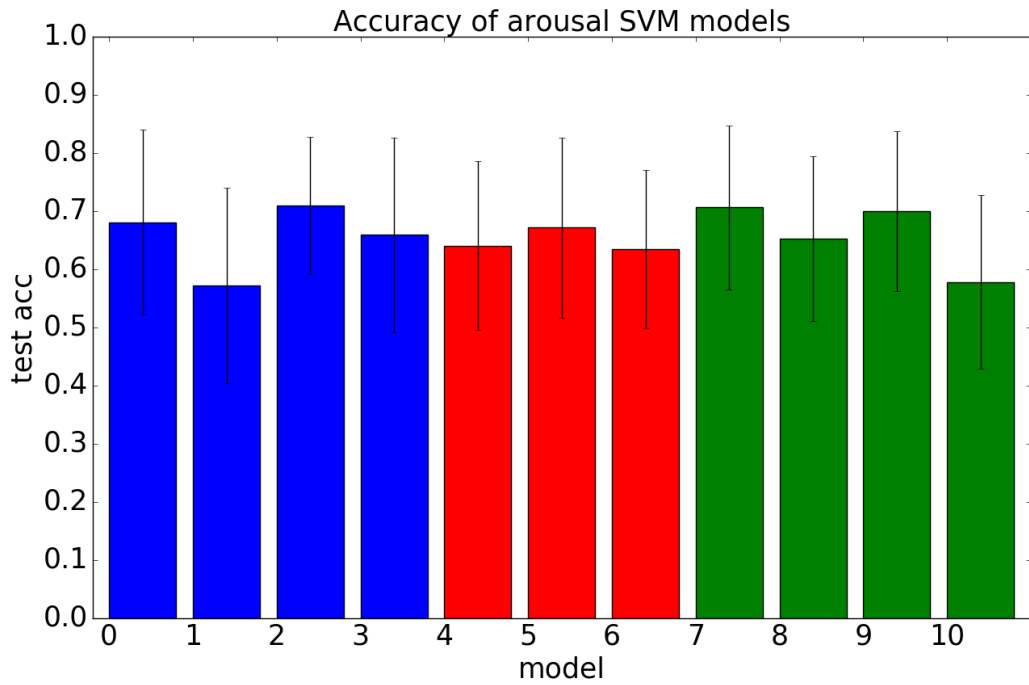


Figure 3.2: Comparison of different feature selection methods for arousal recognition. The y-axis shows the test accuracy averages over all persons as well as the standard deviation. The x-axis shows the different models, each number corresponds to the number in Table 3.1. Blue bars correspond to filter selection methods, red bars correspond to wrapper methods and green bars are used for the embedded methods.

Table 3.1: A comparison of the accuracy of different feature selection methods for arousal. The reported scores are test accuracies averaged over the different persons with their standard deviation..

Number	Feature selection method	Avg test acc - arousal	Std test acc - arousal
0	pearson	0.68125	0.1615199978
1	mutual information	0.571875	0.1708316942
2	distance correlation	0.709375	0.1201058001
3	ANOVA	0.659375	0.1701221098
4	linear regression	0.640625	0.1477997228
5	SVM	0.671875	0.1570583927
6	LDA	0.634375	0.138212961
7	lasso regression	0.70625	0.1435438564
8	ridge regression	0.653125	0.1436491582
9	random forests	0.7	0.1391216687
10	PCA	0.578125	0.1518368713

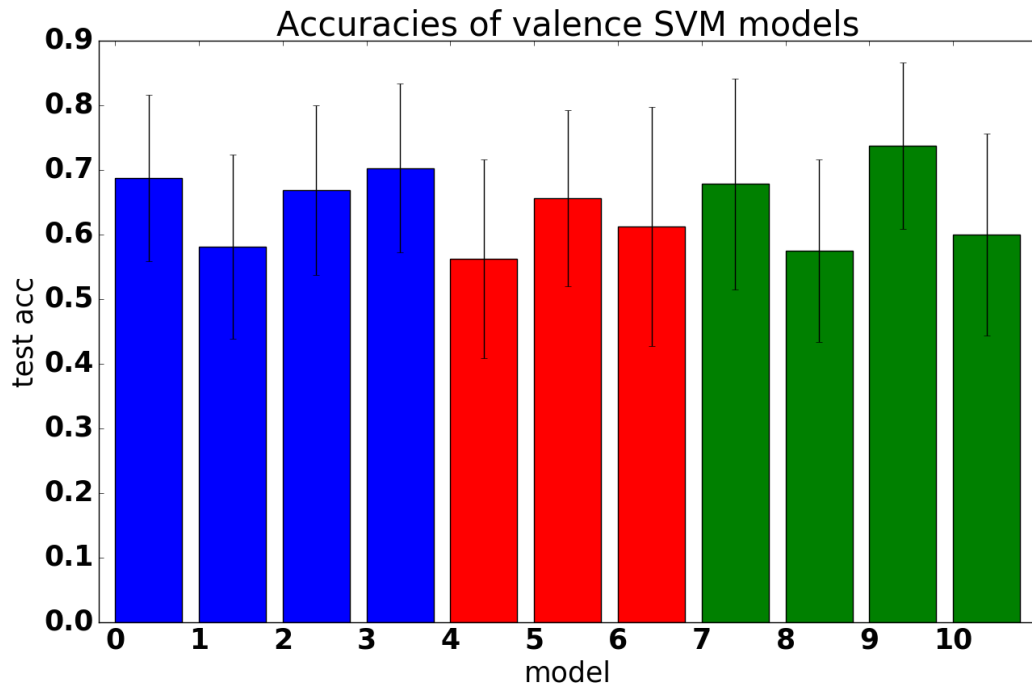


Figure 3.3: Comparison of different feature selection methods for valence recognition. The y-axis shows the test accuracy averages over all persons as well as the standard deviation. The x-axis shows the different models, each number corresponds to the number in Table 3.2. Blue bars correspond to filter selection methods, red bars correspond to wrapper methods and green bars are used for the embedded methods.

Table 3.2: A comparison of the accuracy of different feature selection methods for valence. The reported scores are test accuracies averaged over the different persons with their standard deviation.

Number	Feature selection method	Avg test acc - valence	Std test acc - valence
0	pearson	0.6875	0.1313699529
1	mutual information	0.58125	0.1446631237
2	distance correlation	0.66875	0.1330474085
3	ANOVA	0.703125	0.133161011
4	linear regression	0.5625	0.1560603688
5	SVM	0.65625	0.1389766748
6	LDA	0.6125	0.187943025
7	lasso regression	0.678125	0.1660438632
8	ridge regression	0.575	0.1436842416
9	random forests	0.7375	0.1313699529
10	PCA	0.6	0.1586231078

3.3 Correlation probability and level of valence/arousal

The current model is a classification model, meaning that it divides the valence and arousal into two classes: high and low. The classes are determined by a binary separation. Both valence and arousal range between 1 and 9, so every value between 5 is regarded as a low valence/ arousal. All values above 5 are regarded as high valence/arousal.

It might be interesting to look at the prediction probability a model gives to its output and the distance of the arousal/valence level to this separation boundary. The distance to the separation boundary (sb) of an arousal/valence value v is given by:

$$dist_{v,sb} = |v - sb|$$

Using simple binary classification, the separation boundary has value 5, which simple splits the range into two. A valence level 9 has thus a distance of 4.

It is expected that samples with a valence rating far from the separation boundary, e.g. 9, should be predicted with higher confidence than one with a valence rating close to the separation boundary, e.g. 5 or 6. This should be reflected in the prediction probability, i.e. a model should be more certain of valence/ arousal values that lie further away from the separation boundary. To investigate this, the Pearson correlation coefficient R between the prediction probability and the aforementioned distance to the separation boundary was calculated. These Pearson coefficients are plotted for the model build with the corresponding feature selection methods. The Pearson correlations for arousal are depicted in Figure 3.4 and Figure 3.5 for valence. The legend combined with the precise values, can be found in Table 3.3.

Table 3.3: This table gives the Pearson R correlation coefficients between the prediction probability and the distance between the level of arousal and the separation boundary, i.e. level 9 arousal lies at a distance $|9-5| = 4$, while an arousal of level 7 lies at distance 2. The assumption is that larger distances are easier to recognise, and thus be predicted with a higher confidence. The correlation should thus ideally be positive.

Number	What	arousal	valence
0	pearson	0.03797	0.00957
1	mutual information	-0.09065	0.00805
2	distance correlation	0.08906	0.01725
3	ANOVA	0.07880	-0.01745
4	linear regression	0.05027	0.09465
5	SVM	0.11322	0.02691
6	LDA	-0.06053	0.02876
7	lasso regression	0.05280	0.17024
8	ridge regression	0.02897	0.10253
9	random forests	0.00439	0.10738
10	PCA	0.02182	0.00875

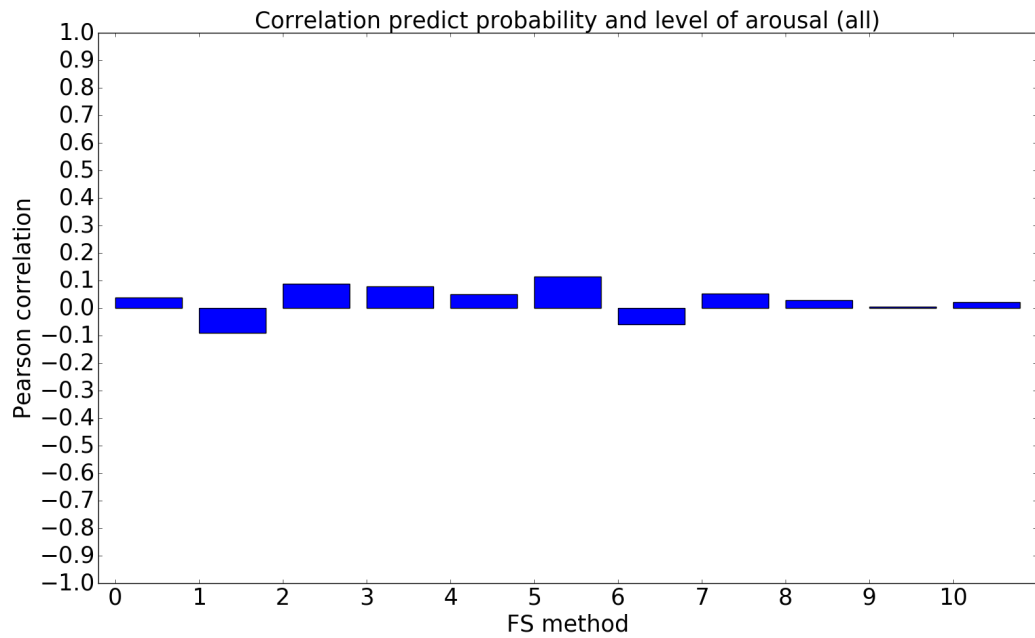


Figure 3.4: The pearson correlations between the model's prediction probability and the distance between the subject's level of arousal and the separation boundary, see Table3.3 for more details.

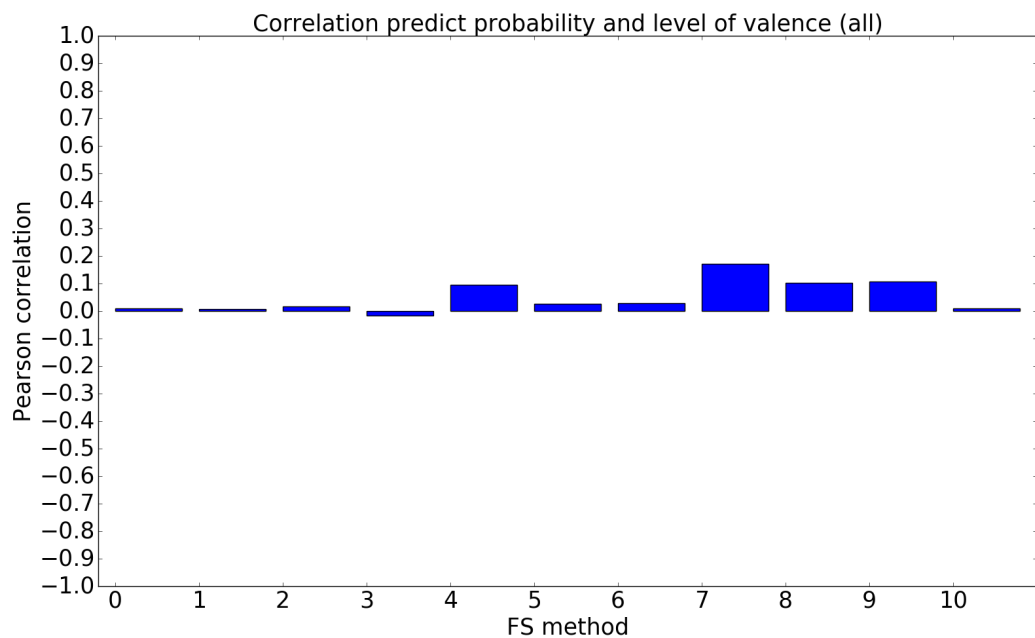


Figure 3.5: The pearson correlations between the model's prediction probability and the distance between the subject's level of valence and the separation boundary, see Table3.3 for more details.

Overall, the correlations are quite low. Some correlations are even negative, meaning that the model is more certain of examples that lie closer to the separation boundary. To explain why, additional research might be needed. At first sight, several explanations for this are possible:

1. The correlation is present, but is more complex than a simple linear correlation. As a result, the Pearson coefficient is not able to capture this correlation well.
2. The assumption that high valence and arousal values are easier to recognise is wrong. It might be possible that a high valence/arousal levels do not correspond to increased physiological responses. Future research could look at the dominance values, that indicate how strong the emotion is perceived. The dominance values are explained in Section 1.1 and were neglected during this work.

On the other hand one can observe that the correlation for valence is a little higher than the correlation for arousal. This indicates that might it be easier to recognize valence.

3.4 Selected features

To compare which features where chosen, the feature set was divided into 8 categories:

1. **Power features:** PSD and FE features of a single EEG channel
2. **Asymmetry features:** DASM, RASM, DCAU and RCAU features that represent a the (a)symmetry between two EEGchannels.
3. **Fractions:** Alpha/beta and fractions of different power ratios of an EEG channels.
4. **Heart rate:** the statistical values of the heart rate.
5. **Galvanic skin response:** the statistical values of the GSR, measuring perspiration.
6. **Respiration:** the statistical values of the respiration.
7. **Blood pressure:** the statistical values of the plethysmograph, indication the person's blood pressure.
8. **Skin temp:** the statistical values of the skin temperature.

The results for arousal are depicted in Figure 3.6, the legend is shown in Figure 3.6l. In each of these plots, a pie chart is shown that gives the distribution of all the selected features for all persons combined. When looking at the different selected features for the different feature selection methods, it becomes clear that the most valuable features are the asymmetry features combined with the power features. All feature selection methods seem to agree that those two categories are most valuable. The amount of asymmetry features is always the highest, except in case of linear, mutual information and lasso regression. These methods are not very advanced, which might explain the difference. Additionally, lasso regression is very prone to noise, as explained earlier in Section 2.4.3. Overall, the most important result for both valence and arousal is therefore that in a person-specific setting, EEG features are clearly dominant over non-EEG features. The non-EEG features are rarely selected by any of the feature selection algorithms.

The conclusion for arousal is that the different feature selection methods agree mostly on what the relevant feature categories. The most import features are the asymmetry features, followed by the power features. The non-EEG features are rarely chose and do not seem to be of importance here. It is also important to note that the fractions of frequency bands is not as important as previously thought. Literature suggested that the fractions of the alpha versus the beta frequency band would give an indication for the arousal of a subject. The main argument for this was the fact that arousal measures how active a person is feeling. A large fraction of alpha and beta power means that the brain is in a relaxed state or in an active and focussed state respectively. Looking at these fractions was therefore supposed to give insight in the arousal level of a subject. These results indicate that the asymmetry and power features are more relevant. This might mean two things, either the asymmetry and power features do contain valuable information for arousal or the algorithm is overfitting on these features.

The results for valence are depicted in Figure 3.7 and the corresponding legend in Figure 3.71. The selected features are similar to the selected features for arousal recognition. The most valuable features are again the asymmetry and power features. These results were expected, as most of the emotion recognition studies agree that the asymmetry features give insight in the valence level of a subject.

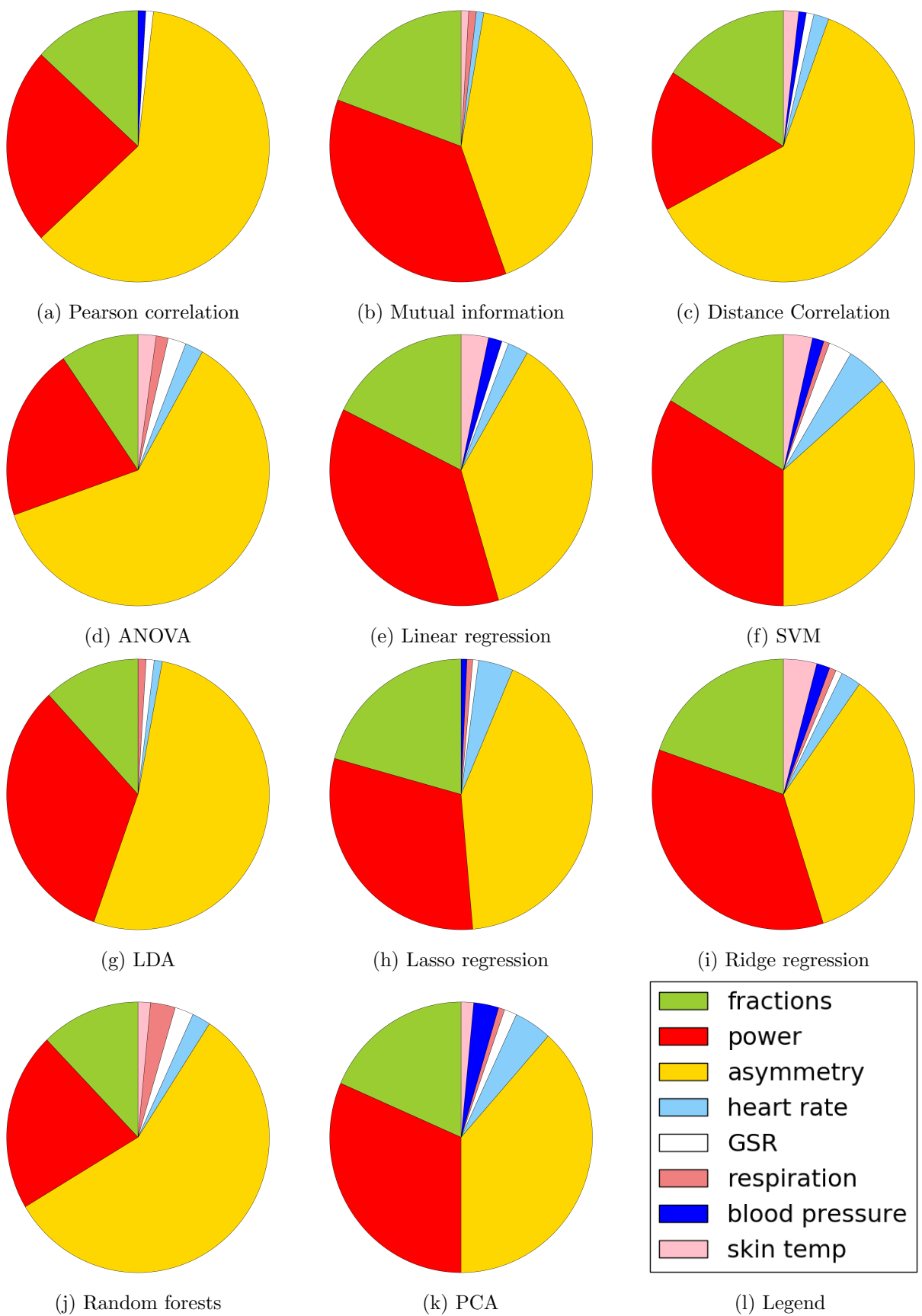


Figure 3.6: The distribution of the selected features for arousal classification of all persons combined of different feature selection methods. It is clear that the most valuable features are the asymmetry features combined with the power features. Furthermore, all feature selection methods agree that EEG features are dominant.

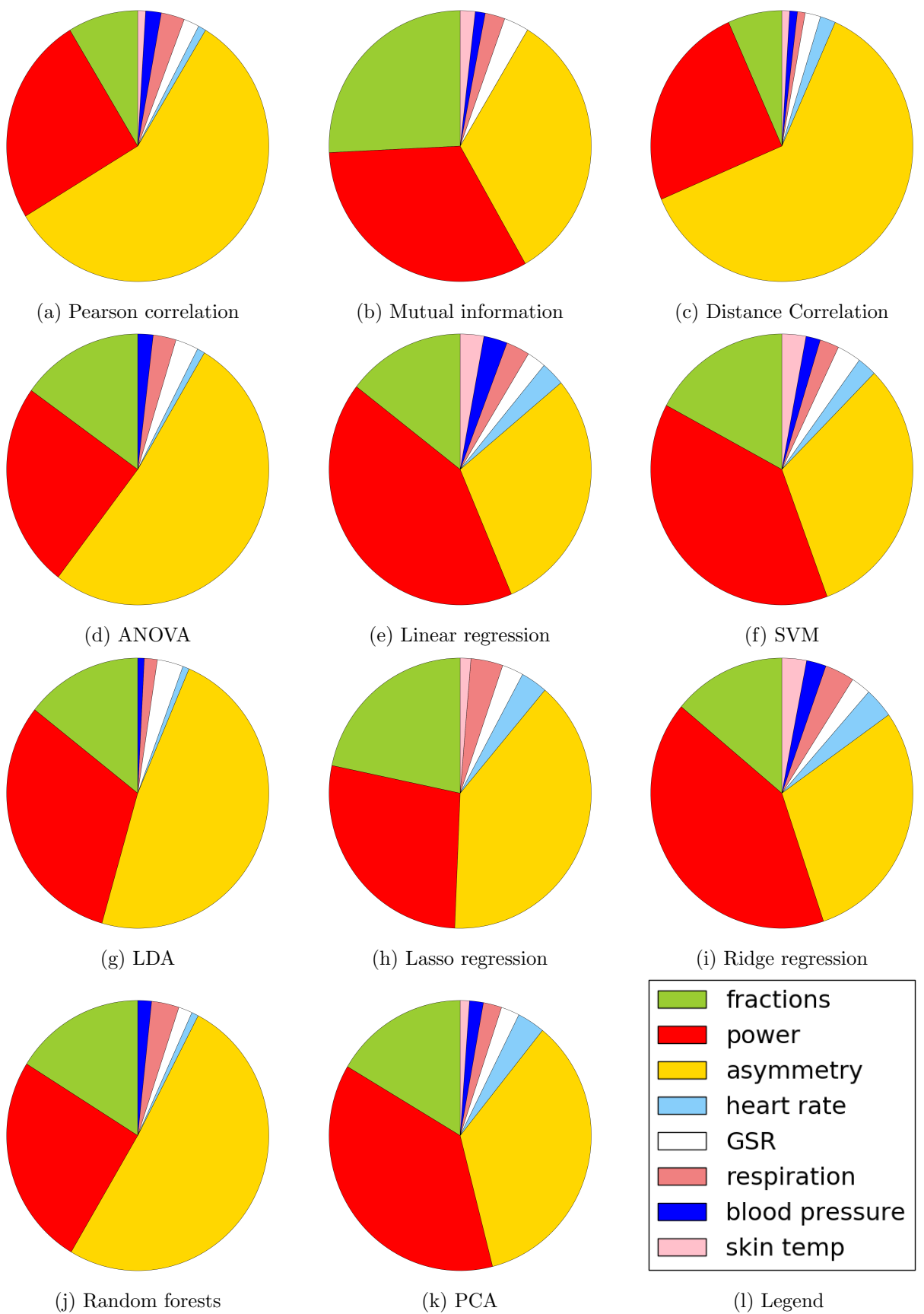


Figure 3.7: The distribution of the selected features for valence classification of all persons combined of different feature selection methods. It is clear that the most valuable features are the asymmetry features combined with the power features. Furthermore, all feature selection methods agree that EEG features are dominant.

The fact that the non-EEG features are almost never chosen might indicate that they are less important. In an attempt to further investigate the difference between EEG features and non-EEG features, the performance of three different feature sets was compared. The first feature set is the previously used feature set with all possible features. The second and third feature sets contained only EEG and non-EEG features respectively. The feature selection was done with random forest, as this method had the best average performance and is the most advanced.

The resulting performances of these different features sets are displayed in Figure 3.8 for arousal and in Figure 3.9 for valence. The exact values are shown in Table 3.4.

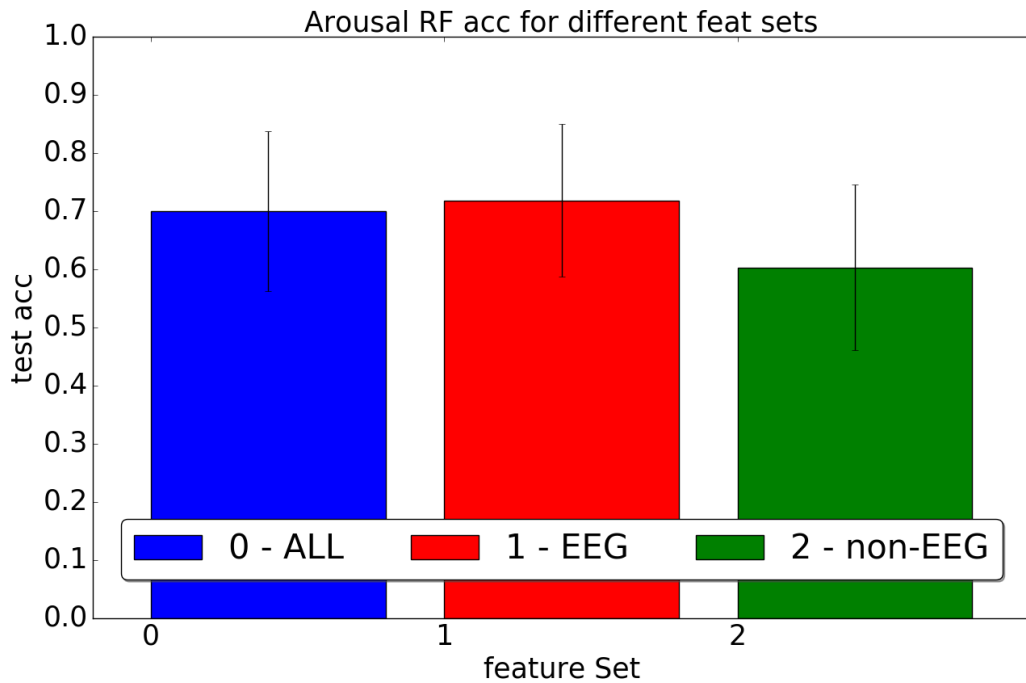


Figure 3.8: The average and standard deviation of the test accuracies of arousal classification for all, EEG and non-EEG features, see also Table 3.4

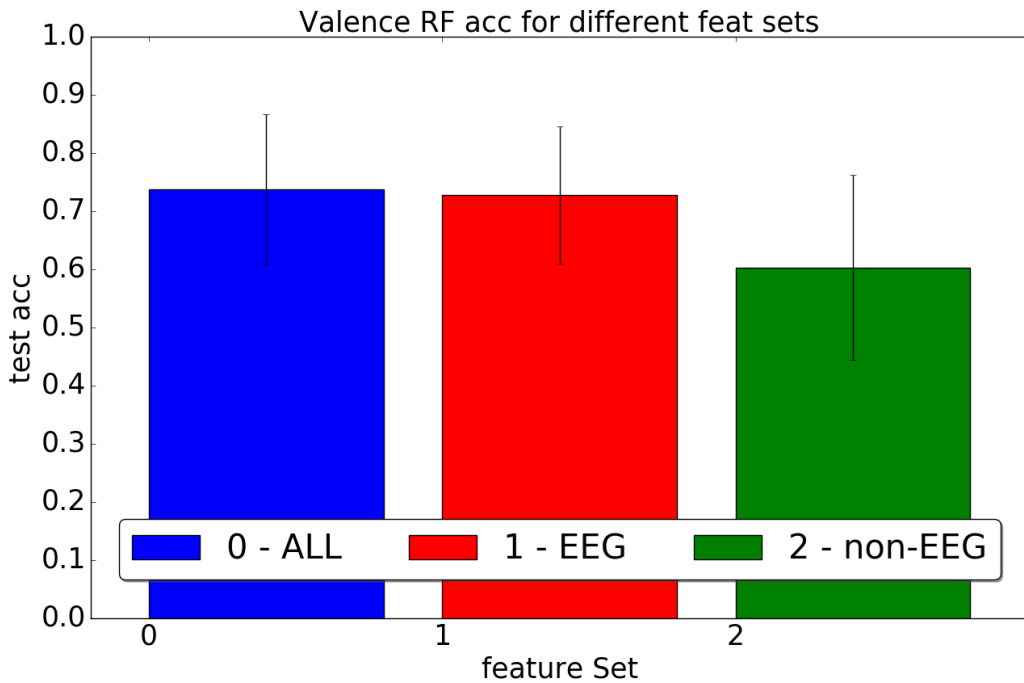


Figure 3.9: The average and standard deviation of the test accuracies of valence classification for all, EEG and non-EEG features, see also Table 3.4

Table 3.4: The average and standard deviation of the test accuracies (over the different persons) for the different feature sets, using the random forest feature selection model.

Feat set	Arousal		Valence	
	avg acc	std acc	avg acc	std acc
all	0.7000	0.1369	0.7375	0.1293
EEG	0.7188	0.1310	0.7281	0.1179
non-EEG	0.6031	0.1425	0.6031	0.1591

It is clear that for both valence and arousal, the average test performances are lower in case only non-EEG features are used. This is confirmed by the p-values in Table 3.5 below:

Table 3.5: P-values for the comparison of the performance of different feature sets.

	all / eeg	all / phy	eeg / phy
Arousal	0.4386	$5.891 * 10^{-7}$	$1.201 * 10^{-4}$
Valence	0.6817	$1.993 * 10^{-9}$	$1.763 * 10^{-6}$

Next, for each of the three feature sets, a comparison of the selected features was made. As you can see on Figure 3.10 for arousal and Figure 3.11, displayed on the following pages, the features are again mostly asymmetry features, followed by the power features. The fraction category gives only limited insight for both valence and arousal. The EEG and ALL set have similar performances, which was expected as they both use very similar features.

The results for the non-EEG features are shown in Figure 3.12 for arousal and Figure 3.13 for valence. Here, no single category can be labelled as most important. This is the case for both arousal and valence. However, the feature that was selected the most as being the most important for one person was the GSR, which measures perspiration. In case of valence, the first selected features were heart rate and GSR.

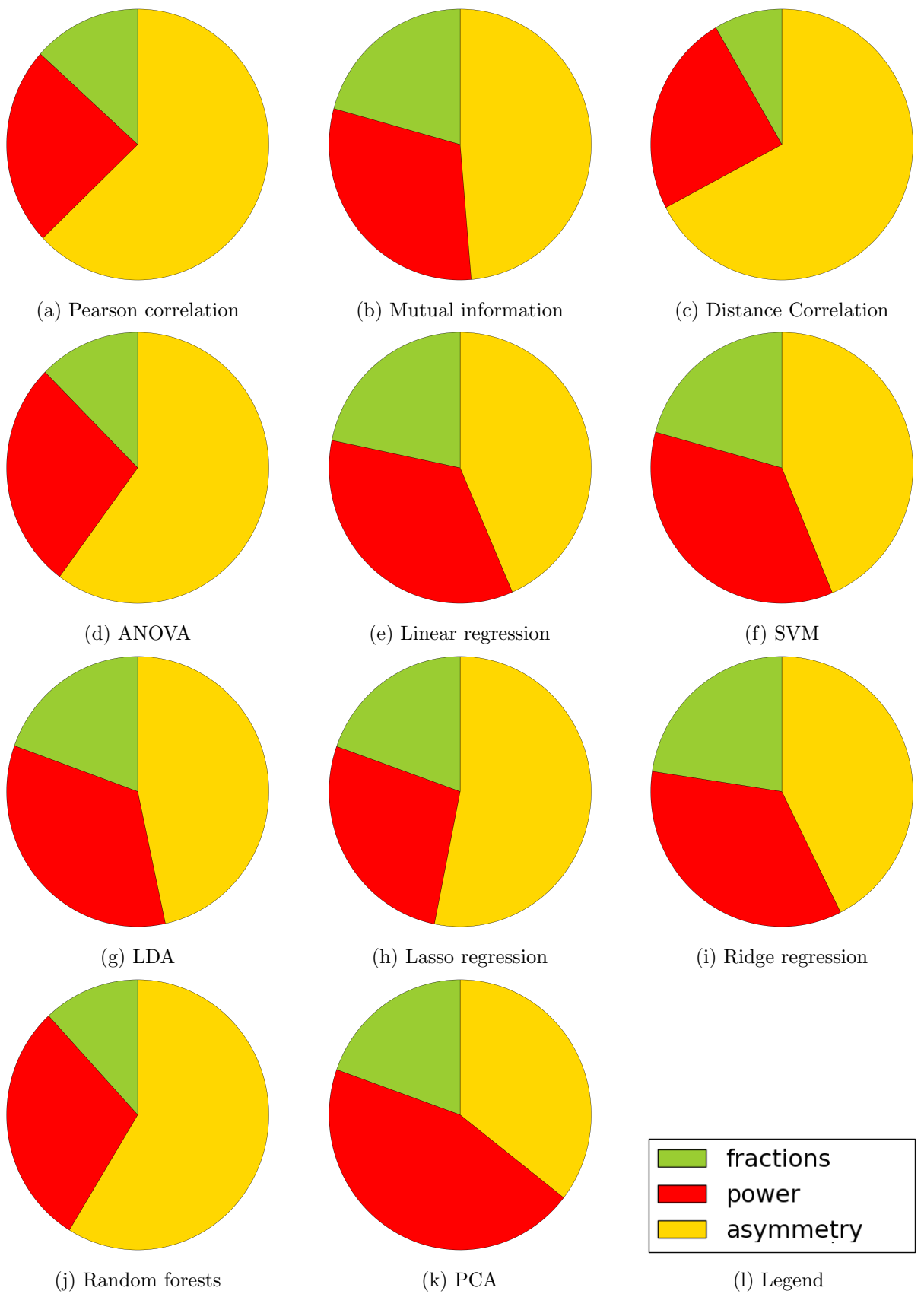


Figure 3.10: The distribution of the selected features for arousal classification of all persons combined of different feature selection methods. The feature set was limited to EEG features only.

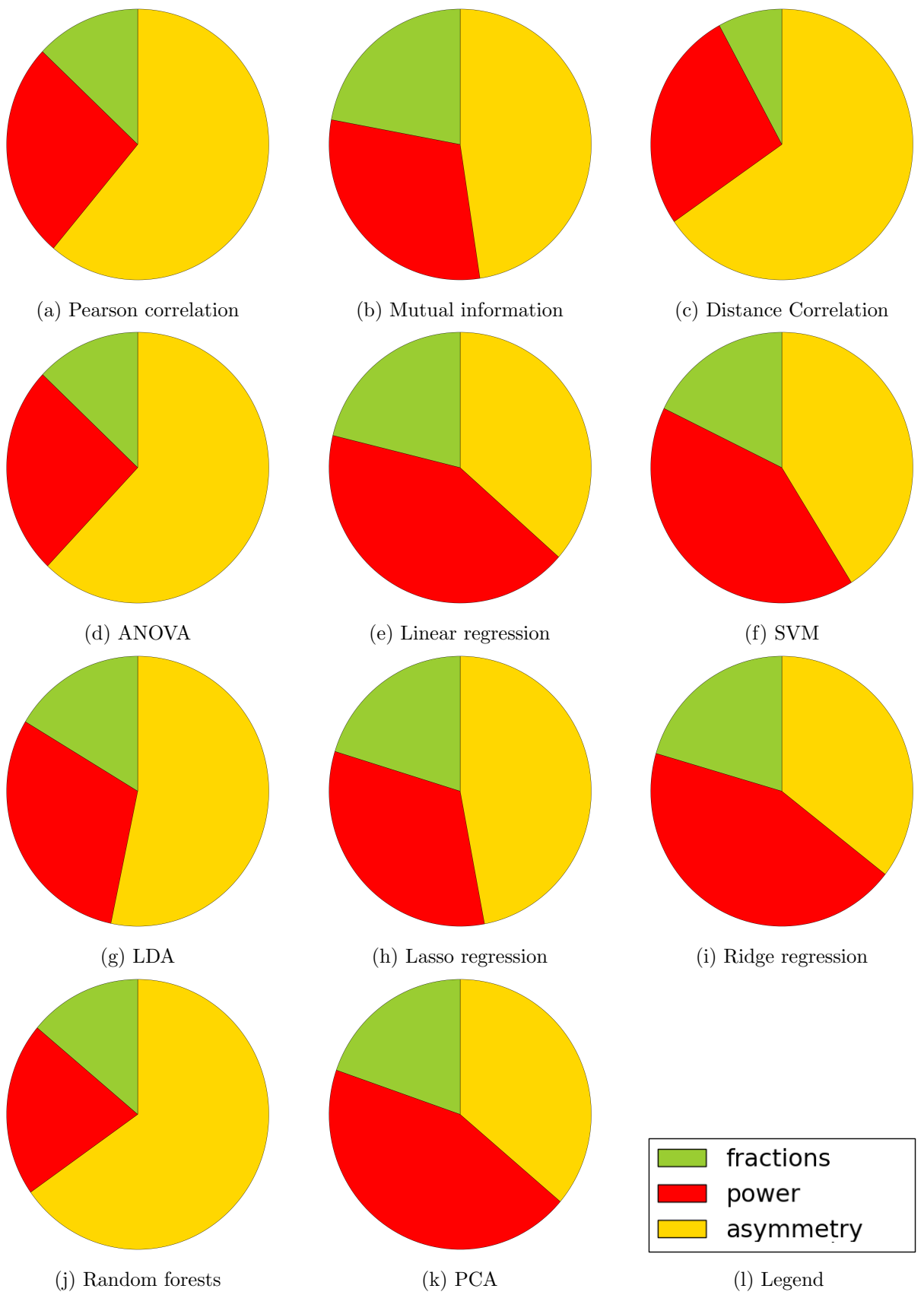


Figure 3.11: The distribution of the selected features for valence classification of all persons combined of different feature selection methods. The feature set was limited to EEG features only.

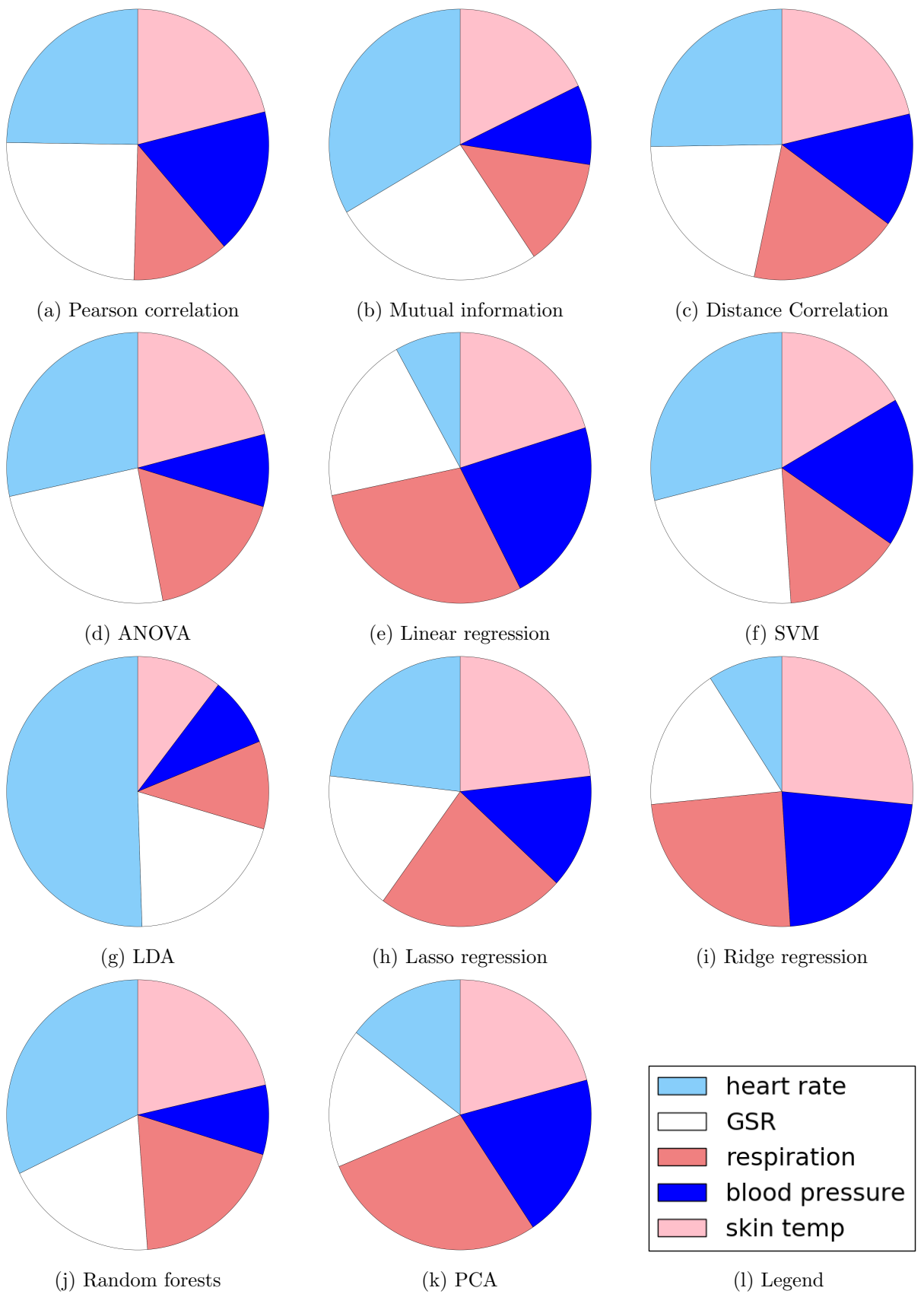


Figure 3.12: The distribution of the selected features for arousal classification of all persons combined of different feature selection methods. The feature set was limited to non-EEG features only.

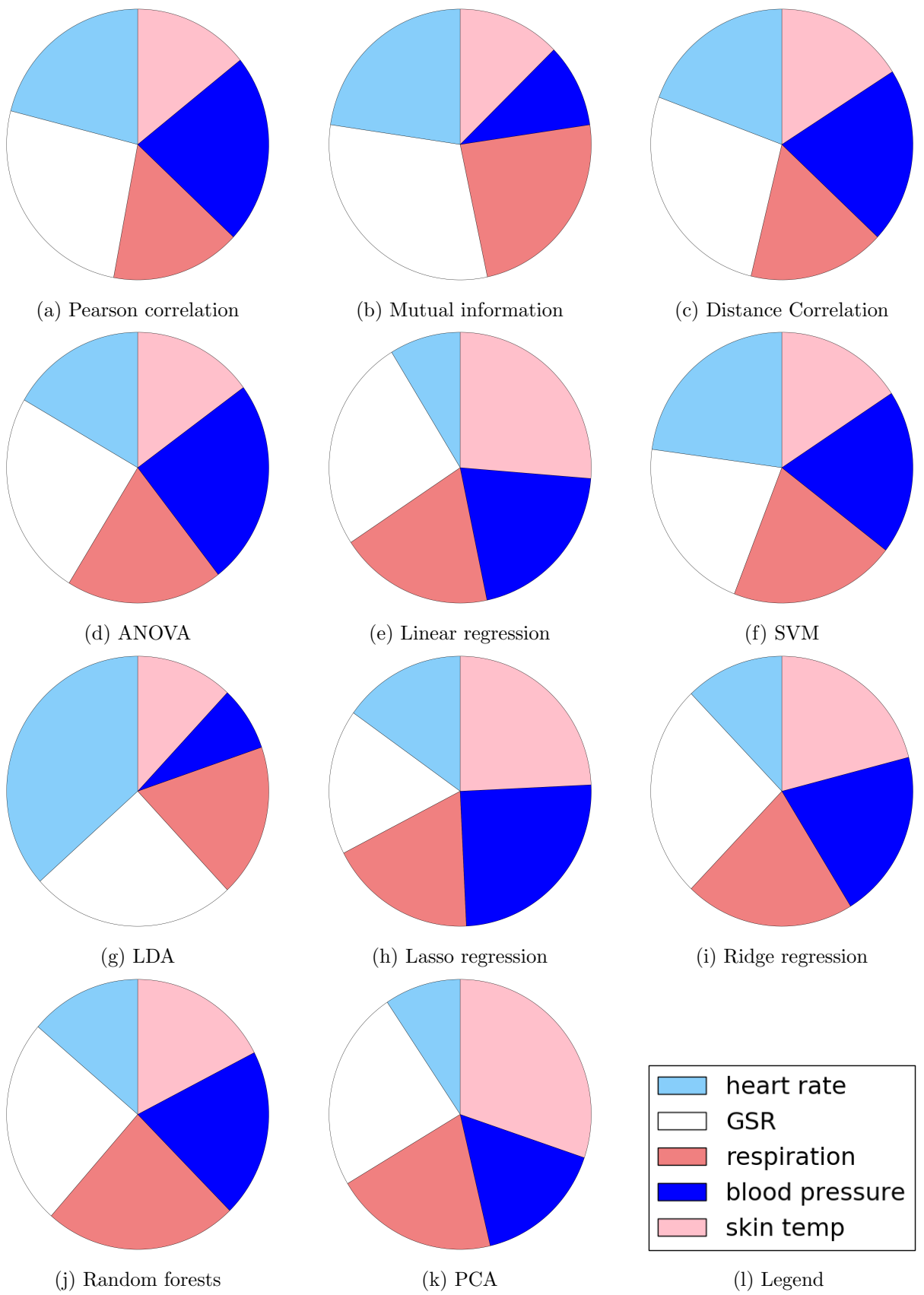
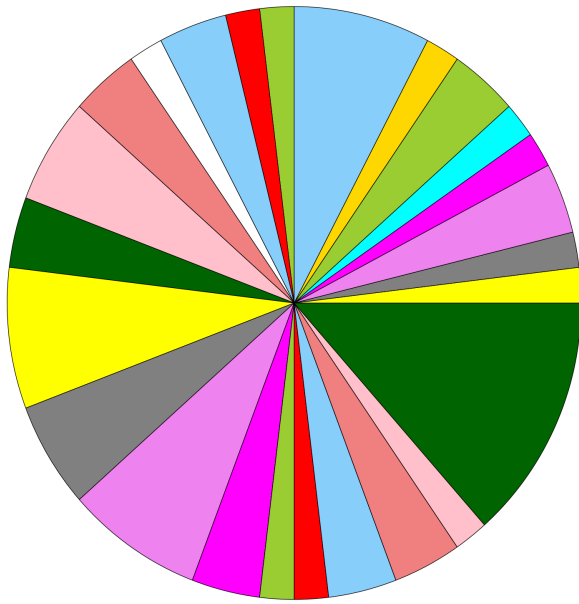


Figure 3.13: The distribution of the selected features for valence classification of all persons combined of different feature selection methods. The feature set was limited to non-EEG features only.

3.5 Important EEG channels

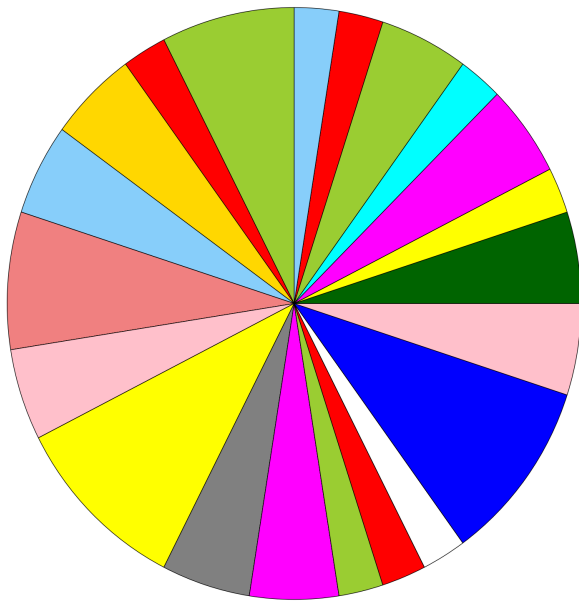
Another component of this work is to dig into the EEG features and find out which channels are most important. This was done by taking the Random forest as a feature selection model and looking at the models that were build. By simply counting the occurrences of different EEG channels in these models, pie charts were constructed. This was done for both valence and arousal. The results are displayed in Figure 3.14a for arousal and Figure 3.15a for valence.



(a) The different selected channels for arousal.

Fp1	P7	FC2
AF3	PO3	Cz
F3	O1	C4
F7	Oz	T8
FC5	Pz	CP6
FC1	Fp2	CP2
C3	AF4	P4
T7	Fz	P8
CP5	F4	PO4
CP1	F8	O2
P3	FC6	

(b) Each color and its corresponding EEG channel.



(a) The different selected channels for valence.

Fp1	P7	FC2
AF3	PO3	Cz
F3	O1	C4
F7	Oz	T8
FC5	Pz	CP6
FC1	Fp2	CP2
C3	AF4	P4
T7	Fz	P8
CP5	F4	PO4
CP1	F8	O2
P3	FC6	

(b) Each color and its corresponding EEG channel.

At first it seems that there is no agreement on the channels, one possible reason for this, might

be that electrodes are not placed exactly. Even though the 10/20 system defines the different locations quite well, it is still possible that small variations in the locations exists. Grouping the channels might give a more clear view of the important regions of the brain. The channels were grouped as follows:

Table 3.6: The region for each EEG channel

Channel	Region	Channel	Region	Channel	Region	Channel	Region
Fp1	front left	CP5	back left	Fp2	front right	C4	back right
AF3	front left	CP1	back left	AF4	front right	T8	back right
F3	front left	P3	back left	Fz	midline	CP6	back right
F7	front left	P7	back left	F4	front right	CP2	back right
FC5	front left	PO3	back left	F8	front right	P4	back right
FC1	front left	O1	back left	FC6	front right	P8	back right
C3	back left	Oz	midline	FC2	front right	PO4	back right
T7	back left	Pz	midline	Cz	midline	O2	back right

These Region are also depicted in Figure 3.16.

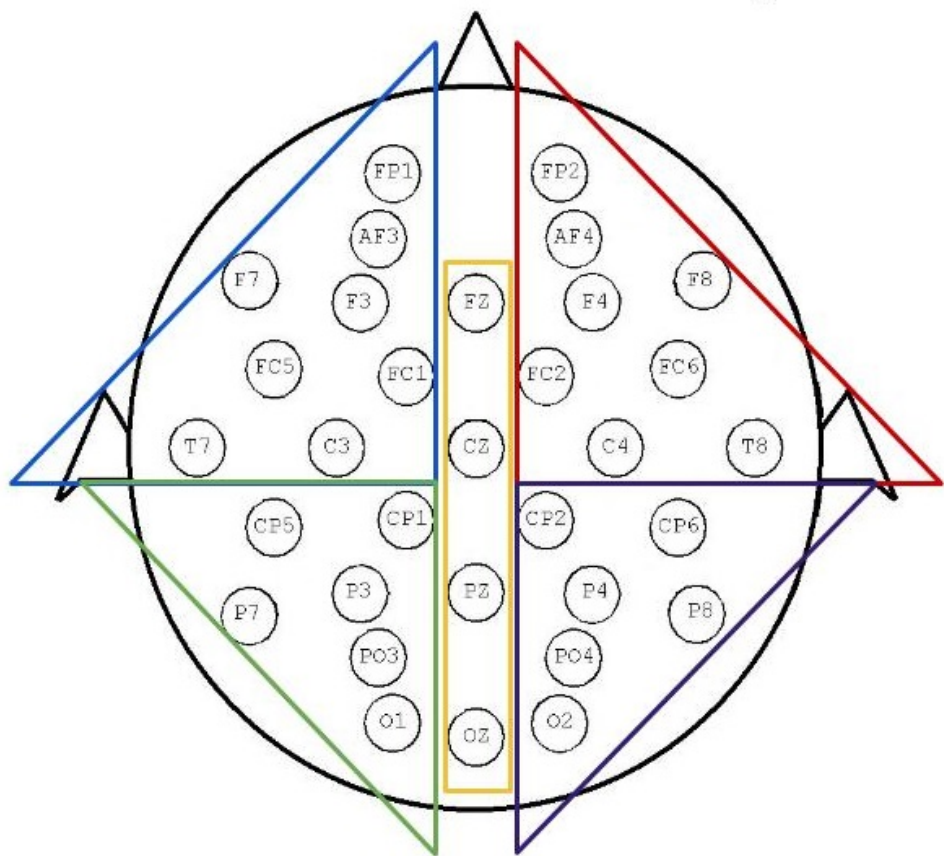
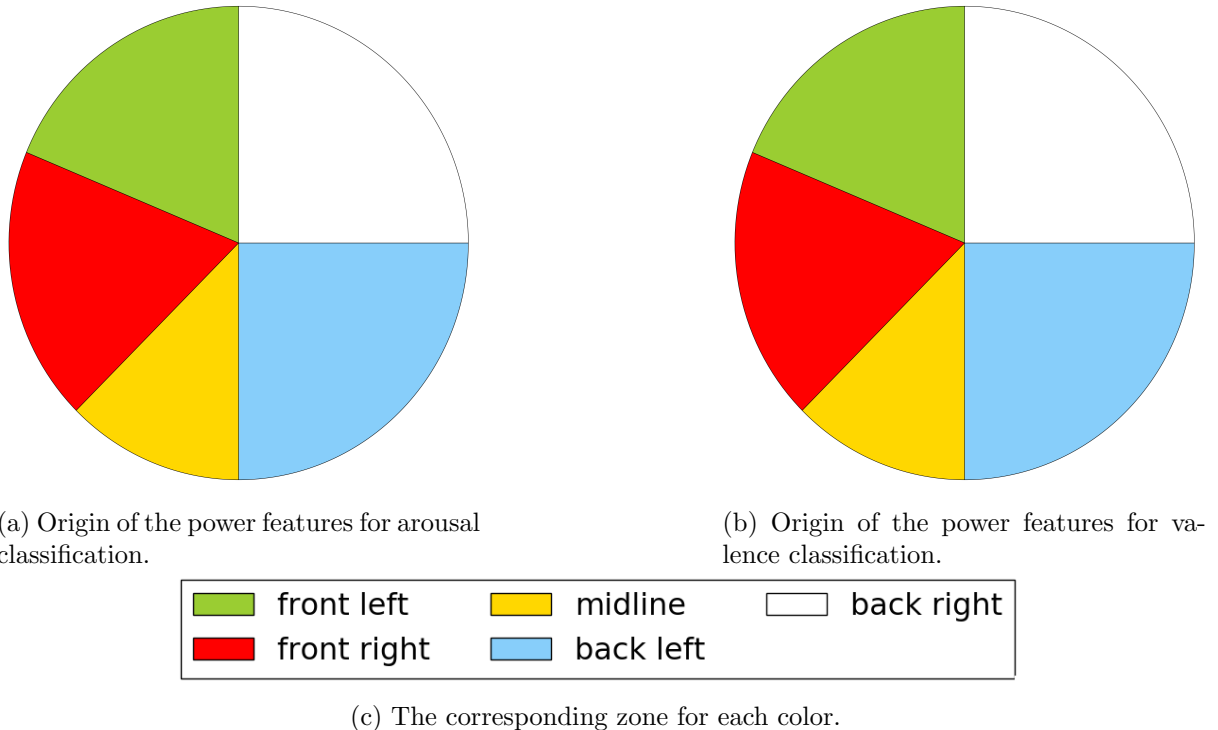


Figure 3.16: All EEG channels were grouped in 4 regions: left-front (blue), right-front (red), left-back(black), right-back (purple) and midline (yellow).

The resulting distributions are shown in Figure 3.17a for arousal and in Figure 3.17b, the legend

is shown in Figure 3.17c.

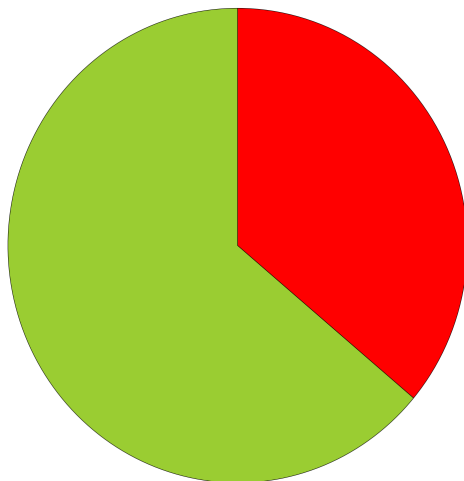


Looking at the pie plots, one can see that there is no clear region used. The back left and right regions appear most often, but the difference with the front left and right is little. It seems that for both valence and arousal, power values of all different regions might be of importance. The distributions for the regions are the same for both valence and arousal, but they differ in terms of channels.

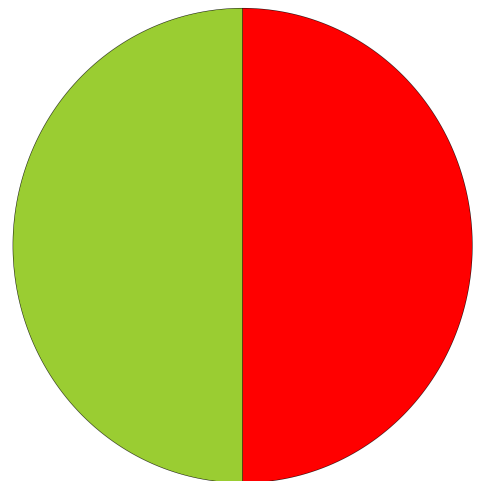
The same principle can be done for the asymmetry features, here a distinction was made between DASM and RASM features on one hand and the DCAU and RCAU features on the other hand. The DASM and RASM features were divided in channel pairs located at the front and back of the brain. A specific list is given in Table 3.7 below.

Table 3.7: the region for each DASM and RASM channel pair

Channel pair	Group	Channel pair	Group
Fp1,Fp2	front	C3,C4	back
AF3,AF4	front	T7,T8	back
F3,F4	front	CP5,CP6	back
F7,F8	front	CP1,CP2	back
FC5,FC6	front	P3,P4	back
FC1,FC2	front	P7,P8	back
		PO3,PO4	back



(a) Origin of the asymmetry features for arousal classification.



(b) Origin of the asymmetry features for valence classification.



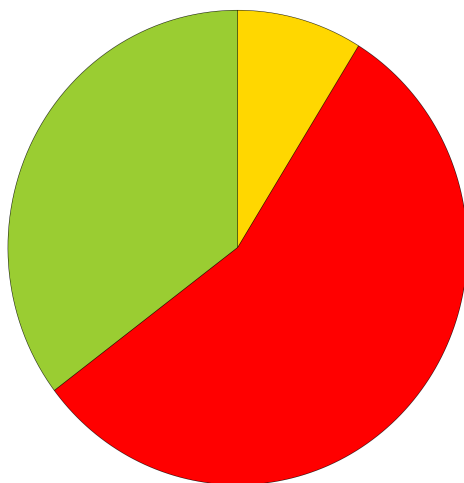
(c) The corresponding zone for each color.

For the DASM and RASM features, it is clear that the asymmetry should be measured at the front of the scalp for arousal. For valence however, features are selected from the front and the back of the scalp. This is in contradiction with the literature, most studies suggest that the frontal asymmetry of alpha power is most valuable.

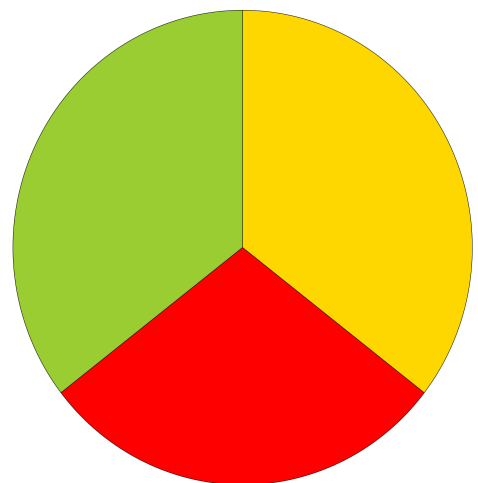
The caudality features also measure asymmetry, but between a frontal and posterior channel. Here, the channel pairs were grouped in three groups: left, right and Fz/Pz, since the Fz/Pz channel pair lies on the central line. The specific grouping is shown in Table 3.8 below.

Table 3.8: The region for each corresponding DASM and RASM channel pair.

Channel pair	Group	Channel pair	Group
FC5,CP5	left	FC6,CP6	right
FC1,CP1	left	FC2,CP2	right
F3,P3	left	F4,P4	right
F7,P7	left	F8,P8	right
Fp1,O1	left	Fp2,O2	right
Fz,Pz			



(a) Origin of the asymmetry features for arousal classification.



(b) Origin of the asymmetry features for valence classification.



(c) The corresponding zone for each color.

For the arousal it seems that the caudality of the right of the brain might be of more interest. Valence uses caudality features from all over the brain.

These results indicate that for valence can be measured with channels from all over the scalp, while arousal seems to rely most on frontal channels.

3.6 Stability

Random forests have the disadvantage that they have an element of randomness, meaning that they might not always select the same features, making them potentially unstable. It is possible to make the random forest algorithm more stable, by adding additional trees or running the algorithm several times and averaging the importance values.

One way to measure the stability is to run the algorithm twice and look at the similarity of the selected features. The similarity can be calculated using the Jaccard index, as explained in Section 2.4.3. The importances of the random forest features selection were averaged over 30 runs to ensure stability. The Jaccard index was measured for several runs for each person. The average and standard deviation over all persons is shown in Table 3.9.

Table 3.9: The Jaccard index of two consecutive features sets for the random forest feature selection method. The indexes are averaged over all persons.

What	runs	Average Jaccard index	STD Jaccard index
valence	1	0.83021	0.20581
valence	5	0.64683	0.21850
valence	10	0.63963	0.24620
valence	20	0.66682	0.25415
valence	30	0.74313	0.24272
valence	40	0.77958	0.22432
valence	50	0.76278	0.24394
arousal	1	0.83318	0.18140
arousal	5	0.61578	0.27061
arousal	10	0.70878	0.24949
arousal	20	0.70873	0.24849
arousal	30	0.79145	0.24380
arousal	40	0.77422	0.21200
arousal	50	0.76370	0.22673

Looking at Table 3.9, the Jaccard index is less stable when fewer runs are used, due to the fact that the importance values are estimated a limited number of times. When the random forest feature selection uses importance values, averaged over 30 runs, the value of the Jaccard index become more or less stable, around 0.75-0.77. One thing to keep in mind though is that the standard deviation of 0.2-0.25 is quite large, which means that the stability of the RF method varies from person to person.

4

Results - Cross-subject

This chapter focusses on features that work well for emotion recognition of several persons. The contents are as follows, first the difference with the person specific approach is explained. Next the performance of different feature selection methods is compared. Then the important features and EEG channels are discussed. This chapter ends with a discussion about the stability of the methods.

The second part of this work was to search for features that work well in a cross-subject setting, meaning that the model was trained on one set of persons/subjects and then tested on another set, containing different persons/subjects. This part is more challenging because physiological signals are very personal by nature [6].

4.1 Approach

The approach from Section 3.1 was modified slightly. The main difference is that the splits in test and train set as well as the cross validation was based on subjects. Once a single sample from a subject is placed in a set, all his other samples are added as well. Special care was taken to ensure that the random forest would also work correctly. The problem with random forest is that it creates an out of bag sample, as explained in Section 2.4.3. Because this out of bag sample is used for validation, a custom random forest was created. This random forest splits the out of bag sample based on the different subject.

4.2 Performance

The performance of the different algorithms is depicted in Figure 4.1 for arousal and Figure 4.2 for valence. The legend, combined with an overview of the accuracy values is given in Table 4.1. The performance in a cross-subject setting is lower than the aforementioned person specific results. This is not surprising, considering that EEG data is very personal by nature. A person specific classifier, using the random forest's build-in feature selection method, achieves a test accuracy around of 70% (stdev. of 14) for arousal and 73% (stdev. of 13) for valence. The performance of the cross-subject classifier is 63% for arousal and 55% for valence. This is a drop of 7 % and 18 %. The performance for the arousal classification is lower in a person specific setting, but drops less when transitioning to a cross-subject setting, when compared to the valence classification. The performance of the valence classification, on the other hand, takes a huge drop. This might indicate that the physiological reactions with respect to valence, might

be more person specific. Another explanation might be that users are more consistent when rating arousal, than rating values. This would mean that everyone has more or less the same idea of active and inactive, while happy and unhappy are less strictly defined.

Table 4.1: A comparison of the test accuracy of different feature selection methods for both arousal and valence. The reported scores are test accuracies averaged over .

Number	Feature selection method	Test acc - arousal	Test acc - valence
0	Pearson R	0.62187	0.51875
1	Mutual information	0.59688	0.56563
2	Distance correlation	0.58125	0.51875
3	Linear regression	0.61562	0.55312
4	Lasso regression	0.59688	0.55312
5	Ridge regression	0.58125	0.55937
6	SVM	0.60938	0.5375
7	Random forests	0.63438	0.55312
8	ANOVA	0.60312	0.53438
9	LDA	0.63438	0.52812
10	PCA	0.62187	0.5375

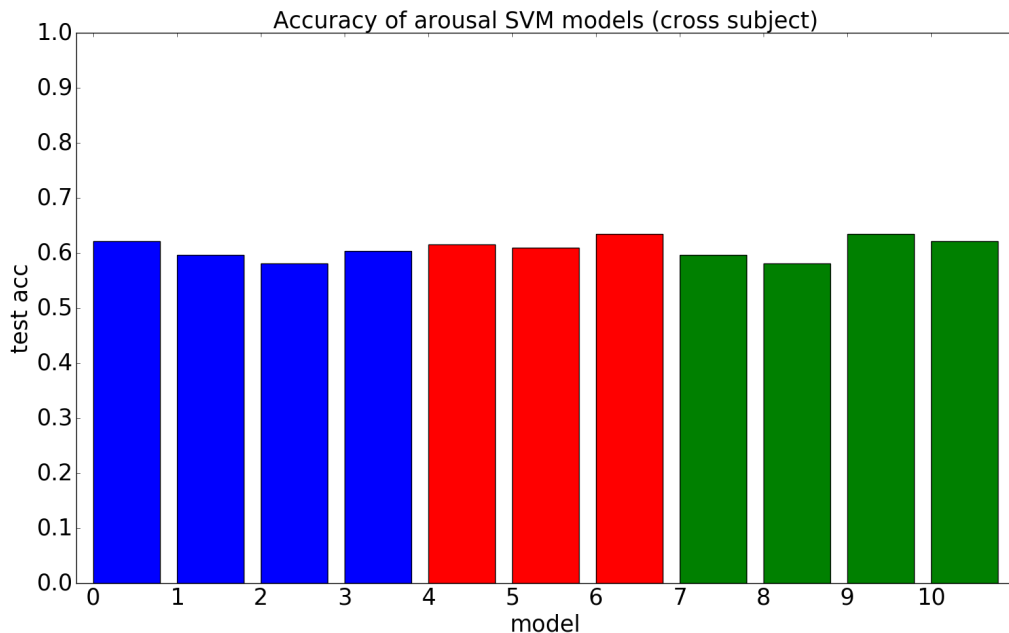


Figure 4.1: Comparison of different feature selection methods' test accuracies for arousal recognition in a cross-subject setting. The blue bars correspond to filter selection methods. Red bars correspond to wrapper methods and green bars are used for the embedded methods.

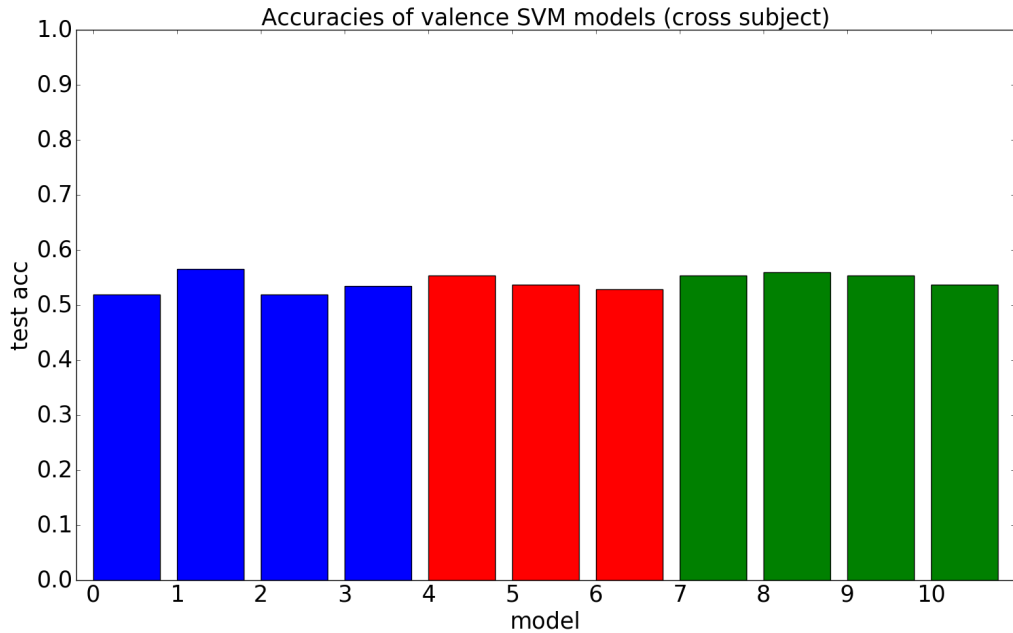


Figure 4.2: Comparison of different feature selection methods' test accuracies for valence recognition in a cross-subject setting. The blue bars correspond to filter selection methods. Red bars correspond to wrapper methods and green bars are used for the embedded methods.

4.3 Correlation probability and level of valence/arousal

The correlation between the prediction probability of a model and the distance of the arousal/valence level from the separation boundary was also research. In an ideal scenario, samples with a clear valence rating, i.e. far from the separation boundary, e.g. 9, should be easier to predict than one with a valence rating close to the separation boundary, e.g. 5 or 6. A model should be more certain of valence/ arousal values that lie further away from the separation boundary.

The Pearson correlation coefficients between the prediction probability and the distance to the separation are shown in Table 4.2. These values were also plotted in Figure 4.3 and Figure 4.4 for arousal and valence respectively.

For arousal, the correlations are quite low, even negative. The distance correlation features, are more promising, but the disadvantage of this method is that it cannot find groups of good features. It might thus be overfitting on a few features that work well for this sample set. This is further supported when looking at the correlations for valence. Here the correlation is even negative.

Table 4.2: The correlations between the prediction probability of the different feature selection methods and the distance to the separation boundary.

Number	FS Method	corr. arousal	corr. valence
0	Pearson	0.03295	-0.05998
1	mutual information	0.02339	-0.09995
2	distance correlation	0.15635	-0.14668
3	ANOVA	0.00430	-0.01410
4	linear regression	-0.00791	0.04455
5	SVM	0.00085	0.07638
6	LDA	-0.02715	0.06226
7	lasso regression	0.02972	0.00575
8	ridge regression	-0.04213	0.03564
9	random forests	0.07254	0.05722
10	PCA	-0.06113861835	-0.07378720791

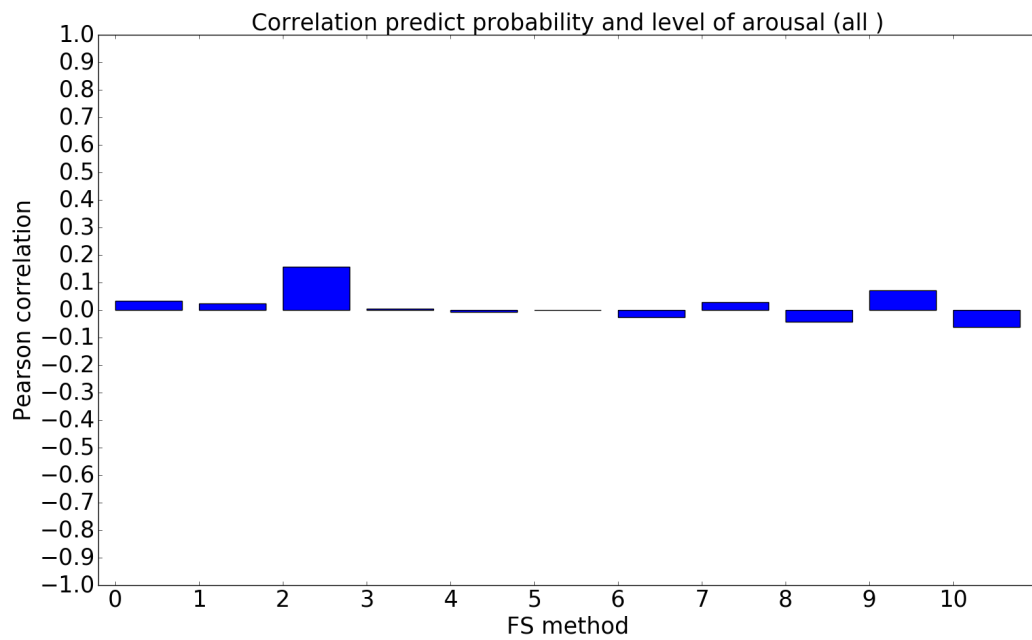


Figure 4.3: The pearson correlations of the model's prediction probability versus the distance between the subject's level of arousal and the separation boundary in a cross-subject setting.

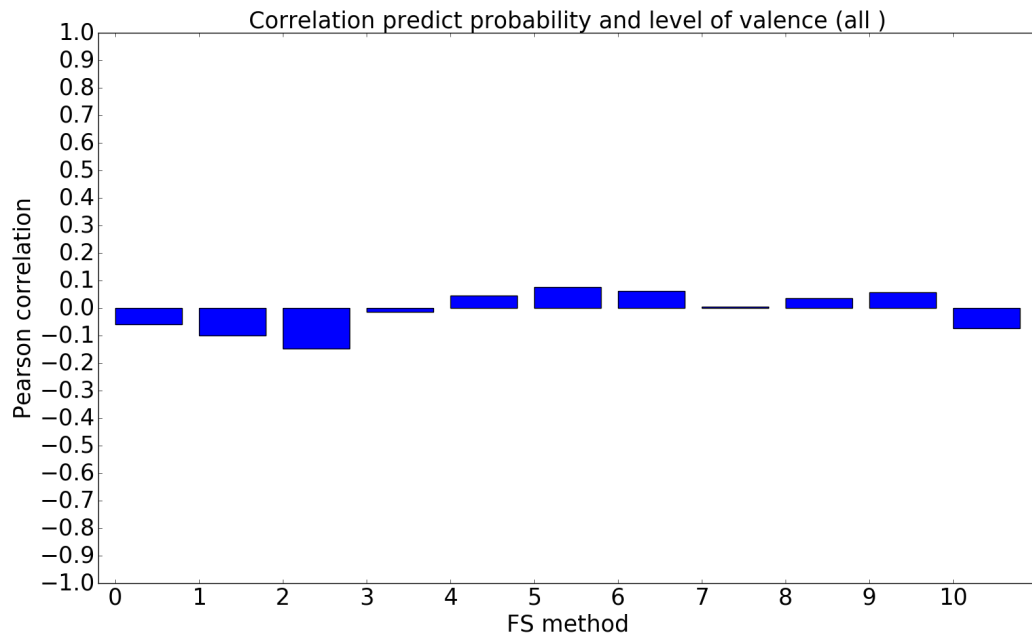


Figure 4.4: The pearson correlations of the model’s prediction probability versus the distance between the subject’s level of valence and the separation boundary in a cross-subject setting.

Similar to the person specific results discussed in Section 3.3, the correlations are quite low. Some correlations are even negative, meaning that the model is more certain of examples that lie closer to the separation boundary. To explain why, additional research might be needed. At first sight, several explanations for this are possible:

1. The correlation is present, but is more complex than a simple linear correlation. As a result, the Pearson coefficient is not able to capture this correlation well.
2. The assumption that high valence and arousal values are easier to recognise is wrong. It might be possible that a high valence/arousal levels do not correspond to increased physiological responses. Future research could look at the dominance values, that indicate how strong the emotion is perceived. The dominance values are explained in Section 1.1 and were neglected during this work.

However one has to keep in mind that it might be difficult to draw conclusions from these results, as the performance of the cross-subject emotion recognition is quite low.

4.4 Selected features

To compare which features where chosen, the feature set was, again divided into 8 categories:

1. **Power features:** PSD and FE features of a single channel
2. **Asymmetry features:** DASM, RASM, DCAU and RCAU features that represent a the (a)symmetry between two channels.

3. **Fractions:** Alpha/beta and fractions of different power ratios of a channels.
4. **Heart rate:** the statistical values of the heart rate.
5. **Galvanic skin response:** the statistical values of the GSR.
6. **Respiration:** the statistical values of the respiration.
7. **Blood pressure:** the statistical values of the plethysmograph.
8. **Skin temp:** the statistical values of the skin temperature.

The selected features are depicted in Figure 4.5 and 4.6 for arousal and valence respectively.

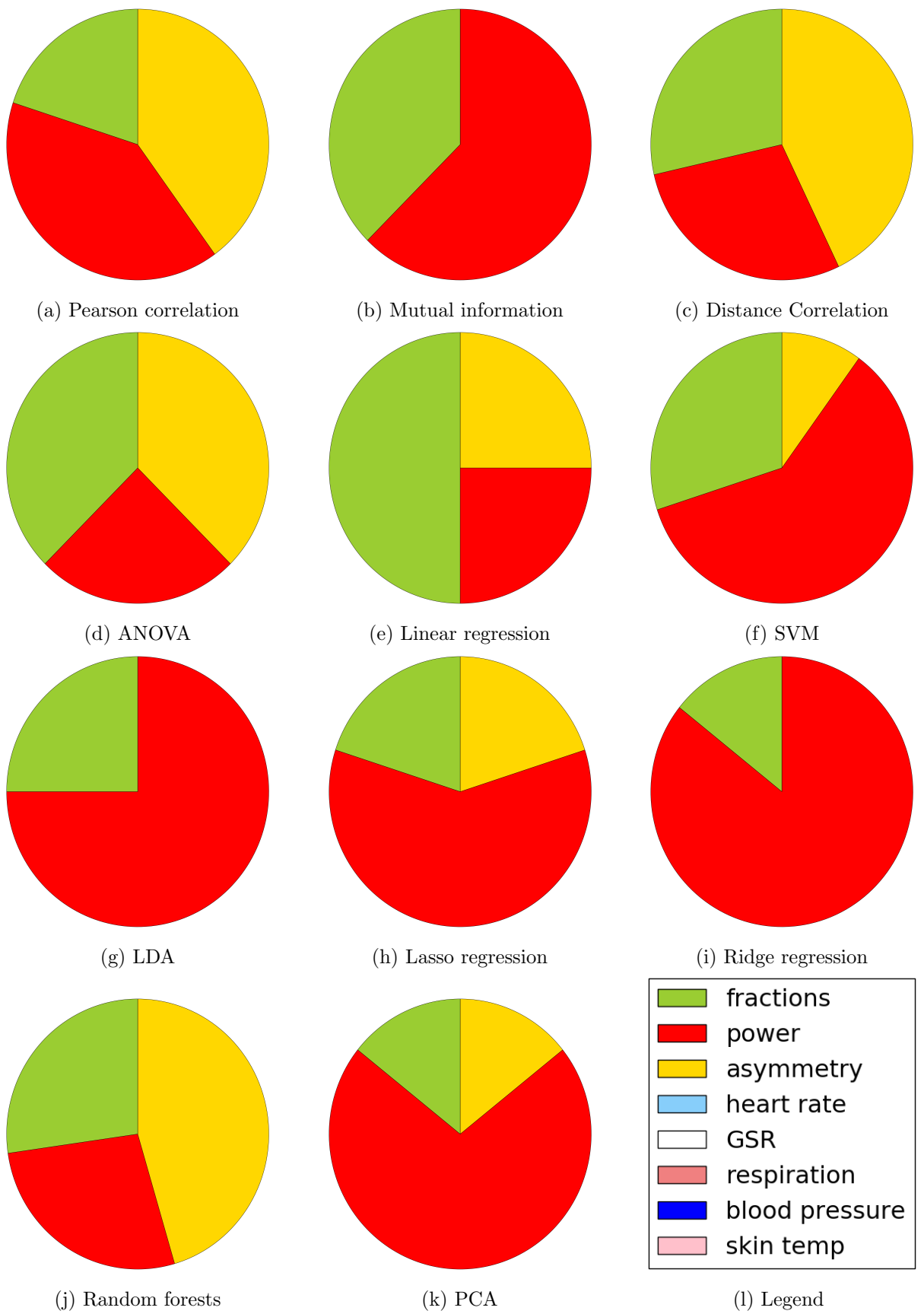


Figure 4.5: The distribution of the selected features for arousal classification in a cross-subject setting for different feature selection methods. It is clear that the most valuable features are the asymmetry features combined with the power features. Furthermore, all feature selection methods agree that EEG features are dominant.

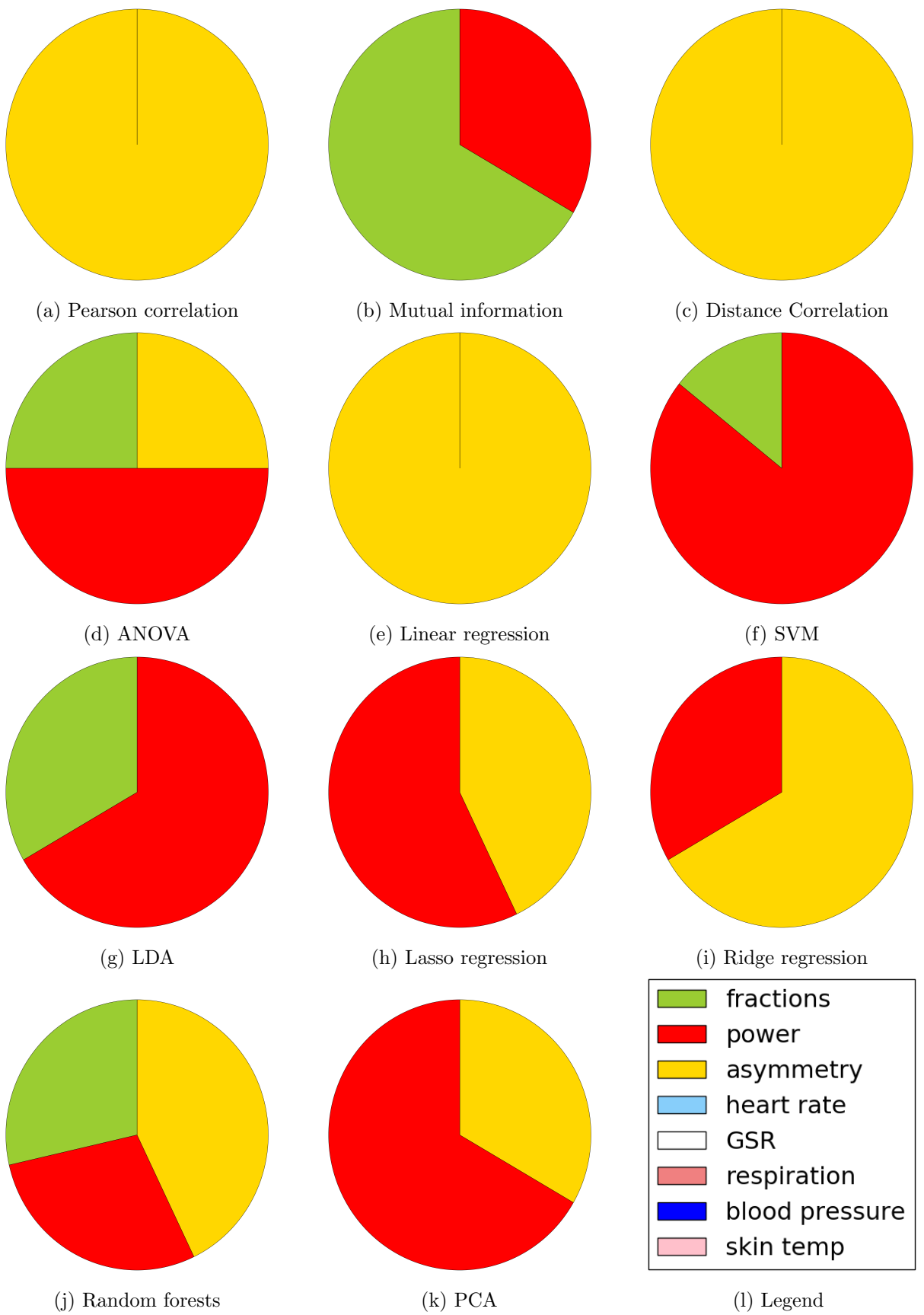


Figure 4.6: The distribution of the selected features for valence classification in a cross-subject setting for different feature selection methods. It is clear that the most valuable features are the asymmetry features combined with the power features. Furthermore, all feature selection methods agree that EEG features are dominant.

For arousal, it is clear that the EEG features are quite dominant. None of the non-EEG features were selected. The EEG features themselves differ from selection method to selection method. One possible explanation for this is that the accuracies of the model are quite low. The models are thus not fitting very well. This may cause unstable behaviour. The random forest method is the most advanced feature selection method and it gives a small preference to asymmetry features. This concurs with the person specific findings.

Similar things can be observed for valence. Again, the asymmetry features are preferred by the random forest, which concurs with similar studies. It might be important to note that there is a high correlation between asymmetry and the valence, which is visible when looking at the Pearson correlation output.

To further look at the difference between EEG and non-EEG features, the random forest selection method was again used three times. The first time, all features were available. The second and third time, only EEG and non-EEG features were available respectively. The results are shown in Figure 4.7, for arousal and Figure 4.8 for valence. The exact values are shown in Table 4.3.

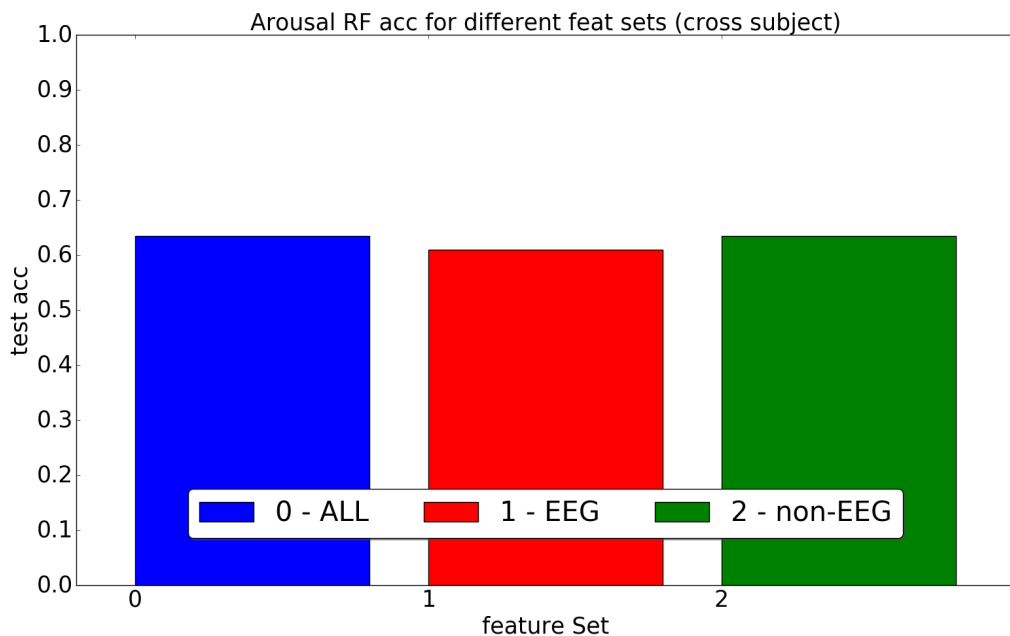


Figure 4.7: The performance of arousal prediction for all, EEG and non-EEG features on the test set in a cross-subject setting.

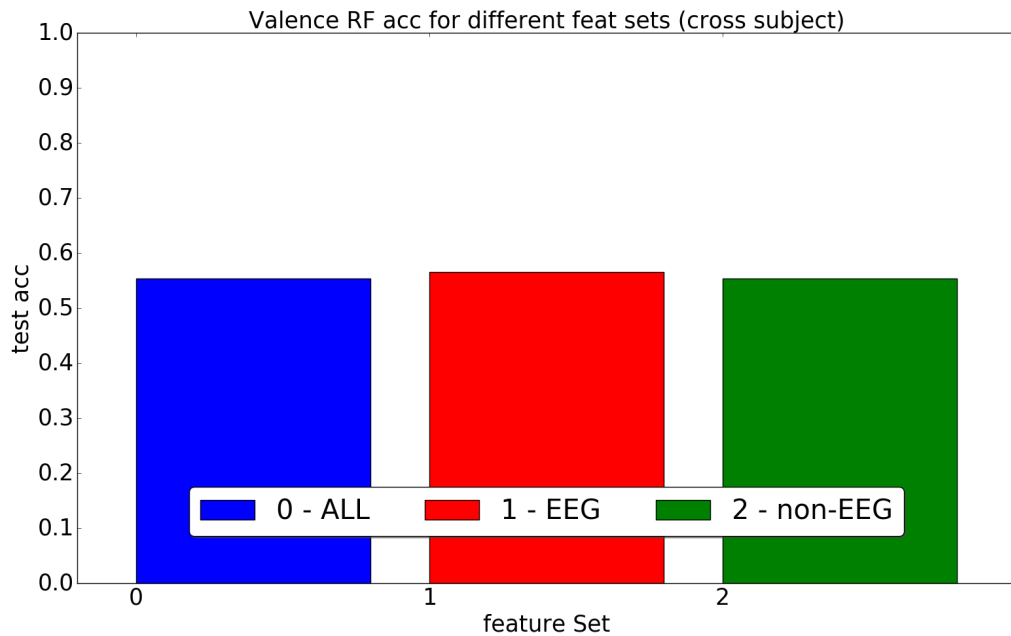


Figure 4.8: The performance of valence prediction for all, EEG and non-EEG features on the test set in a cross-subject setting.

Table 4.3: The test accuracies for both arousal and valence, using different feature sets.

Feat set	Acc - arousal	Acc - valence
All	0.6344	0.5531
EEG	0.6094	0.5656
non-EEG	0.6344	0.5531

Comparing Table 4.3 with Table 3.4, one can see that the difference in accuracy between non-EEG features and all and/or EEG features only is much smaller. This is an indication that the non-EEG features might work better in a cross-subject setting. The reason that the feature selection methods select only EEG features might be due to the fact there are more EEG features available. Given that EEG features often contain a lot of noise, chances are that the selection methods are able to find EEG features that fit the limit sample set well.

To find out which non-EEG feature might be useful, the selected non-EEG features from the random forest selection method were analysed. The resulting model of each feature selection method is quite different. The random forest seems to prefer skin temperature, heart rate and GSR for arousal and blood pressure combined with GSR for valence.

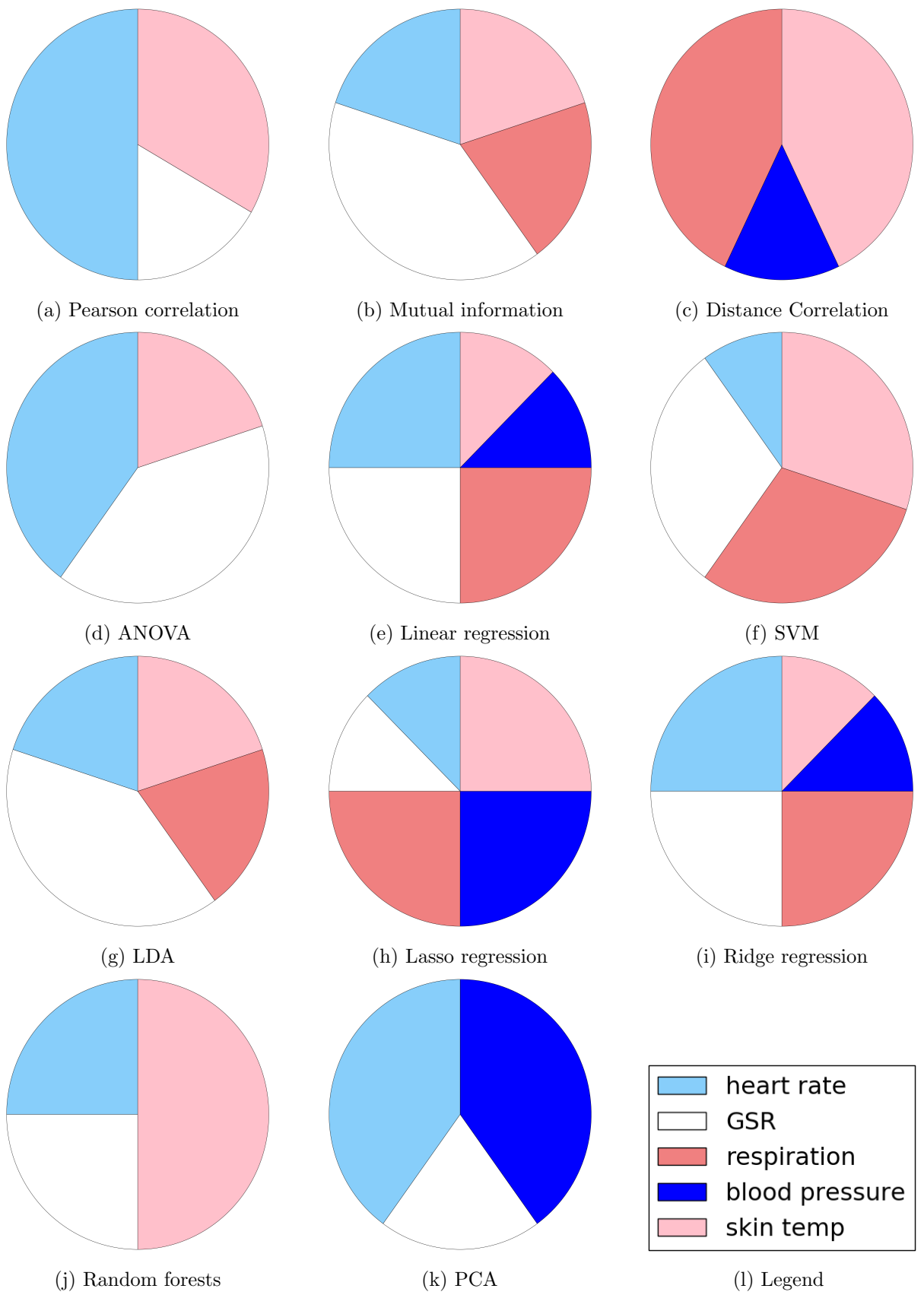


Figure 4.9: The distribution of the selected features for arousal classification in a cross-subject setting for the different feature selection methods. The feature set was limited to non-EEG features only.

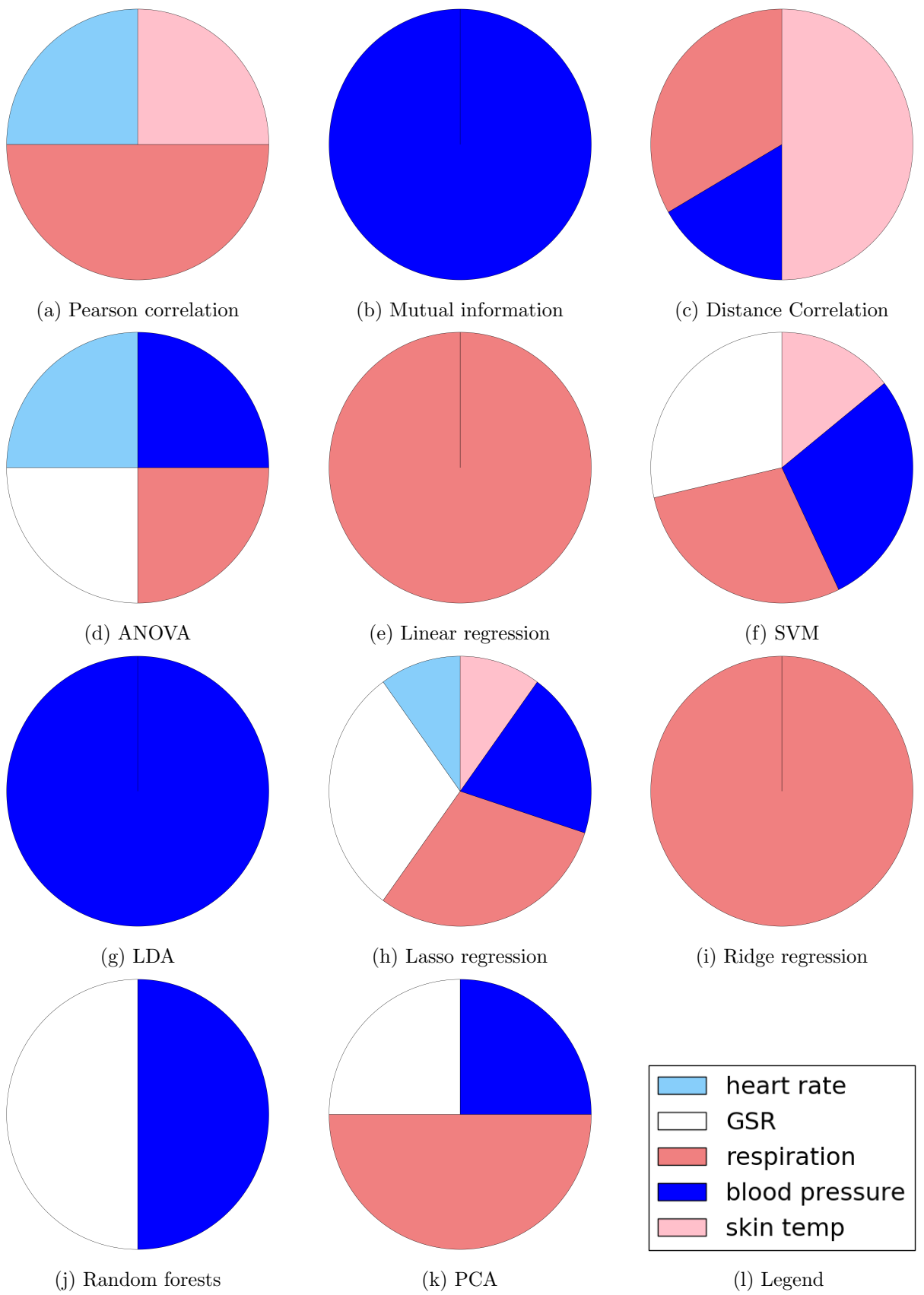


Figure 4.10: The distribution of the selected features for valence classification in a cross-subject setting for the different feature selection methods. The feature set was limited to non-EEG features only.

4.5 Important EEG channels

The features used in the model build with the random forest feature selection for arousal are:

1. DE P4, gamma band
2. DE Cp1, gamma band
3. RCAU Fp2, O2, all bands
4. RCAU FC5, Cp5, all bands
5. DCAU Fz, Pz, all bands
6. fraction Cz, beta band
7. fraction P7, beta band

For valence the features are:

1. DCAU Fz,Pz, beta band
2. DASM CP1,CP2, beta band
3. DE Pz, gamma band
4. DCAU Fz,Pz, gamma band
5. frac Fz, delta band
6. DE Fz, theta band
7. DCAU F4,P4, gamma band
8. frac P3, delta band

In a cross-subject setting, the DCAU features seem to perform well. These features are selected from front and posterior channels. However these results should be treated with caution, especially in case of valence, which only obtained a test accuracy of 55%. If the classifier was not able to predict the emotional states well, one can doubt the selected features.

4.6 Stability

Random forests have the disadvantage that they have an element of randomness, meaning that they might not always select the same features, making them potentially unstable. It is possible to make the random forest algorithm more stable, by adding additional trees or running the algorithm several times and averaging the importance values.

One way to measure the stability is to run the algorithm twice and look at the similarity of the selected features. The similarity can be calculated using the Jaccard index, as explained in Section 2.4.3. The importances of the random forest features selection were averaged over 30

runs to ensure stability. The Jaccard index was measured for several runs, the results are shown in Table 4.4.

Table 4.4: The Jaccard index of two consecutive features sets for the random forest feature selection method.

what	runs	Jaccard index
valence	1	0.89432
valence	5	0.90278
valence	10	0.92562
valence	20	0.90000
valence	30	0.88522
valence	40	0.92930
valence	50	0.90909
arousal	1	0.93048
arousal	5	0.86364
arousal	10	0.86364
arousal	20	0.88025
arousal	30	0.87273
arousal	40	0.89721
arousal	50	0.90190

When comparing the cross-subject results in Table ?? with the person specific results in Table 3.9, it is clear that the random forest selection method is more stable in the cross-subject setting. This is due to the fact that here, training data of different persons is combined, which results in a large data set for the RF method to estimate the importances.

5

Conclusion

This chapter will give the conclusion of this work for both person specific and cross-person emotion recognition.

5.1 Person specific

In case of arousal, the conclusion is that it is possible to achieve accuracies around 73% on the DEAP dataset. The random forest is the best feature selection method as it is more certain when the arousal or valences are more extreme. The most prominent features for arousal recognition, according to this study, were the asymmetry features. Those features are often described as good features for valence recognition though. Repeating this study with more data, might be desired.

For valence, it is indeed confirmed that the asymmetry features work best. These asymmetry features should not be limited to the asymmetry of frontal channels. Posterior channels also seem to contain additional information. A performance of 70% was obtained which is similar, if not better than the state of the art studies described in Section 2.3.

The performance of non-EEG features is statistically proven to be lower than the performance of the all and EEG-only feature sets. One can conclude that adding non-EEG features will not improve performance. This is further supported by the fact that all feature selection methods rarely select non-EEG features.

5.2 Cross-subject

The main conclusion for cross-subject emotion recognition, is that cross-subject emotion recognition is still an open topic for research. Physiological signals are quite personal by nature, which might explain the drop in performance.

A distinction between arousal and valence should be made though. The performance of valence classification was around 55%, while the performance of arousal was around 63%. This indicates that physiological reactions to arousal levels, are more common between persons than reactions to valence levels. The performance for valence was better than the performance of arousal recognition in person specific setting. This means that reactions to changes in a person's valence level, are more distinguishable in physiological signals, but more person specific. Different persons will react different to changes in valence levels.

Arousal levels on the other hand are harder to recognize, but the reaction seem to be more shared. Different persons will react more similar to a change in arousal than a change in valence.

Further research is needed to confirm this, as the problem could also be in the labelling. Each subject rated their own feeling, which might result in biased ratings, i.e. an valence level of 6 might have a different meaning for person A than person B. Following this line of thought, the difference between valence and arousal classification would be that subjects have a more common definition of active/inactive, than they have on happy/unhappy.

Another thing to note is that non-EEG features work better in a cross-subject setting than in a person specific setting. The selected features are again EEG features. When comparing the performance of the ALL, EEG-only and non-EEG-only features sets, the non-EEG set scores higher in a cross-subject setting than a person specific set. This might mean that non-EEG, physiological reactions to changes in an emotional state are more common between different persons than the reaction inside a person's brain features.

To further improve the performance of cross-subject emotion recognition, simple feature selection will not suffice. Instead, more complex techniques like transfer learning are desired.

6

Future Research

This chapter gives an overview of research that can be done on this subject

6.1 Applications for emotion recognition

Emotion recognition has many different applications, e.g. as an improvement for brain computer interfaces or marketing analysis. A Brain Computer Interface (BCI), creates a direct link between the brain and the computer[52], that enables a subject to control the computer using only his mind. This means that physical actions like moving a mouse or typing on a keyboard are no longer needed to control a computer. A BCI is usually composed of two components. The first component is the extraction component, which extracts brain signals from the brain. The second component is a decoder that interprets signals translates them to device commands.

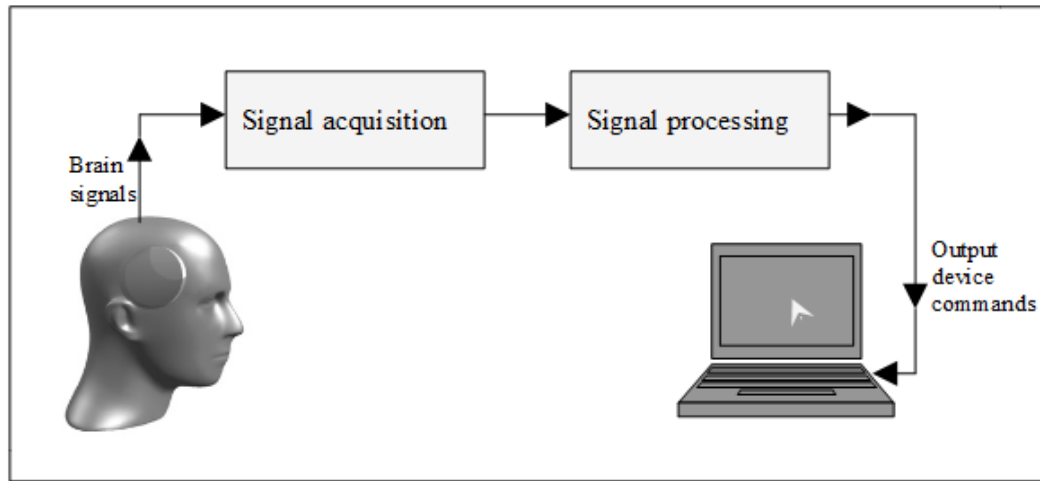


Figure 6.1: The basic components of a BCI system[8]

A very well-known BCI is the P300 speller. The P300 speller is an active topic of research. It uses EEG signals to enable patients with a locked in syndrome to communicate[53]. The basic version uses a six by six grid of characters, each row and column is flashed in a random order while the subject silently counts the number of flashes of a certain character, as shown in figure

6.2. This procedure, where a train of stimuli with some infrequent occurring target stimuli is applied, is called the oddball paradigm[54]. It is known that this technique triggers an increase in the potential difference in the EEG around the parietal lobe. When a potential difference in the brain occurs as a reaction to an event, it is referred to as an event-related potential (ERP). The P300 ERP occurs roughly 300 milliseconds after the stimulus is flashed, hence its name[55]. The presence or absence of the P300 waveform is used by the P300 speller to determine what character the subject was focusing on, which basically allows the subject to spell text.

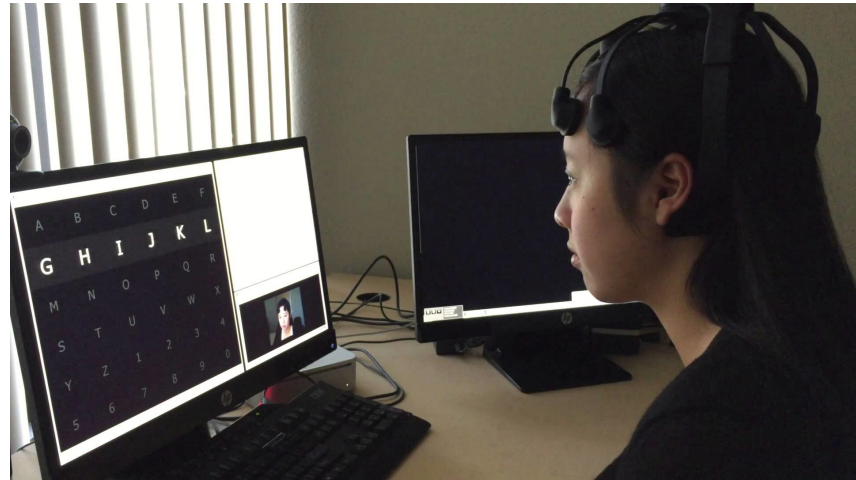


Figure 6.2: Different parts of the P300 speller, found at [9].

Research with visual stimuli on healthy subjects, has shown that emotion has an effect on the auditory P300 wave[56]. Both the P300 peak amplitude and area were highest when viewing neutral pictures and descended further, in decreasing order, for sadness, anger and pleasure. The latency of the P300 ERP speller was shortest for subjects in an emotionally neutral state. The latency increased for pleasure, anger and sadness. It is expected that a visually triggered P300 wave, will also be influenced by emotion. Having a good emotion recognition system, can help a P300 detector in finding the correct latency of the P300 wave. This can then, in turn improve the detection of P300 waves. Additionally knowing a subject's emotional state can help detecting when a subject gets frustrated, e.g. because of mistakes he makes.

An improvement in performance is not the only advantage an emotionally aware P300 speller has. Contrary to what subjects might think, the P300 speller is unable to read the mind and know what a person is thinking about[53]. The P300 speller provides no more than a means of communication that the subject can use. Should he choose to ignore the instructions and focus his attention elsewhere, then the recordings become useless. Nevertheless, ethical questions often remain unanswered. Knowing how the subject feels, can provide more insight for ethical issues, e.g. "How does the subject think about the P300 speller recording and analysing his brain activity?". Information about the subject's emotional state can help answering some of these ethical questions. Integrating the results from this thesis with the P300 speller, is an opportunity for future research.

Another application for emotion recognition is in the field of marketing and customer satisfaction research. Discovering how a person feels about a product is often tricky. Questionnaires is one way to go, but they might contain a lot of noise. Being able to 'read' the emotion straight from a subject's mind, is expected to give more accurate results as it avoids any form of social masking.

Bibliography

- [1] P. C. Trimmer, E. S. Paul, M. T. Mendl, J. M. McNamara, and A. I. Houston, “On the evolution and optimality of mood states,” *behavioral sciences*, vol. 3, pp. 501–521, August 2013.
- [2] Y. Han, S. Suk Oh, J. K. Kang, and H. Park, “Simultaneous measurement of fmri and eeg - principles and applications,” *intech*, May 2014.
- [3] unknown, “Electrode placement,” 2015.
- [4] Konstantin, “A brief history of intelligence,” 2011.
- [5] stackexchange, “When is a model underfitted,” 2016.
- [6] S. Koelstra, C. Muhl, M. Soleymani, J.-S. Lee, A. Yazdani, T. Ebrahimi, T. Pun, A. Ni-jholt, and I. Patras, “Deap: A database for emotion analysis ;using physiological signals,” *Affective Computing, IEEE Transactions on*, vol. 3, pp. 18–31, Jan 2012.
- [7] Citizennet, 2016.
- [8] A. Sangari, “What is a brain computer interface,” 2016.
- [9] Cognionics, “Cognionics dry eeg p300 speller demo,” 2015.
- [10] K. Takahashi, “Remarks on emotion recognition from multi-modal bio-potential signals,” vol. 3, pp. 1138–1143 Vol. 3, Dec 2004.
- [11] K.-E. Ko, Hyun-Chang, and K.-B. Sim, “Emotion recognition using eeg signals with relative power values and bayesian network,” *International Journal of Control, Automation, and Systems*, 2009.
- [12] Y. Lio, O. Sourina, and M. K. Nguyen, “Real-time eeg based human emotion recognition and visualization,” 2010.
- [13] D. O. Bos, “Eeg-based emotion recognition,” 2007.
- [14] F. Dellaert, T. Polzin, and A. Waibel, “Recognizing emotion in speech,” in *Spoken Language, 1996. ICSLP 96. Proceedings., Fourth International Conference on*, vol. 3, pp. 1970–1973 vol.3, Oct 1996.
- [15] J. Wagner, J. Kim, and e. André, “From physiological signals to emotions: implementing and comparing selected methods for feature extraction and classification,” *IEEE*, 2005.
- [16] M. Garces Agustina Correa and E. Laciar Leber, “Noise removal from eeg signals in polisomnographic records applying adaptive filters in cascade,” June 2011.

- [17] M.-K. Kim, M. Kim, E. Oh, and S.-P. Kim, “A review on the computational methods for emotional state estimation from the human eeg,” *Computational and Mathematical Methods in Medicine*, vol. 2013, no. 573734, p. 13, 2013.
- [18] T. C. Technologies, *10/20 System Positioning manual*. Fortis Tower, 2012.
- [19] Brainworks, “What are brainwaves?,” 2015.
- [20] J. Mellinger, G. Schalk, C. Braun, H. Preiss, W. Rosenstiel, and A. Kübler, “A meg-based brain-computer interface (bci),” *Neuroimage*, July 2008.
- [21] S.-g. Kim Cmrr and K. Ugurbil, “Comparison of blood oxygenattion and cerebral blood flow effect in fmri: Estimation of relative oxygen consumption change,” *Magnetic Resonance in Medicine*, vol. 38, no. 1, pp. 59–65, 1997.
- [22] A. Momose, “Demonstration of phase-contrast x-ray computed tomography using an x-ray interferometer,” *Nuclear Instruments and Methods in Physics Research Section A: Accelerators, Spectrometers, Detectors and Associated Equipment*, vol. 352, no. 3, pp. 622 – 628, 1995.
- [23] T. Castermans, D. Matthieu, G. Cheron, and T. Dutoit, “Towards effective non-invasive brain-computer interfaces dedicated to gait rehabilitation systems,” *brain sciences*, vol. 4, 2014.
- [24] A. Villringer, J. Planck, C. Hock, L. Schleinkofer, and U. Dirnagl, “Near infrared spectroscopy (nirs): A new tool to study hemodynamic changes during activation of brain function in human adults,” *Neuroscience Letters*, vol. 154, pp. 101 – 104, 1993.
- [25] P. LanG, M. Greenwald, M. Bradley, and A. Hamm, “Looking at pictures: affective, facial, visceral, and behavioral reactions.,” *Psychophysiology*, vol. 30, pp. 261–273, May 1993.
- [26] S. U. A. NG, “Machine learning,” 2016.
- [27] L. Eikvil, “Optical character recognition,” *citeSeer. ist. psu. edu/142042. html*, 1993.
- [28] C. M. Bishop, *Pattern Recognition and Machine Learning (Information Science and Statistics)*. Secaucus, NJ, USA: Springer-Verlag New York, Inc., 2006.
- [29] X. Zhu, Z. Ghahramani, J. Lafferty, *et al.*, “Semi-supervised learning using gaussian fields and harmonic functions,” vol. 3, pp. 912–919, 2003.
- [30] R. Genuer, J.-M. Poggi, and C. Tuleau-Malot, “Variable selection using random forests,” *Pattern recognition letters*, pp. 2225–2236, 2010.
- [31] D. O. Bos, “Eeg-based emotion recognition the influence of visual and auditory stimuli.”
- [32] Y. P. Lin, C. H. Wang, T. P. Jung, T. L. Wu, S. K. Jeng, J. R. Duann, and J. H. Chen, “Eeg-based emotion recognition in music listening,” *IEEE Transactions on Biomedical Engineering*, vol. 57, pp. 1798–1806, July 2010.
- [33] L. Brown, B. Grundlehner, and J. Penders, “Towards wireless emotional valence detection from eeg,” in *2011 Annual International Conference of the IEEE Engineering in Medicine and Biology Society*, pp. 2188–2191, Aug 2011.

- [34] M. Murugappan, “Human emotion classification using wavelet transform and knn,” in *Pattern Analysis and Intelligent Robotics (ICPAIR), 2011 International Conference on*, vol. 1, pp. 148–153, June 2011.
- [35] W. Zheng, J. Zhu, and B. Lu, “Identifying stable patterns over time for emotion recognition from EEG,” *CoRR*, vol. abs/1601.02197, 2016.
- [36] J. Kim and E. Andre, “Emotion recognition based on physiological changes in music listening,” *IEEE Transactions on Pattern Analysis and Machine Intelligence*, vol. 30, no. 12, pp. 2067–2083, 2008.
- [37] S. Baluja and D. Pomerleau, “Non-intrusive gaze tracking using artificial neural networks,” January 1994.
- [38] R. N. Duan, J. Y. Zhu, and B. L. Lu, “Differential entropy feature for eeg-based emotion classification,” pp. 81–84, Nov 2013.
- [39] Y. Lio and O. Sourina, “Eeg databases for emotion recognition,” *International Conference on Cyberworlds*, 2013.
- [40] Y.-P. Lin, Y.-H. Yang, and T.-P. Jung, “Fusion of electroencephalographic dynamics and musical,” 2014.
- [41] G.-B. Huang, Q.-Y. Zhu, and C.-K. Siew, “Extreme learning machine: theory and applications,” *Neurocomputing*, vol. 70, no. 1, pp. 489–501, 2006.
- [42] Y. Peng, S. Wang, S. Long, and L. B.-L., “Discriminative graph regularized extreme learning machine and its application to face recognition,” *Neurocomputing*, vol. 149, pp. 360–353, 2015.
- [43] S. L. Crawford, “Statistical primer for cardiovascular research,” 2006.
- [44] J. P. Pluim, A. Maintz, and M. A. Viergever, “Mutual-information-based registration of medical images: A survey,” *IEEE Transactions on Medical Imaging*, vol. 22, pp. 986–1003, August 2003.
- [45] G. J. Szekely and M. L. Rizzo, “Brownian distance covariance,” *The annals of Applied Statistics*, vol. 3, no. 4, pp. 1236–1265, 2009.
- [46] A. Coone, “A study on different preprocessing and machine learning techniques for the detection of error-potentials in brain-computer interfaces,” afstudeerwerk, Ghent university, June 2011.
- [47] F. Lee, R. Scherer, R. Leeb, C. Neuper, H. Bischof, and G. Pfurtscheller, “A comparative analysis of multi-class eeg classification for brain computer interface,” in *Proceedings of the 10th Computer Vision Winter Workshop*, pp. 195–204, 2005.
- [48] G. Pfurtscheller, C. Neuper, C. Guger, W. Harkam, H. Ramoser, A. Schlögl, B. Obermaier, and M. Pregenzer, “Current trends in graz brain-computer interface (bci) research,” *IEEE Transactions on rehabilitation Engineering*, vol. 8, pp. 216–219, JUNE 2000.
- [49] T. Pahikkala, A. Airola, and T. Salakoski, “Speeding up greedy forward selection for regularized least-squares,” pp. 325–330, 2010.

- [50] Stackexchange, “Application of machine learning techniques in small sample clinical studies,” 2016.
- [51] Stackexchange, “Number of features vs. number of observations,” 2016.
- [52] H. Verschore, “A brain-computer interface combined with a language model: the requirements and benefits of a p300 speller,” afstudeerwerk, Ghent University, June 2012.
- [53] L. Farwell and E. Donchin, “Talking off the top of your head: toward a mental prosthesis utilizing event-related brain potentials,” *Electroencephalography and clinical Neurophysiology*, vol. 70, no. 70, pp. 510–523, 1988.
- [54] T. Verhoeven, “Brain-computer interfaces with machine learning: an improved paradigm for the p300 speller,” afstudeerwerk, Ghent University, June 2013.
- [55] N. V. Manyakov, N. Chumerin, A. Combaz, and M. M. V. Hulle, “Comparison of classification methods for p300 brain computer interface on disabled subjects,” *Computational intelligence and neuroscience*, 2011.
- [56] Y. Morita, K. Morita, M. Yamamoto, Y. Waseda, and H. Maeda, “Effects of facial affect recognition on the auditory {P300} in healthy subjects,” *Neuroscience Research*, vol. 41, no. 1, pp. 89 – 95, 2001.

